Federal University of Ceará
Department of Teleinformatics Engineering
Postgraduate Program in Teleinformatics Engineering

Radio Resource Management for Single and Two-Hop Device-to-Device Communications

Master of Science Thesis

Author
José Mairton Barros da Silva Júnior

Advisor
Prof. Dr. Tarcisio Ferreira Maciel

Co-Advisor
Dr. Gábor Fodor

Fortaleza – Ceará
October 2014

Universidade Federal do Ceará
Departamento de Engenharia de Teleinformática
Programa de Pós-graduação em Engenharia de Teleinformática

Radio Resource Management for Single and Two-Hop Device-to-Device Communications

Autor
José Mairton Barros da Silva Júnior

Orientador
Prof. Dr. Tarcisio Ferreira Maciel

Co-orientador
Dr. Gábor Fodor

Dissertação apresentada à Coordenação do Programa de Pós-graduação em Engenharia de Teleinformática da Universidade Federal do Ceará como parte dos requisitos para obtenção do grau de ***Mestre em Engenharia de Teleinformática****. Área de concentração: Sinais e sistemas.*

Fortaleza – Ceará
October 2014

UNIVERSIDADE FEDERAL DO CEARÁ
CENTRO DE TECNOLOGIA
PROGRAMA DE PÓS-GRADUAÇÃO EM ENGENHARIA DE TELEINFORMÁTICA

CAMPUS DO PICI, CAIXA POSTAL 6007 CEP 60.738-640
FORTALEZA – CEARÁ - BRASIL
FONE (+55) 85 3366-9467 – FAX (+55) 85 3366-9468

JOSÉ MAIRTON BARROS DA SILVA JR

RADIO RESOURCE MANAGEMENT FOR SINGLE- AND TWO-HOP D2D COMMUNICATIONS

Dissertação submetida à Coordenação do Programa de Pós-Graduação em Engenharia de Teleinformática, da Universidade Federal do Ceará, como requisito parcial para a obtenção do grau de Mestre em Engenharia de Teleinformática.
Área de concentração: Sinais e Sistemas.

Aprovada em: 30/10/2014.

BANCA EXAMINADORA

Prof. Dr. Tarcisio Ferreira Maciel (Orientador)
Universidade Federal do Ceará

Prof. Dr. Yuri Carvalho Barbosa Silva
Universidade Federal do Ceará

Prof. Dr. Francisco Rafael Marques Lima
Universidade Federal do Ceará

Prof. Dr. João Paulo Cruz Lopes Miranda
Fundação CPqD

Dados Internacionais de Catalogação na Publicação
Universidade Federal do Ceará
Biblioteca de Pós-Graduação em Engenharia - BPGE

S58r Silva Júnior, José Mairton Barros da.
Radio resource management for single and two-hop device-to-device communications / José Mairton Barros da Silva Júnior. – 2014.
98 f. : il. color. , enc. ; 30 cm.

Dissertação (mestrado) – Universidade Federal do Ceará, Centro de Tecnologia, Programa de Pós-Graduação em Engenharia de Teleinformática, Fortaleza, 2014.
Área de concentração: Sinais e Sistemas.
Orientação: Prof. Dr. Tarcisio Ferreira Maciel.
Coorientação: Dr. Gábor Fodor.

1. Teleinformática. 2. Agrupamento. 3. Controle de potência. I. Título.

CDD 621.38

Contents

Dedications

In memoriam to my two grandfathers, Raimundo and Manoel, whose teachings helped me to become who I am today.

Acknowledgements

Foremost, I would like to thank God, for his guidance in all moments.

I am very grateful to my advisor Prof. Dr. Tarcisio F. Maciel for the support, incentive, friendship, guidance, and valuable suggestions and comments during the supervision of my studies. I am also indebted and very grateful to Dr. Gábor Fodor, for all the incentive, friendship, understanding, encouragement and time to advise me when I was in Stockholm for my internship. I have really enjoyed working with both of you, and learning what research is all about. I am looking forward to work with you again :)

To my parents, Edna and Mairton, for the advices, love and support throughout my whole life. Once more to my grandfathers, Raimundo and Manoel, who passed away months before I could show this work to them. To my beloved girlfriend Tainá, who stood with me since I began my undergraduation and suffered from my absence when I was in Stockholm and preparing this thesis during evenings, weekends and holidays; giving me enthusiasm, encouragement, understanding and help.

I would like to thank M. Sc. Prof. Alexandre Moreira (Sobral), in memoriam, for introducing me in the world of programming, for all the great advices you gave me throughout my career. If I become a professor, I will do my utmost to follow your steps. I would like to thank Prof. Dr. Fco. Rodrigo P. Cavalcanti for believing in my professionalism, responsibility and collaboration and for giving me the opportunity to improve as a researcher. Also, I would like to thank my colleagues from UFC 33, M. Sc. Rodrigo Batista, M. Sc. Carlos Filipe, Eng. Yuri Victor for the discussions which greatly contributed for my growth as a researcher.

I would like to thank Ícaro Leonardo, Daniel Costa, Níbia Bezerra and Benedito Neto for the friendship, advices and care when I was in Stockholm, it was great and guys, you had a huge impact on that. I would like also to thank Aidilla Pradini, who helped me to start and to keep up with the simulation environment at Ericsson. To my friends from GTEL, Hugo Costa, Yuri Victor, Victor Farias, Marciel Barros, Diego Sousa and Igor Osterno. To my long-time friends, Rogério Guerra, Paulo Vitor, Hercílio Helton, Jael Araripe, Felipe Ramó and Thiago Moura,

Thanks to the Innovation Center, Ericsson Telecomunicações S.A., Brazil, under EDB/UFC.33 Technical Cooperation Contract. I would like also to acknowledge CAPES for the scholarship support.

Fortaleza, October 2014.

José Mairton Barros da Silva Jr.

Abstract

The increasing demand for fast multimedia services and the scarcity of electromagnetic spectrum has motivated the research of technologies able to increase the capacity of wireless systems without requiring additional spectrum. In this context, Device-to-Device (D2D) communication represents a promising technology. By enabling direct and low-power communication among devices, D2D communication leads to an increased and intelligent spatial reuse of radio resources allowing to offload the data transport network. As a result, the overall system capacity and specially the spectral efficiency is increased; and the proximity between devices allows data transfer with low delays and high rates without requiring extra power from devices' batteries.

However, in order to realize the potential gains of D2D communications as a secondary network of the cellular (primary) one, some key issues must be tackled. Assuming that the communicating devices are aware of each other, the actual link (channel) conditions must be evaluated. If beneficial, Radio Resource Management (RRM) techniques would be employed so that the co-channel interference caused in cellular devices would be mitigated. Such techniques may be summarized as: grouping, mode selection, and power control.

In this thesis, I focus my attention on the RRM for D2D communications underlaying a Long Term Evolution (LTE)-like network, and the main RRM techniques to mitigate the co-channel interference. Aiming at the reduction of the intra-cell interference and at the improvement of spectral efficiency, I formulate a joint grouping and power allocation problem. However, due to its complexity I propose suboptimal methods to group cellular and D2D User Equipments (UEs) with the goal of minimizing intra-cell interference, taking into account spatial orthogonality between the UEs that share the same resources. In addition, I analyze methods to decide if D2D-capable UEs should communicate directly to one another or in the conventional way via the Evolved Node B (eNB). The results show that D2D communications can improve the spectral efficiency of the system and that most of this improvement can be achieved by suitably grouping the UEs for sharing resources based on successive orthogonal projections and matching different spatial compatibility metrics.

Moreover, in this thesis I argue that D2D technology can be used to further increase the spectral and energy efficiency if the key D2D RRM algorithms are suitably extended to support network assisted multi-hop D2D communications. Specifically I propose a novel, distributed utility maximizing power control (PC) scheme that is able to balance spectral and energy efficiency while taking into account mode selection and resource allocation constraints that are important in the integrated cellular-D2D environment. The analysis and numerical results indicate that multi-hop D2D communications combined with the proposed PC scheme can be useful not only for harvesting the potential gains previously identified in the literature, but also for extending the coverage of cellular networks.

Keywords: D2D, grouping, mode selection, multi-hop, power control

Resumo

O aumento da demanda por serviços ricos em multimídia e a escassez do espectro eletromagnético têm motivado a pesquisa de tecnologias capazes de aumentar a capacidade de sistemas sem fio sem requerer espectro adicional. Nesse contexto, comunicações Dispositivo-a-Dispositivo (D2D, do inglês *Device-to-Device*) representam uma tecnologia promissora. Ao permitir comunicação direta e de baixa potência entre os dispositivos, comunicações D2D levam a um maior e mais inteligente reuso dos recursos de rádio, permitindo um descongestionamento da rede de transporte de dados. Como resultado, a capacidade total do sistema e especialmente a eficiência espectral são aumentadas; e a proximidade entre os dispositivos permitem transferências de dados com baixo atraso e altas taxas de dados, sem requerer potência extra da bateria dos dispositivos.

Entretanto, com o objetivo de tornar real os potenciais ganhos de comunicações D2D como uma rede secundária da celular (primária), algumas questões chave precisam ser controladas. Assumindo que os dispositivos se comunicando estão cientes um do outro, a condição do enlace (canal) deve ser avaliada. Caso seja benéfica, técnicas de Gestão de recursos de rádio (RRM, do inglês *Radio Resource Management*) são empregadas para que a interferência co-canal causada nos dispositivos celulares seja mitigada. Tais técnicas podem ser resumidas como: agrupamento, seleção de modo e controle de potência.

Nessa dissertação, eu foco a minha atenção para RRM em comunicações D2D subjacentes a redes LTE, e para as principais técnicas de RRM para mitigar a interferência co-canal. Objetivando a redução da interferência intra-celular e na melhoria da eficiência espectral, eu formulo um problema conjunto de agrupamento e controle de potência. Entretanto, devido à sua complexidade eu proponho métodos sub-ótimos para agrupar usuários celulares e D2D com o objetivo de minimizar a interferência intra-celular, levando em conta a ortogonalidade espacial entre os usuários que compartilham o recurso. Além disso, eu analiso métodos para decidir se um candidato D2D deveria se comunicar diretamente ou de modo convencional através da estação rádio-base (eNB, do inglês *Evolved Node B*). Os resultados mostram que comunicações D2D conseguem melhorar a eficiência espectral do sistema e que a maioria dos ganhos pode ser alcançada agrupando de forma adequada os usuários para compartilhar recursos baseando-se em projeções sucessivas e ortogonais, assim como combinando diferentes métricas de compatibilidade espacial.

Além disso, nessa dissertação eu argumento que tecnologias D2D podem ser usadas para aumentar ainda mais a eficiência espectral e energética se os parâmetros chave dos algoritmos de RRM forem adequadamente estendidos para comunicações D2D em múltiplos saltos. Especificamente, eu proponho um novo algoritmo distribuído de controle de potência baseado em maximização da utilidade que é capaz de equilibrar eficiência espectral e energética, enquanto leva em consideração a seleção de modo e restrições na alocação de recursos inerentes à integração do ambiente celular-D2D. Os resultados numéricos mostram que

comunicações D2D em múltiplos saltos combinadas com o algoritmo de controle de potência proposto são úteis não apenas para colher os potenciais ganhos identificados na literatura, mas também para estender a cobertura de redes celulares.

Palavras-chave: D2D, agrupamento, seleção de modo, múltiplos-saltos, controle de potência

List of Figures

List of Tables

List of Algorithms

Nomenclature

The following notation is used throughout this thesis. I use uppercase and lowercase boldface to denote matrices and vectors, respectively. Plain letters are used for scalars. Other notational conventions are summarized as follows:

List of Symbols

$(\cdot)^{\star}$	Optimal value of the argument, page 54
$(\cdot)^{T}$	Transpose of the argument, page 57
$(\cdot)_{\mathbf{t}(i,h)}$	Argument evaluated on route i and hop h, page 53
α	Path loss compensation factor, page 60
β	General path loss attenuation, page 17
$\boldsymbol{\eta}$	Auxiliary vector to form the LP problem, page 57
$\boldsymbol{\lambda}$	Vector of Lagrange multipliers from the power minimization problem, page 55
$\boldsymbol{\lambda}^{(\mathrm{LP})}$	Vector of Lagrange multipliers of the corresponding LP dual problem, page 57
$\boldsymbol{\mu}$	Vector of transmitted power in the reverse link (DL) , page 59
χ	General shadowing attenuation, page 17
$\mathrm{diag}(\cdot)$	Diagonal of a matrix, page 21
ϵ	Step of the projected gradient iterations, page 55
$\exp(\cdot)$	Exponential of the argument, page 55
$\mathbb{C}$	Field of the complex numbers, page 13
$\gamma_{\cdot}$	SINR achieved by a specific UE, page 17
$\gamma_{\cdot}^{tgt}$	SINR target for a specific UE, page 52
$(\cdot)^{\mathrm{H}}$	Hermitian of a matrix, page 20
$\log_a$	Logarithm to base a of the argument, page 17
$\tilde{\mathbf{R}}$	2-dimensional equivalent routing matrix of all resources, page 52
$\mathbf{C}$	Matrix of link capacities, page 53

$\mathbf{c}_q$	Vector of link capacities on resource q, page 53
$\mathbf{p}_q$	Power vector on resource q, page 53
$\mathbf{R}$	3-dimensional routing matrix, page 51
$\mathbf{R}_q$	2-dimensional routing matrix of resource q, page 51
$\mathbf{s}$	Vector of end-to-end rates, page 53
$\mathbf{1}$	Vector of ones, page 57
$\tilde{\mathbf{S}}$	Set of feasible rate vectors, page 54
$\mathbf{t}(i,h)$	Link and resource indexes in route i and hop h, page 52
$\mathcal{G}$	Group comprising cellular and D2D UEs, page 20
$\mathcal{L}(\cdot)$	Lagrangian function with respect to the argument variables, page 55
$\min(\cdots)$	Minimum value among all arguments, page 60
$\mathbf{H}_{r,t}$	Channel matrix between the UEs r and t, page 13
$\mathbf{H}_{u,c}$	Channel matrix between the UE u and cell c, page 13
$\mathbf{I}_A$	Identity matrix with dimension $A \times A$, page 20
$\mathbf{P}^{(\cdot)}$	Power matrix of specific UEs, page 17
$\mathbf{T}_i$	i^{th} iteration of the projection matrix, page 20
$\mathbf{V}$	Auxiliary matrix to form the LP problem, page 57
$\mathbf{X}$	Resource assignment matrix, page 17
$\nabla(\cdot)$	Gradient of the argument, page 55
$\|\cdot\|^2$	Euclidean norm or 2-norm of a vector, page 14
$\nu(\cdot)$	Objective function of the SINR target setting and power control problem, page 54
ω	Weight between rate maximization and power minimization, page 54
$\arg\min_{a\in A} f(a)$	Value of $a \in A$ that minimizes the function $f(\cdot)$, page 42
∂	Partial derivative symbol, page 55
ρ_q	Number of times resource q has been assigned, page 40
ρ_{min}	Number of times the resource least used has been assigned, page 40
σ^2	Average noise power, page 17
$\succeq$	Component-wise inequality, page 53
$\ln(\cdot)$	Natural logarithm of the argument, page 53
$\triangleq$	Equals to by definition, page 54
$\varphi(\cdot)$	Cost of the total transmit power, page 54

$\mathbf{h}_i$	Channel of the i^{th} UE to the eNB, page 20
$\boldsymbol{\nu}_i$	Grouping metric vector for the admission of the i^{th} UE to the group, page 21
$\mathbf{v}_i$	Normalized projected channel of the $(i)^{\text{th}}$ UE, page 20
$\widehat{\mathbf{H}}_i$	Projected channel matrix at the i^{th} iteration, page 20
$\widehat{\mathbf{h}}_{i,j}$	Projected channel between the eNB and the j^{th} UE at the i^{th} projection, page 21
a	Semi-major axis of the ellipse, page 37
b	Semi-minor axis of the ellipse, page 37
c	Specific eNB in cell c, page 13
$e^{(\cdot)}$	Exponential of the argument, page 56
f	Focal distance of the ellipse, page 37
$f(i)$	Number of hops in route i, page 52
$g_{c,t}$	Leakage of the D2D transmitter t to the eNB c, page 14
$g_{c,u}$	Gain of the eNB c from the cellular receiver u, page 14
G_{eq}	Equivalent channel from D2D_{Tx} to its receiver, page 39
$g_{r,m}$	Leakage of the D2D transmitter m to the D2D receiver, page 14
$g_{r,t}$	Gain of the D2D receiver r from the D2D transmitter t, page 14
$g_{r,u}$	Leakage of the cellular transmitter u to the D2D receiver r, page 14
G_{Re-eNB}	General channel coefficient from D2D_{Re} to eNB, page 39
G_{Re-Rx}	General channel coefficient from D2D_{Re} to D2D_{Rx}, page 39
G_{Tx-eNB}	General channel coefficient from D2D_{Tx} to eNB, page 39
G_{Tx-Re}	General channel coefficient from D2D_{Tx} to D2D_{Re}, page 39
h	Specific hop h, page 52
I	Number of routes (source-destination pairs), page 51
L	Number of links (transmitter-receiver pairs), page 51
M	Maximum number of D2D pairs that can be grouped with a cellular UE, page 17
M_C	Number of antennas at the eNB, page 12
M_U	Number of antennas at the UEs, page 12
m_{PRB}	Minimum number of scheduled PRB per user, page 60
N_{CELL}	Number of cells, page 12
N_{PAIR}	Number of D2D pairs in a cell, page 13

N_{PRB}	Number of PRB, page 12
N_{UE}	Total number of UEs, page 12
$P_{(\cdot)}$	Transmit power of a specific node, page 17
$P^{tot}_{\mathbf{t}(i,h)}$	Total received power measured by the receiver on route i and hop h, page 53
P_{IN}	Interference plus noise power, page 60
q	Specific resource q, page 17
r	Specific D2D receiver r, page 14
$R_{(\cdot)}$	Calculated rate for a specific link, page 17
$S(q)$	Sum of the interferences perceived by a specific UE on resource q, page 42
s_i	End-to-end rate between the S-D pair i, page 52
t	Specific D2D transmitter t, page 14
$t_1(i,h)$	Link index l in route i and hop h, page 52
$t_2(i,h)$	Resource index q in route i and hop h, page 52
U	Total number of transmitters in a cell, page 13
u	Specific UE u, page 13
$u_i(\cdot)$	Utility of the S-D pair i, page 53
W	Bandwidth of one PRB, page 53
y	Specific D2D pair y, page 14

Acronyms

The abbreviations and acronyms used throughout this thesis are listed here. The meaning of each abbreviation or acronym is indicated once, when it first appears in the text.

3GPP	3rd Generation Partnership Project
4G	4th Generation
5G	5th Generation
BLER	BLock Error Rate
BRA	Balanced Random Allocation
CAP	Combinatorial Allocation Problem
CDF	Cumulative Distribution Function
CL	Closed Loop
CLPC	Closed Loop Power Control
CPA	Cellular Protection Algorithm
CSI	Channel State Information
D2D	Device-to-Device
DF	Decode and Forward
DIST	Distance-based Grouping
DL	Downlink
D2DM	D2D Mode Selection
ECC	Electronic Communications Committee
eNB	Evolved Node B
EPA	Equal Power Allocation
FDD	Frequency Division Duplex
HMS	Harmonic Mode Selection
INV	Inverted Norm-based Grouping
IoT	Internet of Things
L3	Layer-3
LP	Linear Programming
LTE	Long Term Evolution
LTE-Advanced	Long Term Evolution Advanced
MAC	Medium Access Control
MANET	Mobile Ad hoc Network

MCS	Modulation and Coding Scheme
MG	Maximum Gain
MH	Multi-Hop
MIMO	Multiple Input Multiple Output
MINLP	Mixed Integer Nonlinear Programming
MIP	Mixed Integer Programming
MISO	Multiple Input Single Output
MRT	Maximum Ratio Transmission
MS	Mode Selection
MTC	Machine-Type Communication
MU-MIMO	Multi-User Multiple Input Multiple Output
MU	Multi-User
NLP	Nonlinear Programming
NLOS	Non-Line of Sight
NORM	Normalized Projection-based Grouping
NP	Non-Polynomial Time
NSPS	National Security and Public Safety Services
OFDMA	Orthogonal Frequency Division Multiple Access
OFDM	Orthogonal Frequency Division Multiplexing
OL	Open Loop
PAIR	D2D Pair Gain-based Grouping
PC	Power Control
PL	Pathloss
PRB	Physical Resource Block
PROJ	Projection-based Grouping
ProSe	Proximity Services
QAM	Quadrature Amplitude Modulation
QoS	Quality of Service
RA	Resource Allocation
RB	Resource Block
REF	Reference Grouping
RND	Random Grouping

RRA	Radio Resource Allocation
RRM	Radio Resource Management
RUNE	RUdimentary Network Emulator
SCM	Spatial Channel Model
S-D	Source-Destination
SINR	Signal to Interference-plus-Noise Ratio
SISO	Single Input Single Output
SIMO	Single Input Multiple Output
SNR	Signal to Noise Ratio
TDD	Time Division Duplex
TPC	Transmit Power Control
TTI	Transmission Time Interval
UE	User Equipment
UL	Uplink
WLAN	Wireless Local Area Network
ZF	Zero-Forcing

Chapter 1

Introduction

"You know what happens when you dream of falling? Sometimes you wake up. Sometimes the fall kills you. And sometimes, when you fall, you fly."

Neil Gaiman

This is an introductory chapter where I present the motivation and scope of this master's thesis in Section 1.1. After that I present the state of the art of Device-to-Device (D2D) communications in Section 1.2. The open problems studied and the main contributions are stated in Sections 1.3 and 1.4, respectively. Finally, the main scientific production during the Master course is presented in Section 1.5.

1.1 Thesis Scope and Motivation

With the advent of the 4th Generation (4G) networks, the well known Long Term Evolution (LTE) Advanced [1], and the upcoming 5th Generation (5G), cellular networks have increased their demands of throughput and energy efficiency, requiring higher data rates for the connected users, while reducing the power consumption, leading to longer battery life for the devices [2]. In 5G networks, there are many scenarios of interest, featuring large numbers of close-by nodes wanting to exchange data [1, 2], such as open-air festivals, game matches in stadiums, emergency communications and Machine-Type Communication (MTC) or even Internet of Things (IoT).

Direct communication between wireless devices, the so-called D2D communication, has gradually gained attention in the scientific community and industry over the last years, and became an extensive research field, for it achieves higher throughput gains maintaining a low power consumption. D2D communication is a type of direct wireless communication between two or more nodes similar to the direct mode in professional mobile radio systems (colloquially, walkie talkies). D2D communications can be deployed in ad hoc wireless networks for the unlicensed spectrum use, like Wireless Local Area Network (WLAN), or in cellular networks for the licensed use, such as LTE and LTE Advanced. Moreover, the 3rd Generation Partnership Project (3GPP) is investigating the use of D2D communication both in commercial and National Security and Public Safety Services (NSPS) scenarios [3], while Electronic Communications Committee (ECC) is studying the allocation of spectrum for public protection to provide services in situations when the cellular infrastructure is damaged [4], such as in natural disasters.

The main principle that underlies D2D communication is to exploit the nodes' proximity that may allow very high data rates, low delays, and low power consumption [5]. For the D2D communication between nodes in close proximity when considering a cellular network, the

network operator does not need to be involved in the actual data transport, except (eventually) for the signaling of session setup, billing, and policy enforcement; which off-loads the core network from the data transport.

The other benefits of D2D communication are the reuse gain and hop gain. The reuse gain implies that radio resources may simultaneously be used by cellular and D2D links, narrowing the reuse factor (even for reuse-1 systems). The hop gain refers to the use of a single link in D2D mode rather than using uplink and downlink bands (Frequency Division Duplex (FDD)) or different time slots (Time Division Duplex (TDD)) like in cellular mode [6, 7]. Additionally, at cell boundaries, D2D links may be also used to extend the cell coverage area.

Despite its advantages, the existence of D2D communication poses another new challenge: nodes and network must cope with new interference situations. For example, in cellular networks using Orthogonal Frequency Division Multiplexing (OFDM) technology, the D2D links may reuse some of the allocated resource blocks; and, in such case, the intra-cell (or co-channel) interference is no longer negligible because the orthogonality between links is lost. Moreover, the undesirable proximity of D2D and cellular transmitters/receivers may bring new types of inter-cell interference. Nevertheless, the new types of interference also depend on the duplexing scheme, spectrum bands, and resources allocation algorithms. Furthermore, recent research lines have recognized the potential of using D2D as relay-assisted Multi-Hop (MH) communications, including mobile relays and relay-assisted D2D communications, which can help to meet the requirements of future radio access networks [2, 3].

1.2 State of the Art

The ideas of integrating ad hoc relaying systems into cellular networks are not new [8, 9], but the advantages of D2D communications in cellular spectrum have been identified and analyzed only recently [6, 10]. Specifically, it has been found that D2D communications can increase the spectral and energy efficiency by taking advantage of the proximity, reuse and hop gains when radio resources are properly allocated to the cellular and D2D layers [11]. Hence, the key functions of single- and multi-hop D2D communications comprise: neighbor discovery, physical layer and Medium Access Control (MAC) sublayer procedures, like synchronization and reference signal design, Radio Resource Management (RRM) functions such as mode selection, grouping, power control, and interference coordination [6, 7]. In Figure 1.1 those procedures are presented in a (possible simulation) chain before the link establishment. Note that I named the RRM as the whole picture and the techniques that really deal with resource allocation as RRM for D2D communications.

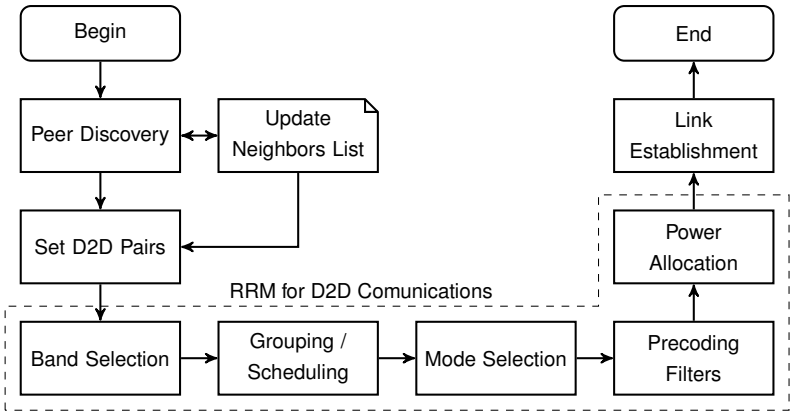

Figure 1.1: RRM procedures for D2D communications and link establishment (based on [7])

The scheduling procedure is responsible for defining which User Equipments (UEs) are

scheduled and determining their required data rates at a specified time, while the resource assignment feature defines which resources will be assigned to the selected flows. Key aspects for designing a mode selection and D2D resource allocation in network-assisted D2D communication, that address both the intra-cell interference and time scale for channel quality estimation, can be found in [6].

Furthermore, the resource allocation between cellular and D2D users has also been addressed in [12–14]. In [12], a greedy heuristic algorithm considering channel gain information appropriately selects the shared radio resources among D2D and cellular users. In [13], the authors exploit the multi-user diversity inherent in cellular systems to improve the network performance. In [14], the D2D users can reuse the resources of more than one cellular user in a system where full Channel State Information (CSI) is assumed, improving the whole system spectral efficiency.

In a scenario with multiple users and a limited number of resources, the selection of which users will be allocated is a key parameter, impacting directly in the throughput of the system. The usage of grouping techniques can improve the total systems' throughput by choosing users which share similar properties, e.g., orthogonality and distance to the Evolved Node B (eNB), to reuse the same resource and so reduce interference.

In [15], the authors propose a spatial subchannel allocation method that sequentially assigns a spatial subchannel to a certain group of channels so that no interference is generated by the currently added spatial subchannel on to any of the previously grouped channels. The interference originated by a certain subchannel on subsequently established subchannels is neutralized by successive encoding following a Zero-Forcing (ZF) criterion. Similarly to [15], in [16] it is proposed to admit UEs to the group in order to improve the channel gain after a projection onto the null space of the channels of the already admitted UEs, so that previously admitted UEs do not see any interference from UEs posteriorly admitted to the group.

Generally speaking, in D2D communications as underlaying a multi-user and multi-cell network, the group can be formed by a D2D pair along with an already scheduled cellular UE based on some grouping metric which measures the compatibility among them. Furthermore, spatial subchannel allocation to create mixed groups of D2D and cellular UEs and its usage with precoding and power allocation techniques are potential techniques to mitigate the interference created by the multiple users inside the group.

Regarding the mode selection, in [10] by allowing D2D communication to underlay the cellular network, the overall throughput in the network may increase up to $65\,\%$ when compared to the traditional case where all traffic is relayed through the cellular network. Moreover, in [17] semi-analytical studies have shown that when D2D communications share the same resources as the cellular network, significant gains in total throughput can be achieved compared to the conventional case, namely by the jointly and optimal allocation. However, numerical analyses have also shown that communication mode selection algorithms need to be designed carefully in order to prevent deteriorating the whole system performance.

In line with the previously mentioned methods of mode selection, in [18], by means of getting optimal communication mode for all devices in the system, equations are derived that capture the network information such as link gains, noise levels, and Signal to Interference-plus-Noise Ratios (SINRs). The results show that the main factors affecting the performance gain of D2D communication are the local communication probability and maximum distance between communicating nodes, as well as the communication mode selection algorithm. As such, designing efficient D2D communication mode algorithms with

minimal interference to the cellular network is seen as a major requirement.

Additionally, in [19] the eNB can decide whether the underlaying D2D pair should reuse cellular resources, get dedicated resources or communicate via eNB. One conclusion drawn from this paper is that optimal communication mode selection strategy does not only depend on the quality of the link between D2D terminals and the quality of the link towards the eNB, but also on the interference situation. In a multi-cell scenario the interference from other cells will affect the decision. In other words, mode selection largely depends on the position of the D2D receiver relative to the cellular terminal when reusing uplink resources, and to the eNB when reusing downlink resources.

Power control is a well-known RRM strategy for interference management in multi-user communication systems. In these systems, the performance of a UE depends on its own transmit power as well as on the transmit powers of interfering UEs. Power control usually improves system performance by adjusting transmit powers of the co-channel UEs so that each of them attains its target Quality of Service (QoS), usually expressed as a SINR value. In this way, links with in-excess QoS will have their transmit powers lowered, thus reducing power consumption as well as interference levels in the system [20–26]. Power control algorithms for cellular systems have been studied with fixed [21, 24, 26] and variable [22, 23, 25] target SINR values considering scenarios with single-antenna [21–23, 27] and multiple-antenna transceivers [24–26].

Particularly, power control algorithms originally designed for cellular systems can be adapted to scenarios with D2D communications by looking at D2D transmitters as the transmitters of interfering cells. Since D2D communications in an LTE-like system can be seen as an underlay, some works focused on limiting the impact of these communications on the cellular network [28–30]. In [28], the SINR distribution of D2D and cellular users is determined, and a simple power control algorithm that limits the impact of D2D communications on the cellular UEs is investigated, while in [29] two power control algorithms are analyzed: a power optimization with greedy sum-rate maximization and a power optimization with rate constraints. Similarly, different power control schemes for D2D UEs communicating in the uplink of an LTE system have been studied in [30]. In these works the authors reached the same conclusions: power control can improve the whole system performance in comparison with a pure cellular system and, with proper scheduling and mode selection algorithms, also minimize the generated interference. Joint problems were also addressed by some authors [31–33], relating power control, mode selection and resource allocation into a single problem. They show that a joint approach achieves a better performance than solving the problems separately.

Integrating MH D2D communications can also help to meet the evolving requirements of next generation wireless networks [2, 3]. In all these cases, both spectral and energy efficiency requirements must be met due to the limited spectrum resources and the requirement on providing broadband services. The combination of D2D and relay technologies is therefore recognized as a potential application of D2D communications [2, 3], but but it has only been studied recently. There are some recent works that consider the usage of fixed and mobile relays to improve the communication [34–36], either on ad hoc or cellular networks, but only a few in the network-assisted D2D communication scenario [37–40]. The main conclusion drawn from these works is that relay-assisted transmission can effectively enhance the performance of D2D, both in spectral and energy efficiency.

1.3 Open Problems

In Section 1.2, I presented different RRM problems for D2D communications that were studied in some scenarios. As shown by the literature review, the community research is aware of the relevance of D2D communications to modern networks what shows the importance of the subject. In this thesis I am also concerned with D2D communications, however, I am motivated by novel aspects about grouping, mode selection, power control and the usage of MH paths in the communication.

Related to these new problems and scenarios, some engineering/scientific topics arise and need to be studied:

i. **Problem formulation and modeling of D2D grouping**: As said before, the grouping of cellular and D2D UEs in a Multiple Input Single Output (MISO) scenario was not yet studied as far as I know. A joint problem is proposed and suboptimal solutions that take into account multiple antennas (either in the eNB or in the UE) are yet to be considered and remains as an open problem.

ii. **Analysis of D2D grouping and other RRM functions**: The joint performance of other RRM functions, such as mode selection, with D2D grouping should still be considered, so as to understand and quantify the importance of them in the same system. This approach remains also as an open problem for D2D grouping.

iii. **Scenarios for underlaying MH D2D communications**: As presented in the literature review, underlaying MH D2D communications has been studied recently and to the best of my knowledge, no standardized scenario from 3GPP for it has been analyzed and therefore remains as an open problem.

iv. **Mode selection for MH D2D communications**: In D2D communications, mode selection is an important function that permits to exploit the proximity gain (when it exists). However, mode selection for MH D2D communications has not been considered yet and remains as open problem.

v. **Power control for MH D2D communications**: Although power control has been extensively studied for ad hoc (common multi-hop networks), its usage on MH D2D communications underlaying cellular networks needs to be addressed, because the multi-resource environment (from cellular networks) must cope with the multi-hop constraints. To the best of my knowledge, this problem has not been studied.

Thus, in order to analyze the performance gains from the usage of grouping in D2D communications, I propose an optimization problem to find the optimal joint grouping and power allocation, but due to its difficulty, suboptimal solutions need to be proposed. Thus, for its suboptimal solution, I consider spatial grouping of cellular and D2D UEs in a MISO scenario, which to the best of my knowledge has not been studied by the literature so far. Concerning MH D2D communications, I propose a mode selection algorithm that selects between legacy cellular communications, single or multi-hop D2D communications, and also I extend a power control algorithm to multi-hop and multi-resource D2D communications. As before, to the best of my knowledge these mode selection and power control strategies have not been considered for underlaying MH D2D communications.

1.4 Contributions and Thesis Organization

In Chapter 2, I concentrate on the resource allocation problem of grouping conventional and D2D-capable UEs for shared resource usage within an LTE-like cellular network. More specifically, I formulate a Mixed Integer Nonlinear Programming (MINLP) optimization problem aiming at the maximization of the overall throughput, where the resources must be shared between cellular UEs and multiple D2D candidates. Since the problem has a high complexity and its optimal solution can not be found in a Transmission Time Interval (TTI) time scale (ms), suboptimal solutions are proposed. Moreover, I formulate a mode selection algorithm and evaluate its performance to better understand the impact of both mode selection and grouping algorithms. The contributions of this chapter help to address the open problems **i** and **ii**.

In Chapter 3, I concentrate on the mode selection and resource allocation problems that are applicable in cellular networks integrating MH D2D communications, where for the two-hop D2D communications I consider two different scenarios that follow 3GPP Proximity Services (ProSe) use cases [3, §5.9, 5.11] within an LTE-like cellular network. The contributions of this chapter help to address the open problems **iii** and **iv**.

In Chapter 4, I propose and analyze heuristic mode selection strategies from Chapter 3 and extend a utility-based, optimal, and distributed Power Control (PC) scheme that takes into account both the achievable rates along MH paths and the overall energy consumption into a multi-resource environment. Moreover, I consider its application on both scenarios proposed in Chapter 3. The contributions of this chapter help to address the open problems **iii** and **v**.

In Chapter 5, I summarize the main conclusions obtained along the thesis. Furthermore, I point out the main research directions that can be considered as extension of the study performed in this thesis.

1.5 Scientific Production

The contents related to mode selection and D2D grouping for single-cell scenarios has been published in the following book chapter:

- [7]: C. F. Silva, **J. Mairton B. da Silva Jr.**, and T. F. Maciel, "Radio Resource Management for Device-to-Device Communications in Long Term Evolution Networks," in Resource Allocation and MIMO for 4G and Beyond, F. R. P. Cavalcanti, Ed. Springer New York, 2014, vol. 105-156.

The contents and contributions present in Chapter 2 were published and submitted with the following information:

- [41]: **J. Mairton B. da Silva Jr.**, T. F. Maciel, R. L. Batista, C. F. M. e Silva, and F. R. P. Cavalcanti, "UE grouping and mode selection for D2D communications underlaying a multicellular wireless system," in IEEE WCNC 2014 - Workshop on Device-to-Device and Public Safety Communications (WCNC'14 - WDPC Workshop), Istambul, Turkey, Apr. 2014, pp. 230–235.

- **J. Mairton B. da Silva Jr.**, T. F. Maciel, C. F. M. e Silva, R. L. Batista and Yuri V. L. de Melo, "User Equipment Grouping for Device-to-Device Communications Underlying a Multi-Cell Wireless System" in EURASIP Journal on Wireless Communications and Networking (submitted).

Two provisional United States patents of the mode selection algorithm proposed in Chapter 3 and one related to admission control on Device-to-Device were filed:

- **J. Mairton B. da Silva Jr.**, G. Fodor, A. Pradini, Tarcisio F. Maciel, "Methods for wireless devices and base station for supporting D2D communication over relay", P41860 WO1
- G. Fodor, **J. Mairton B. da Silva Jr.**, M. Kazmi, M. Belleschi, "A user equipment, a network node, a first and a second core network node, and methods therein for enabling Radio Admission Control (RAC) of Device-to-Device (D2D) services", P42878 WO1

For Chapter 4, its content and contributions were accepted with the following information:

- **J. Mairton B. da Silva Jr.**, G. Fodor, T. F. Maciel, "Performance Analysis of Network-Assisted Two-Hop D2D Communications," in IEEE GLOBECOM 2014 - Workshop on Broadband Wireless Access (BWA) (accepted), Texas, USA, Dec. 2014.

In parallel to the work developed in the Master course that was initiated on the second semester of 2012, I have been working on other research projects, which are in the context of radio resource management for D2D communications. The complete list of articles is presented in the following:

- [42]: R. L. Batista, C. F. M. e Silva, **J. Mairton B. da Silva Jr.**, T. F. Maciel, and F. R. P. Cavalcanti, "Impact of device-to-device communications on cellular communications in a multi-cell scenario," in XXXI Telecommunications Brazilian Symposium (SBrT), Fortaleza, Brazil, Sep. 2013.
- [43]: R. L. Batista, C. F. M. e Silva, **J. Mairton B. da Silva Jr.**, T. F. Maciel, and F. R. P. Cavalcanti, "What happens with a proportional fair cellular scheduling when D2D communications underlay a cellular network?" in IEEE WCNC 2014 - Workshop on Device-to-Device and Public Safety Communications (WCNC'14 - WDPC Workshop), Istambul, Turkey, Apr. 2014, pp. 260–265.
- [44]: R. L. Batista, C. F. M. e Silva, **J. Mairton B. da Silva Jr.**, T. F. Maciel, and F. R. P. Cavalcanti, "Power prediction prior to scheduling combined with equal power allocation for the OFDMA UL," in European Wireless 2014 (EW2014), Barcelona, Spain, May 2014.
- [45]: Y. Victor L. Melo, R. L. Batista, T. F. Maciel, C. F. M. e Silva, **J. Mairton B. da Silva Jr.**, and F. R. P. Cavalcanti, "Power control with variable target SINR for D2D communications underlying cellular networks," in European Wireless 2014 (EW2014), Barcelona, Spain, May 2014.

In the context of the same project, I have participated on the following technical reports:

- [46]: **J. Mairton B. da Silva Jr.**, R. L. Batista, C. F. M. e Silva, Y. Victor L. Melo, T. F. Maciel, and F. R. P. Cavalcanti, "Network-Assisted Device-to-Device Communications", GTEL-UFC-Ericsson UFC.33, Tech. Rep., Aug. 2014, Fourth Technical Report.
- [47]: R. L. Batista, C. F. M. e Silva, **J. Mairton B. da Silva Jr.**, Y. Victor L. Melo, T. F. Maciel, and F. R. P. Cavalcanti, "Network-Assisted Device-to-Device Communications", GTEL-UFC-Ericsson UFC.33, Tech. Rep., Jan. 2014, Third Technical Report.
- [48]: **J. Mairton B. da Silva Jr.**, R. L. Batista, C. F. M. e Silva, Y. Victor L. Melo, T. F. Maciel, and F. R. P. Cavalcanti, "Network-Assisted Device-to-Device Communications", GTEL-UFC-Ericsson UFC.33, Tech. Rep., Aug. 2013, Second Technical Report.

- [49]: R. L. Batista, C. F. M. e Silva, **J. Mairton B. da Silva Jr.**, T. F. Maciel, and F. R. P. Cavalcanti, “Network-Assisted Device-to-Device Communications”, GTEL-UFC-Ericsson UFC.33, Tech. Rep., Feb. 2013, First Technical Report.

Chapter 2

User Equipment Grouping for Device-to-Device Communications

2.1 Introduction

Device-to-Device (D2D) communications underlying cellular networks have been a topic of intense research and appear as a relatively new area offering potentially high benefits in terms of capacity for future wireless networks. In fact, D2D communications underlying cellular systems offer improved spectrum and energy efficiency by exploiting resource reuse and proximity gains [6]. By taking advantage of proximity among communicating devices, direct low-power communication can be employed, thus allowing to offload cellular network through such direct links and reducing congestion in both Downlink (DL) and Uplink (UL).

Moreover, D2D communications should play an important role in 5th Generation (5G) networks in which many scenarios of interest, such as open-air festivals, game matches in stadiums, and Machine-Type Communication (MTC) or even Internet of Things (IoT) scenarios feature large numbers of close-by nodes wanting to exchange data [1]. These are examples of scenarios for which resource reuse and proximity gains can be richly exploited. In Europe, for example, the Electronic Communications Committee (ECC) is considering the allocation of spectrum resources for public protection and disaster relief to provide *broadband* services in situations in which the cellular infrastructure is partially dysfunctional [4]. Meanwhile, 3rd Generation Partnership Project (3GPP) is investigating the use of D2D communication both in commercial and National Security and Public Safety Services (NSPS) scenarios [3].

D2D communications in cellular networks give rise to new types of inter-cell and especially intra-cell interference so that efficient interference coordination becomes a major issue in cellular networks supporting D2D communications [6, 42]. An introduction to D2D communications underlaying a 3GPP Long Term Evolution (LTE)-Advanced network is provided in [10] and key issues related to the potential benefits of implementing D2D communication within cellular systems are identified and discussed.

Two relevant problems in this context are to determine if resource sharing by D2D communications would improve the system spectral efficiency or if conventional cellular communication should be preferred and the other one is how to select which cellular and D2D links should share a resource. These problems are a *mode selection* and a *grouping problem*, respectively.

2.1.1 Related Work

As mentioned before, a major problem for D2D communications underlying a cellular system is the interference they cause in the cellular spectrum due to the resource reuse among conventional cellular and D2D-capable User Equipments (UEs) [11]. There are many techniques to deal with this interference, such as power control [7, 28, 30], mode selection [18, 19] and resource allocation [12, 50, 51], as well as joint schemes using two or more of these approaches [33, 52].

In [28], it is shown for a single circular cell that the interference between cellular and D2D links can be coordinated with proper power control. In [30], four power control schemes based on the LTE power control are proposed and the authors concluded that resource allocation needs to be additionally taken into account with power control in order to decrease the critical interference between cellular and D2D-capable UEs. In [7], it is shown for a single-cell system different power control, resource allocation and mode selection algorithms, that try to improve the system's performance. It concludes that the gains of D2D communications underlaying a cellular network can be harvested considering these different Radio Resource Management (RRM) techniques.

The decision on whether D2D-capable UEs in the proximity of each other should communicate directly — in the so called D2D mode — or via the Evolved Node B (eNB) — in cellular mode — plays an important role on the interference caused by D2D communications. In [18, 19], it is shown that a proper mode selection procedure ensures a reliable D2D communication with limited interference on the cellular network.

In [12], resource allocation for cellular and D2D communications on shared radio resources is studied. Therein, an eNB transmits in DL to the cellular UE on the resource in which the channel gain is the highest. On this resource, the D2D transmitter whose interfering channel gain towards the receiving cellular UE is the lowest is grouped with the former for sharing the resource. Analogously, in UL the D2D transmitter whose interfering gain to the eNB (the receiver) is the lowest is grouped with the cellular UE for sharing the resource. Thus, the D2D link will share the resource with the cellular UE with the lowest channel gain between them, while the $D2D_{Tx\text{-}Rx}$ channel gain is not taken into account.

In [50] the resource allocation for cellular and D2D communications is also studied in a single-cell scenario for the DL with an auction-based approach. Therein, a Combinatorial Allocation Problem (CAP) is proposed, which yields a Non-Polynomial Time (NP)-hard problem. A suboptimal solution is then proposed, resulting in improvements compared to a random allocation. However, the proposed suboptimal algorithm takes too many iterations to converge even in a single-cell scenario and despite the fact that fast fading is considered, its impacts on the algorithm are not. Moreover, the lack of information about the variables and parameters used in simulations make it difficult to reproduce the simulation results presented therein.

In [51] the resource allocation for D2D communications in a hotspot open area network without cellular communications is studied. Therein, a graph coloring approach is proposed to mitigate the interference between the UEs. The numerical experiments show that the proposed solution can significantly improve the throughput performance of a D2D network.

In [52], a reduced-complexity algorithm to solve mode selection and resource allocation for a single-cell scenario is evaluated, showing that joint usage of power allocation and mode selection can improve system's performance. Although the $D2D_{Tx\text{-}Rx}$ channel gain has been considered, the D2D cellular channel gain has not. In [33], a joint power control and resource allocation is formulated for an indoor single-cell scenario in the UL as a

mixed-integer programming problem yielding an NP-hard problem, for which the column generation method is presented as a near-optimal solution [53]. Results therein show that the overall transmission power increases with the spectrum reuse.

2.1.2 Contributions

In this chapter, I concentrate on the resource allocation problem of grouping conventional and D2D-capable UEs for shared resource usage within an LTE-like cellular network. More specifically, I formulate a Mixed Integer Nonlinear Programming (MINLP) optimization problem aiming at the maximization of the overall throughput, where the resources must be shared between cellular UEs and multiple D2D candidates. Unfortunately, the problem has a high complexity and its optimal solution can not be found on a Transmission Time Interval (TTI) basis (ms), and thus suboptimal solutions need to be considered. In addition, I formulate a mode selection algorithm and evaluate its performance to better understand the impact of both mode selection and grouping algorithms.

I adopt a three-step approach: firstly, conventional cellular UEs (further on termed simply cellular UEs) are assigned with resources according to a Maximum Gain (MG) scheduling policy. Secondly, I apply a mode selection rule to determine if the D2D UEs will communicate directly – in D2D mode – or via the eNB – in conventional cellular mode. Both steps are done by the eNB which decides for the best rate arrangement.

Lastly, I select one or more D2D-capable UEs (further on termed simply D2D UEs) to share these resources with the cellular UEs. Notice that D2D-capable UEs are willing to communicate with their respective receiver by using D2D communications. Since resource reuse leads to intra-cell interference that has to be suitably treated, I propose a simple yet efficient grouping algorithm that greedily selects the D2D UEs that have the best compatibility with the cellular UEs preselected on each resource; where compatibility is quantified according to different proposed grouping metrics.

The combination of this greedy grouping algorithm with different grouping metrics and the mode selection results in grouping algorithms with different performances in terms of spectral efficiency and capacity. Differently from previous works which evaluated only the UL [33, 52] or only the DL [50], herein I evaluate the performance of the proposed grouping and mode selection algorithms for both UL and DL directions.

Moreover, differently from [7, 33, 50, 52] which only considered single-cell analyzes, I consider a multi-cell scenario with wrap-around, thus capturing the impact of inter-cell interference on the performance of the proposed algorithms.

Differently from [12, 33, 50, 52] which considered single-antenna scenarios, I consider that the eNB in each cell is equipped with M_C antennas and can service simultaneously multiple single-antenna UEs on a same resource, i.e., I consider Multi-User (MU) Multiple Input Single Output (MISO) and Single Input Multiple Output (SIMO) scenarios in the DL and UL, respectively. Moreover, some of the proposed metrics consider the spatial compatibility [54] among the channels of grouped UEs based on the idea of successive orthogonal projections presented for cellular communications in [15].

I present five different grouping algorithms that can cope with the interference created by the resource reuse and with different channel knowledge for each one, such as the D2D cellular and $\text{D2D}_{\text{Tx-Rx}}$ channel gains, in order to be suitable for many situations. In summary, the main contributions of this chapter are:

- Proposal of a mode selection algorithm that determines the most suitable arrangement for a D2D to communicate;

- Proposal of a grouping algorithm and different grouping metrics that allow for efficient resource allocation in terms of the overall spectral efficiency of the system;
- Performance evaluation of the proposed methods considering a MU MISO and SIMO multi-cellular system scenario for DL and UL, respectively.

The remaining sections are organized as follows. In Section 2.2 the system modeling is presented as well as the main simulation parameters; in Section 2.3 the concept of mode selection is explained as well as the algorithm is presented; in Section 2.4 the joint grouping and power control problem is defined; in Section 2.5 the concept of D2D UE grouping is explained as well as the algorithms are presented; in Section 2.6 the algorithms presented are evaluated; the chapter ends with conclusions and some perspectives, in Section 2.7.

2.2 System Modeling

In this section, I present the models adopted to evaluate the performance of the cellular system with D2D underlay considered in this chapter. I will not mention any physical layer parameter herein, because its construction was abstracted. Let us assume that each eNB is placed at the center of a site, which is represented by a regular hexagon. The considered scenario corresponds to a multi-cell network with wrap-around [55], performed in order to avoid border effects and with the eNBs placed over its coverage area. The propagation environment considered is urban-microcell, cf. [56]. In the urban-microcell environment, each site comprises a single-cell [56]. Graphically, the multi-cell scenario is shown in Figure 2.1.

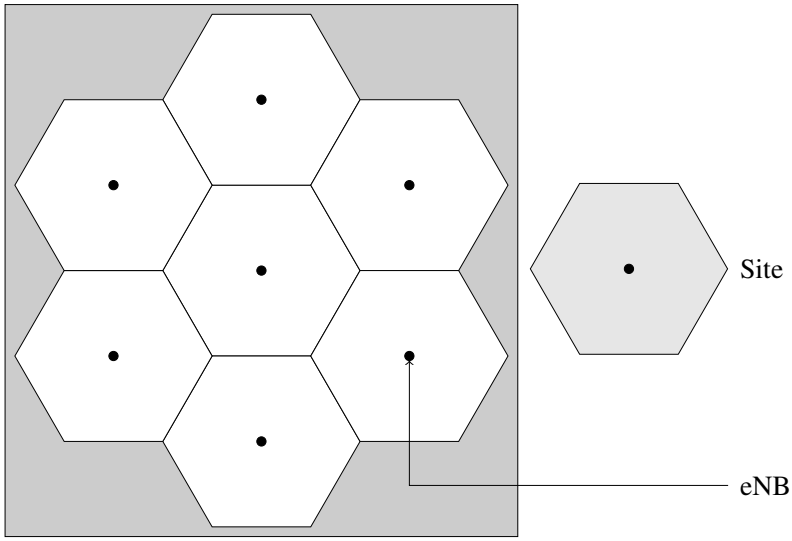

Figure 2.1: The scenario is composed of seven cells (sites) with the eNB at their centers

In the considered notation, it is assumed that the multi-cell scenario is composed of N_{CELL} cells, each one serving N_{UE} UEs uniformly distributed over its coverage area. Also, it is assumed that frequency resources can be fully reused in all cells. Furthermore, each eNB is equipped with M_C co-located antennas, which are omnidirectional in the urban-microcell environment [56] as well as each UE is equipped with M_U omnidirectional co-located antennas. In the MISO scenario (as well as in the SIMO), pre- and post-processing are performed at each side.

The Physical Resource Block (PRB) is the minimum allocable resource unit that can be allocated to a link by RRM in the considered LTE-like system. For both DL and UL, each frame is composed of N_{PRB} PRBs, which have frequency and time dimensions. In the frequency domain, due to signaling constraints, Orthogonal Frequency Division Multiple Access

(OFDMA) subcarriers are not allocated individually, but in blocks of adjacent subcarriers, which represent the PRBs [57]. Each PRB comprises 12 contiguous Orthogonal Frequency Division Multiplexing (OFDM) subcarriers spaced of $15\,\mathrm{kHz}$, which gives a PRB bandwidth of $180\,\mathrm{kHz}$. In the considered model, for a given PRB, the complex channel coefficients corresponding to the middle subcarrier of the PRB are considered as representative for the whole PRB, i.e., I assume that the channel coherence bandwidth is larger than the bandwidth of a PRB, thus leading to a *flat fading channel* over each PRB. In the time domain, the PRB is composed by 14 OFDM symbols, which correspond to one TTI whose duration is $1\,\mathrm{ms}$. Moreover, I consider that each TTI is totally dedicated for data, that is, the control information is not modeled in the frame.

The modeling of the complex channel coefficients includes propagation effects on the wireless channel, namely, pathloss, shadowing, short-term fading as well as it includes the antenna gains. The short-term fading is modeled by the stochastic channel model developed by 3GPP – which is termed Spatial Channel Model (SCM) – for evaluating Multiple Input Multiple Output (MIMO) system performance [56]. The distance dependent Non-Line of Sight (NLOS) pathloss in the microcell environment is based on the COST 231 Walfish-Ikegami NLOS model. Slow channel variations due to shadowing are modeled by a zero-mean lognormal distribution with variance σ^2. Particular aspects of the large-scale fading model for the urban-microcell environment are described in [56, 57] and its basic parameters are presented in Table 2.1.

Table 2.1: Parameters of the large-scale fading model for cellular links

Parameter	**Urban-microcell**
Inter-site distance	$500\,\mathrm{m}$
eNB transmit power	$38\,\mathrm{dBm}$
UE transmit power	$24\,\mathrm{dBm}$
Pathloss model	$34.5 + 38\log_{10}(d)$ dB
Shadowing variance	$10\,\mathrm{dB}$

For D2D communications, the shadowing is defined in Table 2.1 and the pathloss model employed is given by $PL = 37 + 30\log_{10}(d)$, where d is the distance in meters [58]. The received power (either by the $\mathrm{D2D_{Rx}}$, eNB and cellular UE) is given by $P_r[dBm] = P_t[dBm] - PL[dB] - \chi[dB]$ [59], where P_t is the transmitted power by the UE or eNB and χ is the log-normal random variable with zero mean and variance σ^2 that represents the shadow fading. For the middle subcarrier of a given PRB and considering low mobility of UEs, while the channel response for the link between the UE u and cell c can be represented by a channel matrix $\mathbf{H}_{u,c} \in \mathbb{C}^{M_U \times M_C}$, the channel response for the link between the UEs r and t can be represented by $\mathbf{H}_{r,t} \in \mathbb{C}^{M_U \times M_U}$.

The existence of hotspots is important to analyze cases where a pair of D2D-capable UEs are close to each other. Hotspots are placed near the cell-edge in order to evaluate D2D communications in a scenario where they are likely to happen and near the eNB to evaluate D2D communications in a scenario when it is not likely to happen. They have rectangular shape and can accommodate different loads expressed as a number of UEs inside the hotspot area (only D2D candidates are placed inside). Herein, $50\,\%$ of the total number of UEs within the cell are clustered inside the hotspot zone. After all neighbors able to establish D2D communication with a reference UE are detected by a peer-discovery procedure (not covered in this thesis but in other references [7, 60]), D2Ds pairs are obtained by a random pairing procedure. Herein, the number N_{PAIR} of D2D pairs inside the hotspot is given by $N_{\mathrm{PAIR}} = \dfrac{N_{\mathrm{UE}}}{4}$, which is also the total number of D2D transmitters (either UL or DL) inside a cell. In addition,

I denote by $U = \frac{N_{\text{UE}}}{2} + N_{\text{PAIR}}$ the total number of transmitters in a cell, where $\frac{N_{\text{UE}}}{2}$ is the number of cellular UEs.

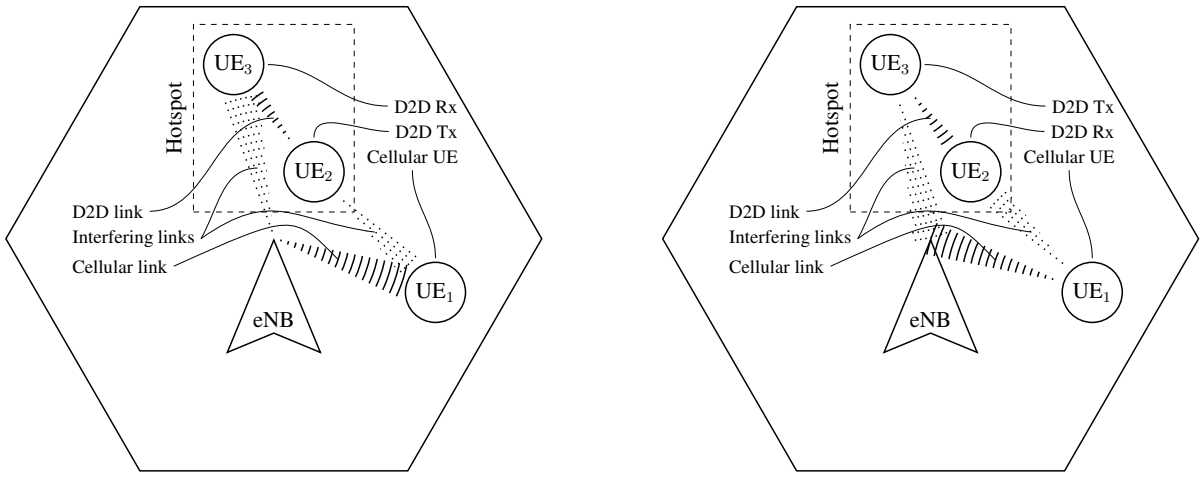

(a) Shared-resource communications in DL **(b)** Shared-resource communications in UL

Figure 2.2: Figures 2.2(a) and 2.2(b) represent the shared-resource communication within a cell for both directions (DL and UL), where the solid lines describe the interesting links and the dashed lines represent the interfering links.

For the urban-microcell environment, there is no need for a special positioning of the hotspot in different directions, since the antennas of the eNB are omnidirectional. Figures 2.2(a) and 2.2(b) exemplify cellular and D2D communications in such hotspot zones in the urban-microcell environment for the DL/UL communication phase, where the term "gain" and "leakage" are associated with the gains of interest and interfering links, respectively.

From Figure 2.2(a), while one pair of UEs is grouped within the hotspot for D2D communications, one cellular UE is serviced by the cellular system. Let us consider that t and r denote, respectively, the transmitter and receiver in a D2D pair $y = (r, t)$, and that c and u denote, respectively, the transmitter and receiver in a cellular communication. The measures for the channel gains of desired and interfering links among cellular and D2D communications within a cell c for a given resource can be defined as follows:

- Gain of the D2D receiver r from the D2D transmitter t: $g_{r,t} = \|\mathbf{H}_{r,t}\|^2$.
- Gain of the eNB c from the cellular receiver u: $g_{c,u} = \|\mathbf{H}_{c,u}\|^2$.
- Leakage of the D2D transmitter t to the eNB c: $g_{c,t} = \|\mathbf{H}_{c,t}\|^2$.
- Leakage of the cellular transmitter u to the D2D receiver r: $g_{r,u} = \|\mathbf{H}_{r,u}\|^2$.
- Leakage of the D2D transmitter m to the D2D receiver r: $g_{r,m} = \|\mathbf{H}_{r,m}\|^2$.

2.2.1 Link-to-System Interface

In this chapter the link-to-system interface is addressed, which is used to map the Signal to Interference-plus-Noise Ratio (SINR), into link-level performance figures of merit, such as BLock Error Rate (BLER). The link adaptation chooses a proper Modulation and Coding Scheme (MCS) for each link in order to maximize the throughput for each transmission based on effective gains achieved by the Radio Resource Allocation (RRA) algorithm [61]. In order to keep the simplicity, the MCS for each PRB and stream of UE is adapted independently.

In accordance with LTE, a set of fifteen MCSs based on different Quadrature Amplitude Modulation (QAM) and code rates is available for link adaptation [62]. In Figure 2.3 it is

shown the BLER and the average throughput curves available for link adaptation, from MCS-1 (leftmost) to MCS-15 (rightmost).

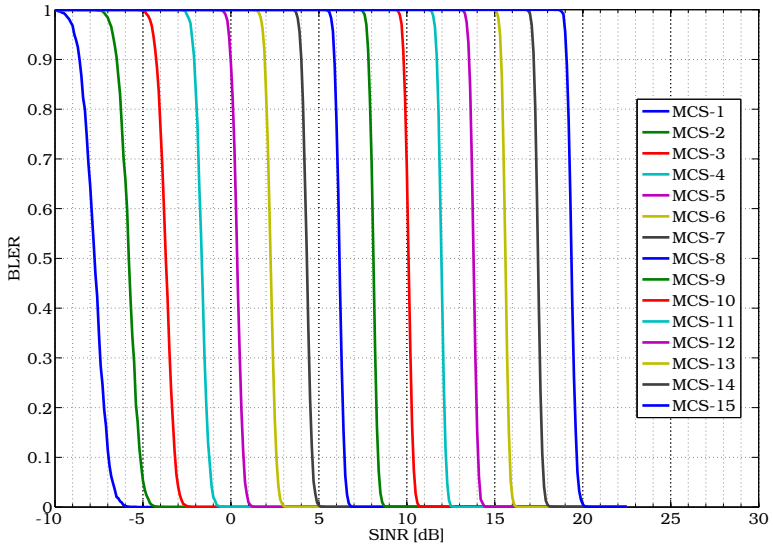

(a) BLER

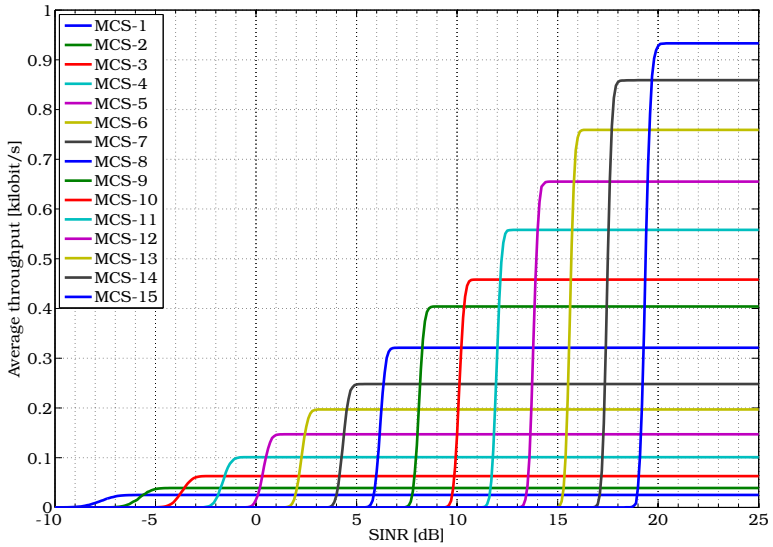

(b) Average throughput

Figure 2.3: Curves of link-level used for link adaptation.

In each transmission, the MCS that yields the maximum average throughput is selected by the link adaptation interface. SINR thresholds are determined for each MCS, i.e. , minimal SINR values required to use each MCS. The MCSs considered in this work and its respective SINR thresholds are summarized in Table 2.2.

Notice that the lowest SINR value of $-6.2\,\mathrm{dB}$ was determined in order to obtain a BLER of $1\,\%$ on transmissions with MCS-1. Also, it is important to notice that the link adaptation can be affected by random variations on the interference levels in the system. I consider that rates are computed considering ideal link adaptation following the link level results from Figure 2.3 and the communications occur error-free, i.e. , there is no packet reception errors and all transmitted data is successfully received.

Table 2.2: SINR thresholds for link adaptation [62].

MCS	**Modulation**	**Code rate** [×1024]	**Rate** [Bits/symbol]	**SINR threshold** [dB]
MCS-1	4-QAM	78	0.1523	−6.2
MCS-2	4-QAM	120	0.2344	−5.6
MCS-3	4-QAM	193	0.3770	−3.5
MCS-4	4-QAM	308	0.6016	−1.5
MCS-5	4-QAM	449	0.8770	0.5
MCS-6	4-QAM	602	1.1758	2.5
MCS-7	16-QAM	378	1.4766	4.6
MCS-8	16-QAM	490	1.9141	6.4
MCS-9	16-QAM	616	2.4062	8.3
MCS-10	64-QAM	466	2.7305	10.4
MCS-11	64-QAM	567	3.3223	12.2
MCS-12	64-QAM	666	3.9023	14.1
MCS-13	64-QAM	772	4.5234	15.9
MCS-14	64-QAM	873	5.1152	17.7
MCS-15	64-QAM	948	5.5547	19.7

2.2.2 Network-assisted RRM Techniques for D2D Communications

The main problem to be solved by the network-assisted RRM techniques for D2D communications is the spatial scheduling of a group of cellular UEs and D2D pairs spatially compatible in each cell, that is, a group that can efficiently share the same resource in the space domain while the levels of interference are kept under control. The assignment decisions are taken independently for each cell, PRB and TTI. Thus, I omit PRB, TTI and link (either UL or DL) indices for simplicity of notation.

In the following, network-assisted RRM techniques exploiting the spatial reuse of radio resources, such as D2D grouping and mode selection are discussed. Figure 2.4 presents the flowchart of the network-assisted RRM techniques for D2D communications developed in this chapter, which are detailed as follows:

1) The initialization step includes peer-discovery and pairing procedures, as mentioned in Section 2.2. Given the list of discovered UEs by the peer-discovery procedure at each reference UE, the pairing procedure shall find the UE that is predisposed to communicate with another, as it could happen in real life. Herein, only UEs inside the hotspot are D2D-capable UEs and they are paired randomly. As output, there are N_{PAIR} D2D pairs able to perform D2D communications.

2.1) Afterwards, the resource allocation is performed, which comprises the cellular scheduling and D2D grouping. Actually, the cellular scheduling is not considered an RRM technique for D2D communications since it schedules cellular UEs independently of the choice of D2D pairs.

2.2) The grouping of D2D pairs takes into account the cellular scheduling decisions in order to establish D2D communications and manage the intra-cell interference in the same resource.

3) The mode selection procedure can be combined with the D2D grouping in order to verify if the grouped D2D pair will obtain more gains communicating via eNB or directly.

In this chapter, the network-assisted RRM techniques for D2D communications are developed considering a certain cellular scheduling policy of the conventional network to assign the available resources to cellular communications. Usually, the number of UEs is larger than the number of available resources. Thus, resources are scheduled to UEs by a

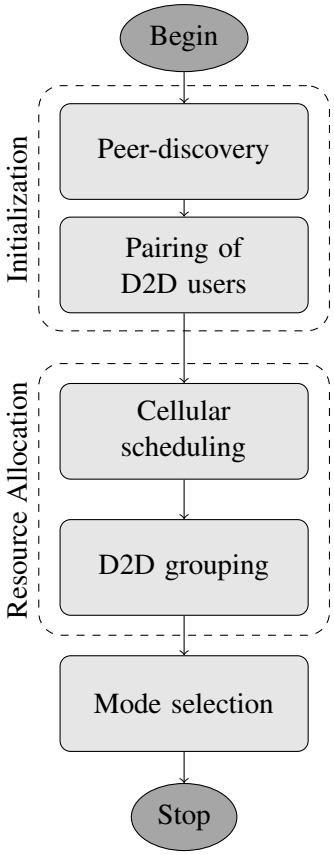

Figure 2.4: Flowchart of the network-assisted RRM techniques for D2D communications.

scheduling policy, i.e., cellular scheduling herein is the process of dynamically allocating the available PRBs at each eNB to the UEs for either data transmission or data reception, based on a set of rules. For the cellular system, the assignment decisions are taken independently for each TTI, PRB and cell by using a scheduling metric, which measures the quality of each link. Herein, the scheduling metric considered is Maximum Gain (MG).

Considering the MG metric, the system throughput is maximized by assigning each frequency-time resource at each cell c to the UE $u^\star$ experiencing the highest channel gain, i.e., with the MG metric one assigns a resource to the UE $u^\star$ with the highest channel gain according to

$$u^\star = \arg\max_u \{g_{u,c}\}\,. \tag{2.1}$$

2.3 Mode Selection Strategies

Herein, the basic idea of mode selection is letting the eNB determine if higher rate (spectral efficiency) is obtained when D2D-capable UEs communicate directly – i.e., in D2D mode –, or via the eNB – i.e., in cellular mode. Figure 2.2 illustrates a cell with one eNB, one cellular UE – UE_1 –, and one D2D pair – D2D_{Tx} and D2D_{Rx} as UE_2 and UE_3 – at the cell edge. As the D2D_{Tx} is close to the D2D_{Rx} and far from the eNB, D2D communications can exploit proximity and reuse gains to improve system performance.

In this work, three modes are analyzed: *cellular mode*, which sets all the D2D-capable UEs to communicate via the eNB in spite of potential gains achievable from direct communication; *D2D mode*, which forces the UEs in D2D pairs to communicate directly disregarding potential interference created to cellular communications; and *rate-based mode selection*, which estimates rate values for D2D and cellular communications to select either cellular or D2D mode.

The rate-based mode selection estimates rates applying Shannon's capacity formula on SINR values calculated using only long-term fading information and verifies if the estimated rate using D2D communication is larger than the one using cellular communication and orthogonal resources [7]. Thus, I assume that the large-scale fading measurements for the link between the nodes are available (e.g., provided by the eNB) and use these measurements as representative of the signal strength.

For D2D communication in the UL, UE_1 transmits to its serving eNB, this corresponding to the link 1, and the $\mathrm{D2D}_{\mathrm{Tx}}$ transmits to the $\mathrm{D2D}_{\mathrm{Rx}}$, this corresponding to the link 2. For links 1 and 2, $\mathrm{D2D}_{\mathrm{Tx}}$ to the eNB and UE_1 to the $\mathrm{D2D}_{\mathrm{Rx}}$ are the interfering links, corresponding to links 3 and 4. For link 1, the closer the UE_1 is to the eNB and the farther $\mathrm{D2D}_{\mathrm{Tx}}$ is from the eNB, the higher its rate (see Figure 2.2(b)). For link 2, the closer the $\mathrm{D2D}_{\mathrm{Tx}}$ is to $\mathrm{D2D}_{\mathrm{Rx}}$ and the farther UE_1 is from $\mathrm{D2D}_{\mathrm{Rx}}$, the higher its rate.

For cellular communication in the UL, all nodes use orthogonal resources and there are two phases: in phase 1, UE_1 transmits to its serving eNB while $\mathrm{D2D}_{\mathrm{Tx}}$ is off; in phase 2, $\mathrm{D2D}_{\mathrm{Tx}}$ transmits to its serving eNB while UE_1 is off, this corresponding to the link 3. I consider that the sum rate in the cellular mode is (roughly) half the sum of the rate obtained in each phase since it uses two resources (in time) [7].

For communications in the UL, cellular and D2D communications work in similar manner with UE_1 and eNB being transmitter and receiver, respectively (see Figure 2.2(a)). In the following, I describe the rate-based mode selection in more details considering the UL. The rate-based mode selection decides which mode to use – cellular or D2D communication – for each TTI, resource and cell, based on the rate estimates:

$$R_1^{\mathrm{D2D}} = \log_2\left(1 + \frac{P_{\mathrm{UE}_1}\beta_1\chi_1}{P_{\mathrm{D2D}_{\mathrm{Tx}}}\beta_3\chi_3 + \sigma^2}\right), \tag{2.2a}$$

$$R_2^{\mathrm{D2D}} = \log_2\left(1 + \frac{P_{\mathrm{D2D}_{\mathrm{Tx}}}\beta_2\chi_2}{P_{\mathrm{UE}_1}\beta_4\chi_4 + \sigma^2}\right), \tag{2.2b}$$

$$R_1^{\mathrm{cell}} = \log_2\left(1 + \frac{P_{\mathrm{UE}_1}\beta_1\chi_1}{\sigma^2}\right), \tag{2.2c}$$

$$R_2^{\mathrm{cell}} = \log_2\left(1 + \frac{P_{\mathrm{D2D}_{\mathrm{Tx}}}\beta_3\chi_3}{\sigma^2}\right), \tag{2.2d}$$

where R_1^{D2D} is the rate calculated for link 1, R_2^{D2D} is the rate calculated for in the link 2, R_1^{cell} is the rate calculated in the link 1 when $\mathrm{D2D}_{\mathrm{Tx}}$ is off, and R_2^{cell} is the rate calculated in the link 3 between $\mathrm{D2D}_{\mathrm{Tx}}$ and eNB when UE_1 is off. In equation (2.2), $P_{(\cdot)}$ is the transmit power of a specific node, σ^2 is the average noise power, and β and χ are the path loss attenuation and shadowing of the previously described links and for the link 4 between UE_1 to $\mathrm{D2D}_{\mathrm{Rx}}$, which are all assumed to be known.

Hence, the rate-based mode selection scheme will decide to use direct D2D communication if the inequality

$$R_1^{\mathrm{D2D}} + R_2^{\mathrm{D2D}} \geq \frac{1}{2}\left(R_1^{\mathrm{cell}} + R_2^{\mathrm{cell}}\right) \tag{2.3}$$

is satisfied, otherwise cellular communication is selected. The rate-based mode selection is presented in Algorithm 2.1, where I consider intercell interference but I do not account for it to estimate rates, since I do not assume any kind of knowledge related to it in the system.

2.4 D2D Grouping Optimization

The fundamental idea behind D2D grouping is to put together D2D pairs and cellular UEs as to obtain resource reuse gains through D2D communications while preventing excessive

Algorithm 2.1 Rate-based Mode Selection Algorithm

1: Calculate the rate estimates R_1^{D2D}, R_2^{D2D}, R_1^{cell}, and R_2^{cell}
2: **if** $R_1^{\text{D2D}} + R_2^{\text{D2D}} \geq \frac{1}{2}\left(R_1^{\text{cell}} + R_2^{\text{cell}}\right)$ **then**
3: Choose D2D communications
4: **else**
5: Choose cellular communications
6: **end if**

reduction on the performance of cellular communications.

In our problem, each resource in each cell is assigned to a cellular UE and then one or more D2D pairs composed by a D2D transmitter (D2D_{Tx}) and a D2D receiver (D2D_{Rx}) are grouped with the pre-selected cellular UE, as illustrated in Figure 2.5, for shared resource usage.

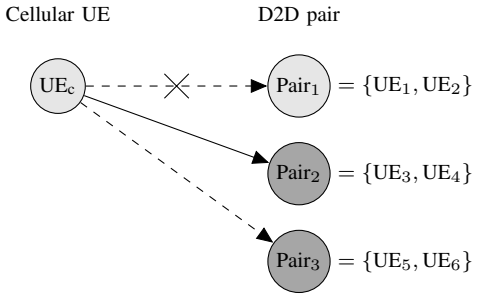

Figure 2.5: The cellular UE is the first UE in the group, followed by the D2D Pair 2 and 3, where the first pair is considered incompatible and thus is not chosen to compose the group.

I define M as the maximum number of D2D pairs that can be grouped together with a cellular UE, which is limited by the total number N_{PAIR} of D2D pairs in a cell. I define $\mathbf{X} \in \{0, 1\}$ the assignment matrix with dimensions $[U \times N_{\text{PRB}}]$, whose $x_{o,q}$ express the relation between user o (either cellular or D2D_{Tx}) and the resource q, i.e., $x_{o,q} = 1$ means that resource q has been assigned to user o. Moreover, I define $\mathbf{P}^c$ and $\mathbf{P}^d$ as the power matrices of cellular and D2D UEs with dimensions given by $\left[\frac{N_{\text{UE}}}{2} \times N_{\text{PRB}}\right]$ and $[N_{\text{PAIR}} \times N_{\text{PRB}}]$, respectively.

In the following, I consider an UL communication, but its adaptation to the DL is similar and can be derived in the same way. The SINR for the transmitting cellular UE u on resource q is measured at the eNB c and defined as

$$\gamma_q^u = \frac{P_{u,q} g_{c,u}}{\sigma^2 + \sum_{t=1}^{M} x_{t,q} P_{t,q} g_{c,t}}, \tag{2.4}$$

where $P_{u,q}$ and $P_{t,q}$ are the assigned power levels to the cellular UE u and D2D_{Tx} t on resource q and σ^2 is the noise power per RB. Notice that there is only one cellular UE per Resource Block (RB), while it may have several D2D UEs sharing the resource. Similarly, the SINR for the D2D_{Tx} UE t on resource q is measured at theD2D_{Rx} r of the same pair and defined as

$$\gamma_q^t = \frac{P_{t,q} g_{r,t}}{\sigma^2 + \sum_{m \neq t}^{M} x_{m,q} P_{m,q} g_{r,m} + \sum_{u=M+1}^{M+\frac{N_{\text{UE}}}{2}} x_{u,q} P_{u,q} g_{r,u}}, \tag{2.5}$$

where now the D2D_{Rx} of pair y has to take into account the interference from other D2D and cellular UE transmitters. Along with the definition of the SINR, I define the throughput of the eNB c from the cellular transmitter u and of the D2D_{Rx} r from the D2D_{Tx} t as

$$R_q^u = \log_2(1 + \gamma_q^u), \tag{2.6}$$

$$R_q^t = \log_2(1 + \gamma_q^t). \tag{2.7}$$

I want to maximize the total throughput of the cell, with the following constraints:

i. Cellular communications are orthogonal, which means that cellular UEs do not share resource with each other;

ii. Power constraint per user, where each UE has a maximum power budget.

Therefore I propose the optimization problem below to find the assignment matrix $\mathbf{X}$ and power levels for cellular ($\mathbf{P}^c$) and D2D ($\mathbf{P}^d$) UEs that maximize the total throughput:

$$\underset{\mathbf{P}^c,\mathbf{P}^d,\mathbf{X}}{\text{maximize}} \sum_{q=1}^{N_{\text{PRB}}} \left(\sum_{t=1}^{N_{\text{PAIR}}} R_q^t + \sum_{u=N_{\text{PAIR}}+1}^{U} R_q^u \right) \tag{2.8}$$

$$\text{subject to} \sum_{t=1}^{N_{\text{PAIR}}} x_{t,q} \leq M, \ \forall q, \tag{C1}$$

$$\sum_{u=N_{\text{PAIR}}+1}^{U} x_{u,q} \leq 1, \ \forall q, \tag{C2}$$

$$p_{u,q} \leq P_{\max}, \ \forall u, q, \tag{C3}$$

$$p_{dn} \leq P_{\max}, \ \forall t, q, \tag{C4}$$

$$\mathbf{X} \in \{0,1\}^{U \times N_{\text{PRB}}}. \tag{C5}$$

Problem (2.8) is an MINLP, which contains both continuous variables (power matrices $\mathbf{P}^c, \mathbf{P}^d$) and binary variables (assignment matrix $\mathbf{X}$). In constraints (C1) and (C2) I restrict the number of D2D and cellular UEs that can share a resource to M D2D_{Tx} and 1 cellular UE, respectively. Constraints (C3) and (C4) set the maximum power for cellular and D2D UEs, while constraint (C5) restricts $\mathbf{X}$ to be binary.

2.5 D2D Suboptimal Grouping Strategies

Usually, MINLPs are hard to solve, due to their composition of two subclasses of problems: the combinatorial essence of Mixed Integer Programming (MIP) and the non-convexity of some Nonlinear Programming (NLP) problems. Therefore, I need to develop heuristics to solve quickly the throughput maximization problem at the eNB of each cell and for each TTI. For the grouping of one or more D2D pairs with these cellular UEs, I propose five grouping metrics and use other two as benchmark, which combined with our greedy grouping method render seven grouping algorithms where each of them has particular characteristics, namely:

- Random Grouping (RND)
- Reference Grouping (REF)
- Distance-based Grouping (DIST)
- D2D Pair Gain-based Grouping (PAIR)
- Projection-based Grouping (PROJ)
- Normalized Projection-based Grouping (NORM)
- Inverted Norm-based Grouping (INV)

In our modeling, I assume Equal Power Allocation (EPA) among the RBs and that the cellular UE is assigned to a resource according to a MG scheduling policy, i.e., each resource is assigned to the cellular UE with the highest channel gain on the considered resource. In

order to improve the system performance, the UEs to be grouped shall be chosen based on grouping metrics capable of measuring the compatibility among D2D pairs and the cellular UE. Note that the MG scheduling policy is aligned with the objective of improving spectral efficiency of cellular communications and, therefore, the cellular UEs closest to the eNB will likely be assigned with resources.

The existence of multiple antennas at eNBs in the MISO scenario allows us to exploit the spatial dimension of the wireless channel, so that a wise allocation of the spatial subchannels to UEs can improve the spectral efficiency of the system [54]. Considering perfect Channel State Information (CSI) at the eNB, the spatial compatibility among UEs can be estimated as function of the orthogonality among the UEs' spatial channels and taken into account when grouping UEs. In [15, 54], the spatial compatibility among UEs is estimated in DL by the norm of UEs' channels after successive null-space projections in a successive spatial subchannel allocation procedure. Differently from those works, herein I adequate the idea of successive null-space projections for usage in both UL and DL with the objective of selecting a set of spatially decoupled subchannels that allows to enhance the system spectral efficiency considering D2D communication.

For successive null-space projections on a given resource, one projects the channel of a selected UE i onto the null space of the i' UEs already admitted to the group of UEs. If the channel of a UE is "highly" orthogonal to the channels of the UEs previously admitted to the group, the norm of its projected channel will remain close to its original value, otherwise, it will be reduced. These norms measure the channel gain of the UE's after and before the null-space projection. In Figure 2.6, null-space (orthogonal) projections considering a cellular and a D2D_{Tx} UE are illustrated, where $\mathcal{N}_1$ and $\mathcal{N}_2$ denote the null-space of the cellular UE and of the D2D_{Tx} spatial channels.

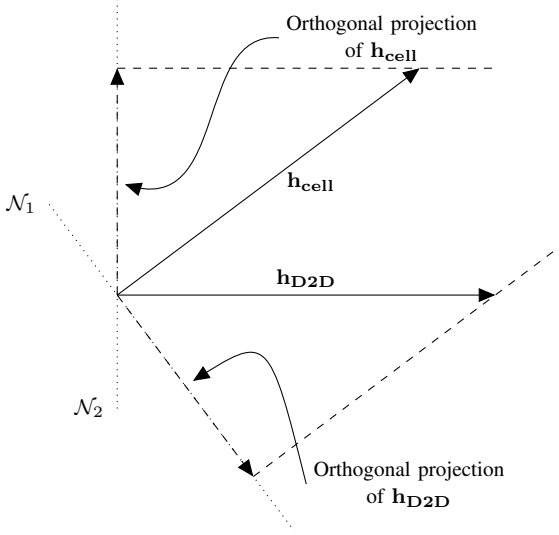

Figure 2.6: Null-space (orthogonal) projections considering a cellular and D2D_{Tx} UEs are illustrated, where the spatial channels are relatively spatially uncorrelated and, consequently, their orthogonal projections preserve much of their original gains.

Therein, the spatial channels are relatively spatially uncorrelated and, consequently, their orthogonal projections preserve much of their original gains. UEs with (close to) orthogonal spatial channels can efficiently share a resource using, e.g., spatial precoding allowing to obtain spatial multiplexing (reuse) gains [54]. In a group $\mathcal{G}$ with $i-1$ already admitted UEs, the channel $\mathbf{h}_i$ of the UE i would be projected onto the joint null-space of the channels $\mathbf{h}_{i'}$, $i' = 1, 2, \ldots, i-1$.

In the following, I consider a single DL resource (for UL it is necessary to transpose the vectors) and for simplicity of notation I omit any index for resources. Let $\mathbf{H} \in \mathbb{C}^{(N_{\text{PAIR}}+1)\times M_C}$ denote the channel matrix formed by stacking the channel $\mathbf{h}_{\text{cell}}$ of the cellular UE and channels $\mathbf{h}_{\text{D2D}_i}$ of the D2D transmitters to the eNB with $i = 1, 2, \ldots, N_{\text{PAIR}}$, i.e.,

$$\mathbf{H} = \left[\mathbf{h}_{\text{cell}}^{\text{T}} \ \mathbf{h}_{\text{D2D}_1}^{\text{T}} \ \cdots \ \mathbf{h}_{\text{D2D}_{N_{\text{PAIR}}}}^{\text{T}}\right]^{\text{T}} \tag{2.9}$$

Therefore, considering the group of UEs that will share the DL resource, let $\mathbf{T}_i \in \mathbb{C}^{M_C \times M_C}$ denote the matrix that projects the channel $\mathbf{h}_i$ of the D2D_{Tx} i onto the null-space of the channels of UEs i'. Note that, for the cellular UE, i.e., the first UE in the group, there is no prior UE in the group and, consequently, $\mathbf{T}_1 = \mathbf{I}_{M_C}$, where $\mathbf{I}_{M_C}$ denotes an $M_C \times M_C$ identity matrix. Then, denoting by $\widehat{\mathbf{H}}_i$ the projection of all UEs' channel in $\mathbf{H}$ of (2.9) for the selection of i^{th} UE of the group, I can write

$$\widehat{\mathbf{H}}_i = \mathbf{H}\mathbf{T}_i, \tag{2.10}$$

where

$$\mathbf{T}_i = \begin{cases} \mathbf{I}_{M_C}, & \text{for } i = 1, \\ \mathbf{T}_{i-1} - \mathbf{v}_{i-1}^{\text{H}}\mathbf{v}_{i-1}, & \text{for } i = 2, 3, \ldots, M, \end{cases} \tag{2.11}$$

and $\mathbf{v}_{i-1}$ is the normalized projected channel of $(i-1)^{\text{th}}$ UE admitted to the group, i.e., it corresponds to the normalized row of $\widehat{\mathbf{H}}_{i-1}$ in (2.10), which is the channel of the $(i-1)^{\text{th}}$ UE selected to be part of the group of UEs sharing the DL resource.

Depending on the grouping algorithm, the idea of successive null-space projections described by (2.10) and (2.11) will be employed considering either $\mathbf{H}$ of (2.9) or an equivalent channel matrix $\widetilde{\mathbf{H}}$, whose definition is in accordance with the objective of each specific grouping algorithm, which will then be used to build $\widehat{\mathbf{H}}_i$ in (2.10). In all the cases, however, the basis grouping algorithm (which is greedy) will admit to the group the UE with highest projected equivalent channel norm. Therefore, if I define the grouping metric vector $\boldsymbol{\nu}_i$ for the admission of the i^{th} UE to the group as

$$\begin{aligned} \boldsymbol{\nu}_i &= \operatorname{diag}\left(\widehat{\mathbf{H}}_i\widehat{\mathbf{H}}_i^{\text{H}}\right) \\ &= \left[\nu_{i,1} \ \nu_{i,2} \ \ldots \ \nu_{i,j} \ \ldots \ \nu_{i,N_{\text{PAIR}}+1}\right]^{\text{T}}, \end{aligned} \tag{2.12}$$

the selected UE $j^\star$ will be

$$j^\star = \arg\max_j \left\{\nu_{i,j}\right\}, \tag{2.13}$$

where $\operatorname{diag}(\mathbf{X})$ denotes the vector formed by the main diagonal of matrix $\mathbf{X}$.

The grouping metrics idealized in this chapter take into account different measurements (which can be made available at the eNB) for the compatibility among cellular UE and D2D UEs, which are:

- The large-scale fading gain g_{cell} of the channel between the eNB and a UE (either a cellular or a D2D);
- The large-scale fading gain g_{D2D} of the channel between the D2D transmitter and D2D receiver;
- The large-scale fading gain $g_{\text{cell-D2D}}$ of the channel between the D2D transmitter and the cellular UE already using the resource;

- The norm $\|\widehat{\mathbf{h}}_{i,j}\|$ of the projected channel $\widehat{\mathbf{h}}_{i,j}$ between the eNB and the j^{th} UE at the i^{th} projection;
- The norm $\|\mathbf{h}_{\text{cell}}\|$ and the squared norm value $\|\mathbf{h}_{\text{cell}}\|^2$ of the channel between the eNB and the cellular UE;

These measurements are used and/or combined in order to capture effects related with spectral efficiency improvement and interference reduction for the groups of UEs sharing a resource. The measurements employed as part of the grouping metrics of each grouping algorithm are indicated in Table 2.3.

Table 2.3: Channel measurements employed by grouping algorithms

Algorithm	**Measurement**					
	g_{cell}	$g_{\text{cell-D2D}}$	g_{D2D}	$\|\widehat{\mathbf{h}}_{i,j}\|$	$\|\mathbf{h}_{\text{cell}}\|$	$\|\mathbf{h}_{\text{cell}}\|^2$
RND	–	–	–	–	–	–
DIST	✓	–	–	–	–	–
REF	–	✓	–	–	–	–
PAIR	–	–	✓	–	–	–
PROJ	–	–	–	✓	–	–
NORM	–	–	✓	✓	✓	–
INV	–	–	✓	✓	–	✓

All the grouping algorithms run at the eNB of each cell, for each TTI and RB. Note that the description above has been presented for the DL direction. However, its adaptation to the UL is similar and can be derived in the same way, with only the eNBs and the cellular UEs exchanging their roles of transmitters and receivers, respectively. Since I assume perfect CSI, the eNB performs all calculations required by the scheduling and grouping algorithms.

The motivation and reasoning behind each measurement and its usage on the different grouping metrics will be described in the following subsections, which detail each of the grouping algorithms. All the grouping algorithms are based on the same greedy procedure. Despite this fact, I opted for clarity sake to describe each algorithm separately in the following.

2.5.1 Random Grouping Algorithm

In order to have a simple D2D grouping algorithm to serve as a benchmark on each resource and cell, the Random Grouping (RND) randomly selects M D2D pairs from the hotspot zone to share the resource with the cellular UE scheduled by the MG policy in this cell. As it can be seen in Table 2.3, this grouping algorithm does not use channel information/measurement. The RND algorithm is shown in Algorithm 2.2. As it has been just mentioned, Algorithm 2.2 (as well as the other algorithms) is applied for each cell, TTI and RB.

Algorithm 2.2 Random Grouping (RND)

1: Select a cellular UE using the MG scheduling policy
2: Select randomly M D2D pairs
3: Form a group with the M D2D pairs and the cellular UE selected in the previous step

2.5.2 Distance-based Grouping Algorithm

Due to the MG scheduling policy, cellular UEs getting resources are likely close to the eNB and, consequently, the interference created by D2D transmitters near the cell-edge to such cellular UEs is low. The basic idea of the Distance-based Grouping (DIST) [41] algorithm is to group the D2D transmitters that are farthest from the eNB with the scheduled cellular UEs as to obtain resource reuse gains without much losses to cellular communications performance.

On a given resource of a cell, whenever $M > 1$, firstly the $D2D_{Tx}$ with the lowest value of g_{cell} is grouped with the scheduled cellular UE. Then, the DIST algorithm looks for the $D2D_{Tx}$ with the second lowest value of g_{cell} and adds it to the group, and so on. As it can be seen in Table 2.3, this grouping algorithm uses only a large-scale fading measurement. The DIST algorithm is shown in Algorithm 2.3.

Algorithm 2.3 Distance-based Grouping (DIST)

1: Select the cellular UE using the MG scheduling policy
2: **while** the number of grouped D2D pairs $\leq M$ **do**
3: Select the non-grouped D2D pair with lowest g_{cell} value
4: Add the selected D2D pair to the group with the cellular UE and D2D pairs selected in the previous steps
5: **end while**

Note that this algorithm tries to protect cellular communications from D2D interference, but ignores the interference that cellular communications cause to $D2D_{Rx}$ UEs (and interference within the hotspot area).

2.5.3 Reference Grouping Algorithm

In order to have a reference grouping algorithm, I consider the one proposed by Zulhasnine et al [12]. The basic idea of REF is to group D2D UEs that have a weak link over the cellular UE already using that resource. On a given resource of a cell, whenever $M > 1$ firstly the $D2D_{Tx}$ with lowest value of $g_{cell\text{-}D2D_{Tx}}$ is grouped with the scheduled cellular UE. Then, REF looks for the $D2D_{Tx}$ with the second lowest value of $g_{cell\text{-}D2D_{Tx}}$ and adds it to the group, and so on. As it can be seen in Table 2.3, this grouping algorithm uses the large-scale fading measurement between cellular and D2D UEs, which needs a high signaling traffic. The REF algorithm is shown in Algorithm 2.4.

Algorithm 2.4 Reference Grouping (REF) from Zulhasnine et al [12]

1: Select the cellular UE using the MG scheduling policy
2: **while** the number of grouped D2D pairs $\leq M$ **do**
3: Select the non-grouped D2D pair with lowest $g_{cell\text{-}D2D_{Tx}}$ value
4: Add the selected D2D pair to the group with the cellular UE and D2D pairs selected in the previous steps
5: **end while**

2.5.4 Pair Gain-based Grouping Algorithm

The D2D Pair Gain-based Grouping (PAIR) method is based on the fact that the proximity between $D2D_{Tx}$ and $D2D_{Rx}$ is an important parameter for D2D communications. I assume that the large-scale fading gain g_{D2D} for the link between these nodes is made available to the eNB, which uses it to represent the effective radio distance between nodes. This gain can be estimated and reported to the eNB by the $D2D_{Tx}$, $D2D_{Rx}$ or both. For this algorithm, whenever $M > 1$ the D2D pairs with smallest distance between the transmitter and D2D receiver are likely to be grouped with the scheduled cellular UE. The PAIR algorithm is shown in Algorithm 2.5.

Algorithm 2.5 D2D Pair Gain-based Grouping (PAIR)

1: Select the cellular UE using the MG scheduling policy
2: **while** the number of grouped D2D pairs $\leq M$ **do**
3: Select the non-grouped D2D pair with highest g_{D2D} value
4: Add the selected D2D pair to the group with the cellular UE and D2D pairs selected in the previous steps
5: **end while**

2.5.5 Projection-based Grouping Algorithm

The successive allocation of spatial subchannels follows the idea that if I have spatially uncorrelated UEs in a group sharing a resource, there will exist less interference among them, leading to higher data rates. The spatial correlation between the channel of the i^{th} UE to be admitted to a group of UEs and the channels of the $i-1$ UEs already admitted

to this group can be estimated by the norm $\|\widehat{\mathbf{h}}_{i,j}\|$ of the j^{th} row of the projected channel matrix $\widehat{\mathbf{H}}_i$ of (2.10), which corresponds to the channel of the UE j projected onto the joint null space of the channels of the UEs already admitted to the group. The greater is the norm, the lower is the spatial correlation between the UE j and the $i-1$ UEs already in the group. In Algorithm 2.6, the Projection-based Grouping (PROJ) algorithm is presented.

The application of successive null-space projections made by the PROJ algorithm of Section 2.5.5 for the DL is similar to its original usage in [15, 54]. Since for this grouping algorithm (and the subsequent ones) the equivalent channel matrix $\widetilde{\mathbf{H}}$ must be composed, I included in the algorithm a description of all the steps required to build the projected channels of (2.10), the projection matrices of (2.11) and to compute the grouping metric vector $\boldsymbol{\nu}_i$ of (2.12).

Algorithm 2.6 Projection-based Grouping (PROJ)

1: Select the cellular UE using the MG metric
2: $i \leftarrow 1$
3: Set $\mathbf{T}_i$ using (2.11), i.e., $\mathbf{T}_1 \leftarrow \mathbf{I}_{M_C}$
4: Set $\widehat{\mathbf{H}}_i$ using (2.10), i.e., $\widehat{\mathbf{H}}_1 \leftarrow \mathbf{H}$
5: $j^\star \leftarrow 1$
6: Add UE $j^\star$ to the group, i.e., the cellular UE
7: Set $\mathbf{v}_i \leftarrow \dfrac{\widehat{\mathbf{h}}_{i,j^\star}}{\|\widehat{\mathbf{h}}_{i,j^\star}\|}$, i.e., $\mathbf{v}_i \leftarrow \dfrac{\mathbf{h}_{\text{cell}}}{\|\mathbf{h}_{\text{cell}}\|}$
8: **while** $i \leq M$ **do**
9: $\quad i \leftarrow i+1$
10: $\quad$ Update $\mathbf{T}_i$ using (2.11)
11: $\quad$ Update $\widehat{\mathbf{H}}_i$ using (2.10)
12: $\quad$ Compute $\boldsymbol{\nu}_i$ using (2.12)
13: $\quad$ Select the UE $j^\star$ with highest value of $\nu_{i,j}$ using (2.13)
14: $\quad$ Update $\mathbf{v}_i \leftarrow \dfrac{\widehat{\mathbf{h}}_{i,j^\star}}{\|\widehat{\mathbf{h}}_{i,j^\star}\|}$
15: $\quad$ Add the D2D UE $j^\star$ to the group
16: **end while**

After the selection of the transmitting cellular UE at step 1, the PROJ algorithm defines the first projection matrix and the first projected channel matrix. Then, the channels of all UEs are projected onto the null-space of the scheduled cellular UE in steps 10 and 11, used to build the equivalent channel matrix from which $\boldsymbol{\nu}_i$ is computed in step 12. Note that according to these steps, the metric $\nu_{i,j}$ for any UE belonging to the group will be zero, since their channels are projected onto their own null-spaces. Thus, in step 13 the UE that does not belong to the group and has the highest norm for its channel after the null-space projections is admitted to the group. After that, the procedure is repeated for adding new UEs to the group.

2.5.6 Normalized Projection-based Grouping Algorithm

Selecting the D2D pair whose D2D_{Tx} has the highest projected channel norm prioritizes D2D UEs that are close to the eNB, which might be undesirable. Now, I propose the Normalized Projection-based Grouping (NORM) algorithm, which prioritizes the proximity gain among D2D_{Tx} and D2D_{Rx} in the D2D pairs (it favors D2D pairs with minimum D2D_{Tx}-to-D2D_{Rx} distance) and the spatial orthogonality among the UEs placed in the same group.

In order to capture the orthogonality among UEs, I first normalize their channels vectors $\mathbf{h}_{\text{D2D}_i}$ of (2.9), thus generating unitary vectors that preserve only channel directions, and then rescale them by multiplying each normalized channel by the channel gain g_{D2D_i} between D2D_{Tx} and D2D_{Rx} of D2D pair i. For this purpose, I define the equivalent channel matrix $\widetilde{\mathbf{H}}$ as

$$\widetilde{\mathbf{H}} = \left[\mathbf{h}_{\text{cell}}^{\text{T}} \;\; \frac{g_{\text{D2D}_1}\mathbf{h}_{\text{D2D}_1}^{\text{T}}}{\|\mathbf{h}_{\text{D2D}_1}\|} \;\; \cdots \;\; \frac{g_{\text{D2D}_{N_{\text{PAIR}}}}\mathbf{h}_{\text{D2D}_{N_{\text{PAIR}}}}^{\text{T}}}{\|\mathbf{h}_{\text{D2D}_{N_{\text{PAIR}}}}^{\text{T}}\|}\right]^{\text{T}}, \tag{2.14}$$

which is used for the algorithm instead of $\mathbf{H}$ in (2.9). In Algorithm 2.7, the NORM algorithm is presented.

Algorithm 2.7 Normalized Projection-based Grouping (NORM)

1: Select the cellular UE using the MG metric
2: $i \leftarrow 1$
3: Set $\mathbf{T}_i$ using (2.11), i.e., $\mathbf{T}_1 \leftarrow \mathbf{I}_{M_C}$
4: Set $\widehat{\mathbf{H}}_i$ using (2.10), but using the equivalent channel $\widetilde{\mathbf{H}}$ of (2.14) instead of $\mathbf{H}$, i.e., $\widehat{\mathbf{H}}_1 \leftarrow \widetilde{\mathbf{H}}$
5: $j^\star \leftarrow 1$
6: Add UE $j^\star$ to the group, i.e., the cellular UE
7: Set $\mathbf{v}_i \leftarrow \dfrac{\widehat{\mathbf{h}}_{i,j^\star}}{\|\widehat{\mathbf{h}}_{i,j^\star}\|}$, i.e., $\mathbf{v}_i \leftarrow \dfrac{\mathbf{h}_{\text{cell}}}{\|\mathbf{h}_{\text{cell}}\|}$
8: **while** $i \leq M$ **do**
9: $\quad i \leftarrow i + 1$
10: $\quad$ Update $\mathbf{T}_i$ using (2.11)
11: $\quad$ Update $\widehat{\mathbf{H}}_i$ using (2.10) with $\widetilde{\mathbf{H}}$ of (2.14) instead of $\mathbf{H}$
12: $\quad$ Compute $\boldsymbol{\nu}_i$ using (2.12)
13: $\quad$ Select the UE $j^\star$ with highest value of $\nu_{i,j}$ using (2.13)
14: $\quad$ Update $\mathbf{v}_i \leftarrow \dfrac{\widehat{\mathbf{h}}_{i,j^\star}}{\|\widehat{\mathbf{h}}_{i,j^\star}\|}$
15: $\quad$ Add the D2D UE $j^\star$ to the group
16: **end while**

Note that it is not necessary to normalize the channel of the cellular UE, since it is always the first UE admitted to the group of UEs sharing the resource. Also the NORM algorithm disregards the distance of D2D UEs to the eNB. Except for the modified metric, the NORM algorithm works in a very similar way to that of the PROJ algorithm.

2.5.7 Inverted Norm-based Grouping Algorithm

Similarly to the NORM algorithm, the INV algorithm described in this section tries to improve the system's performance by combining measures of the orthogonality between UE sharing a resource and the proximity gain between UEs in the D2D pair. However, the INV algorithm takes into account the gain g_{cell_i} from the D2D_{Tx} of the D2D pair i to the eNB in its metric as to prioritize the UEs farthest from the eNB.

For this purpose, I redefine the equivalent channel matrix $\widetilde{\mathbf{H}}$ as

$$\begin{aligned}\widetilde{\mathbf{H}} &= \left[\mathbf{h}_{\text{cell}}^{\text{T}} \;\; \frac{g_{\text{D2D}_1}\mathbf{h}_{\text{D2D}_1}^{\text{T}}}{g_{\text{cell}_1}\|\mathbf{h}_{\text{D2D}_1}\|} \;\; \cdots \;\; \frac{g_{\text{D2D}_{N_{\text{PAIR}}}}\mathbf{h}_{\text{D2D}_{N_{\text{PAIR}}}}^{\text{T}}}{g_{\text{cell}_{N_{\text{PAIR}}}}\|\mathbf{h}_{\text{D2D}_{N_{\text{PAIR}}}}^{\text{T}}\|}\right]^{\text{T}} \\ &= \left[\mathbf{h}_{\text{cell}}^{\text{T}} \;\; \frac{g_{\text{D2D}_1}\mathbf{h}_{\text{D2D}_1}^{\text{T}}}{\|\mathbf{h}_{\text{D2D}_1}\|^2} \;\; \cdots \;\; \frac{g_{\text{D2D}_{N_{\text{PAIR}}}}\mathbf{h}_{\text{D2D}_{N_{\text{PAIR}}}}^{\text{T}}}{\|\mathbf{h}_{\text{D2D}_{N_{\text{PAIR}}}}^{\text{T}}\|^2}\right]^{\text{T}},\end{aligned} \tag{2.15}$$

which is used for the algorithm instead of $\mathbf{H}$ of (2.9). Since I already assume the knowledge of short-term fading for the channels between UEs and the serving eNB, I replace the long-term fading gain g_{cell_1} by the corresponding channel norm $\|\mathbf{h}_{\text{D2D}_i}\|$ leading to the squared norms shown in (2.15). In Algorithm 2.8, the INV algorithm is presented.

Note that, similarly to the NORM algorithm, it is not necessary to modify the channel of the cellular UE, since it is always the first UE admitted to the group of UEs sharing the resource. Also the INV algorithm works in a way very similar to the NORM algorithm, except by its metric that takes into account the distance between UEs and the serving eNB.

2.6 Numerical Results and Discussion

In order to evaluate and compare the performance of the proposed UE grouping algorithms, I performed *system-level simulations* considering an LTE-like cellular system using MATLAB, whose main parameters are summarized in Table 2.4 and are based on 3GPP LTE architecture [56–58, 63].

Algorithm 2.8 Inverted Norm-based Grouping (INV)

1: Select the cellular UE using the MG metric
2: $i \leftarrow 1$
3: Set $\mathbf{T}_i$ using (2.11), i.e., $\mathbf{T}_1 \leftarrow \mathbf{I}_{M_C}$
4: Set $\widehat{\mathbf{H}}_i$ using (2.10), but using the equivalent channel $\widetilde{\mathbf{H}}$ of (2.15) instead of $\mathbf{H}$, i.e., $\widehat{\mathbf{H}}_1 \leftarrow \widetilde{\mathbf{H}}$
5: $j^\star \leftarrow 1$
6: Add UE $j^\star$ to the group, i.e., the cellular UE
7: Set $\mathbf{v}_i \leftarrow \dfrac{\widehat{\mathbf{h}}_{i,j^\star}}{\|\widehat{\mathbf{h}}_{i,j^\star}\|}$, i.e., $\mathbf{v}_i \leftarrow \dfrac{\mathbf{h}_{\text{cell}}}{\|\mathbf{h}_{\text{cell}}\|}$
8: **while** $i \leq M$ **do**
9: $\quad i \leftarrow i + 1$
10: $\quad$ Update $\mathbf{T}_i$ using (2.11)
11: $\quad$ Update $\widehat{\mathbf{H}}_i$ using (2.10) with $\widetilde{\mathbf{H}}$ of (2.15) instead of $\mathbf{H}$
12: $\quad$ Compute $\boldsymbol{\nu}_i$ using (2.12)
13: $\quad$ Select the UE $j^\star$ with highest value of $\nu_{i,j}$ using (2.13)
14: $\quad$ Update $\mathbf{v}_i \leftarrow \dfrac{\widehat{\mathbf{h}}_{i,j^\star}}{\|\widehat{\mathbf{h}}_{i,j^\star}\|}$
15: $\quad$ Add the D2D UE $j^\star$ to the group
16: **end while**

As stated before, the selected scenario is a urban-microcell environment with 7 cells, each serving 16 UEs equally divided into cellular and D2D UEs. The MG scheduling policy is applied to assign resources to the cellular UEs, while the maximum number of D2D pairs that can be grouped to share a resource with a cellular UE has been limited by the number of antennas at the eNB. Therefore, for a 2×1 MISO system, only one D2D pair ($M = 1$) can be grouped with one cellular UE, while for a 4×1 MISO system, three D2D pairs ($M \leq 3$) can be grouped with one cellular UE.

In a network employing D2D communications, its *percentage impact on cellular communications* is often seen as a decrease in the performance of this set of users, while the *percentage gain of D2D communications* is often measured as a gain in the system spectral efficiency. Therefore, the simulation results are presented in terms of the performance achieved by users employing cellular communications, users employing D2D communication, and all users together in the system, which are measured in terms of the system spectral efficiency[1] [bps/Hz/cell].

Initially, in order to understand and quantify the effect of both RRM techniques in the system, the RND and DIST grouping algorithms of Section 2.5 are combined with the different communication modes described in Section 2.3. After that, all the grouping algorithms presented in Section 2.5 are compared using the D2D mode. The results are shown in bar charts, where the y axis is adjusted in each figure as to better shown the differences among the algorithms which have their names shown in the x axis.

2.6.1 Performance Analysis for Mode Selection - SISO System

In Figure 2.7 I concentrate the analysis on the aggregate spectral efficiency values (UL+DL) achieved with each mode, for the cellular, D2D UEs and for the whole system considering the RND and the DIST grouping algorithms. Regarding the cellular UEs with RND in Figure 2.7(a), the cellular mode presents the highest spectral efficiency with gains above $50\,\%$ compared to the other modes. Its good performance is expected since there is no D2D communications and, consequently, no additional D2D interference to harm cellular communications. With the DIST, the performance of the cellular mode has not changed, since D2D-capable UEs operate as conventional cellular UEs.

For the D2D UEs in Figure 2.7(b), the cellular mode is not presented, since there is no D2D communications in that mode. For the D2D users with RND, the D2D mode presents a better performance than the rate-based one, with a relative gain of approximately $12\,\%$.

[1]The system spectral efficiency measures the number of bits received per time/frequency unit per cell.

Table 2.4: Simulation parameters

Parameter	**Value**
Number of eNBs (N_{CELL})	7 (with wrap-around)
Hotspot size	$50 \times 100\,\text{m}$
Hotspot positioning	Cell-edge
Percentage of hotspot UEs	$50\,\%$
Communication links	Downlink (DL) and Uplink (UL)
Central carrier frequency	$1.9\,\text{GHz}$
System bandwidth	$5\,\text{MHz}$
Number of PRBs (N_{PRB})	25 PRBs [57]
Noise power	$-116.4\,\text{dBm}$
Average user speed	$3\,\text{km/h}$ [57]
Channel model	3GPP Spatial Channel Model (SCM) [56]
Antenna pattern	$-\min\left\{12\left[\frac{\theta}{70^o}\right]^2, 20\right\}\,\text{dB}$ [56]
CSI knowledge	Ideal
Interference margin	Last estimated inter-cell interference
Link adaptation	15 Modulation and Coding Schemes (MCSs) [63, 64]
Required SNR at cell-edge	$-6.2\,\text{dB}$
Spatial precoding	Maximum Ratio Transmission (MRT)
Power allocation among PRBs	Equal Power Allocation (EPA)
Traffic model	Full buffer [56]
Number of UEs per cell (N_{UE})	16
Antenna configuration ($M_C \times M_U$)	1×1, 2×1, 4×1
Effective TTI duration	$1\,\text{ms}$
Number of Monte Carlo realizations	150
Snapshot duration	$1\,\text{s}$

This gain comes at the expenses of the degradation of the cellular links, as it can be noted in Figure 2.7(a). For D2D users, comparing the usage of RND and DIST grouping in D2D mode and rate-based mode, I notice that the performance with the DIST grouping is worse than that of RND grouping. This occurs because the DIST limits the D2D pairs that can be selected by taking into account the scheduled cellular UE thus leaving out D2D pairs that would attain high rates but that would do more harm to cellular communications. This does not happen with the RND, which limits neither the selection of D2D pairs nor their impact on the cellular communications, as it can be verified in Figure 2.7(a). The DIST grouping does not only intend to increase spectral efficiency of D2D UEs, but also *to limit interference* caused by D2D communications to the cellular UEs.

Considering the rate-based mode selection with DIST, I notice that both D2D and rate-based modes have achieved almost the same spectral efficiency. Thus, the rate-based mode selection offers protection to the cellular UEs, which have higher spectral efficiency considering both RND and DIST grouping algorithms, as shown in Figure 2.7(a).

Figure 2.7(c) shows the total system spectral efficiency, i.e., the sum of the spectral efficiencies of cellular and D2D UEs shown in Figure 2.7(a) and Figure 2.7(b). In Figure 2.7(c), it can be seen that D2D and rate-based modes with RND grouping achieved gains in the spectral efficiency of about $19\,\%$, compared to the cellular mode. Thus, the results show that D2D communications, whether using D2D or rate-based modes, cause a decrease in the spectral efficiency of cellular UEs, due to the interference that it creates, but improve the overall spectral efficiency of the system. Moreover, the rate-based mode achieves better performance than the D2D mode in which all the D2D-capable UEs communicate directly disregarding the interference caused to cellular communications.

In spite of the fact that the rate-based mode achieved the best results, its relative gain to

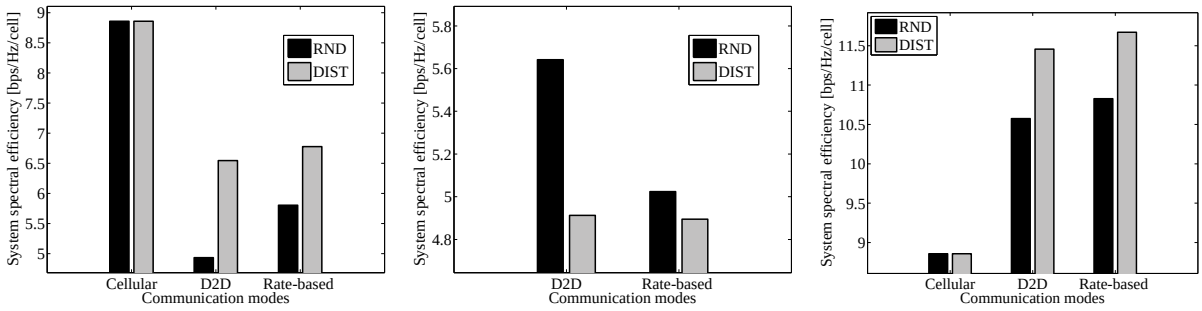

(a) Cellular UEs **(b)** D2D UEs **(c)** Total system spectral efficiency

Figure 2.7: System spectral efficiency for cellular, D2D UEs and for all the UEs. Notice that the usage of D2D communication and a proper mode selection can improve system performance (either D2D or rate-based mode). Moreover, most of the performance gains came from usage of a suitable D2D grouping strategy and not from the mode selection algorithm.

the D2D mode is only about $2\,\%$. Regarding the usage of DIST, there is a gain compared to the RND in the D2D and rate-based modes, about $8\,\%$, while the relative gain between the D2D and rate-based modes is only about $1\,\%$.

Hence, although the cellular mode reached the highest spectral efficiency for the cellular UEs, its total spectral efficiency was the lowest, which shows that the usage of D2D communication and a proper mode selection can improve system performance. The D2D and rate-based modes presented almost the same spectral efficiency, which implies that the usage of the D2D mode, where all the D2D-capable users are underlaid by the cellular network, can be recommended for cases where the complexity is a key parameter. Moreover, most of the performance gains came from usage of a suitable D2D grouping strategy, which might be sufficient for a scheme that aims at suitably increasing spectral efficiency and might dispense the usage of a mode selection scheme.

2.6.2 Performance Analysis for Grouping Algorithms - 2×1 MISO System

In Figure 2.8, the performance of the seven D2D UE grouping techniques described in Section 2.5 will be presented for a 2×1 antenna configuration with the MRT precoding algorithm (i.e., the interference between streams is not canceled) being applied to multi-antenna link between the eNB and cellular UE and with the D2D mode, since it achieves a similar performance with less complexity than rate-based mode. Initially, the grouping algorithms that do not use orthogonal projections are presented (RND,REF,DIST and PAIR) and then PROJ, NORM and INV are compared with the best algorithm among the ones shown before. Figures 2.8(a) and 2.8(b) show the system spectral efficiency for cellular and D2D UEs, respectively, which is the sum of the spectral efficiency of DL and UL phases.

Regarding the cellular UEs, the RND algorithm presents the worst result, followed by the REF algorithm with a relative gain of approximately $3\,\%$ compared to RND. The PAIR algorithm presents a small gain over REF ($\approx 3\,\%$), but over RND the gain is about $19\,\%$. The DIST algorithm shows the highest spectral efficiency, with a relative gain of approximately $19\,\%$ to RND. Although the DIST algorithm shows the highest spectral efficiency for cellular UEs, its relative gain against the other two best grouping algorithms is only about $3\,\%$.

For the D2D UEs in Figure 2.8(b), the DIST and REF algorithms present the worst results, being even worse than that of RND algorithm, where RND presents a relative gain of approximately $18\,\%$ and $9\,\%$ compared to both algorithms, respectively. The PAIR algorithm shows the highest spectral efficiency and its relative gain compared to REF algorithm is about $53\,\%$. This difference is even larger if it is compared with the DIST algorithm, reaching

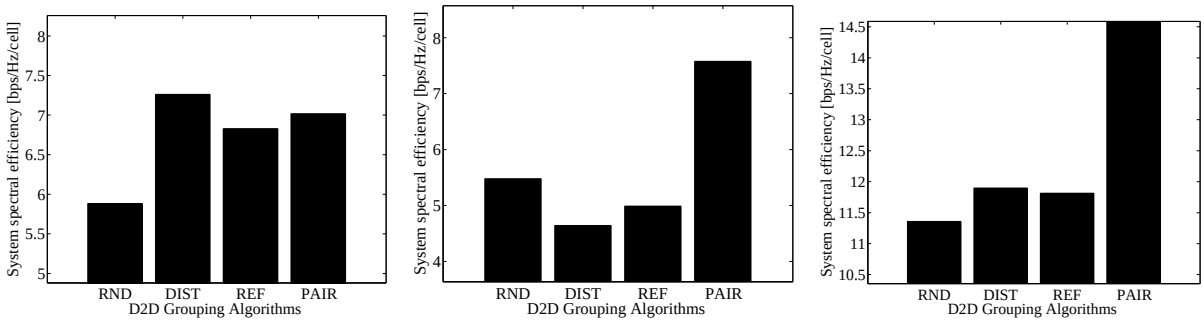

(a) Cellular UEs **(b)** D2D UEs **(c)** Total aggregated

Figure 2.8: System spectral efficiency for 2×1 **MISO**, which illustrate that compatibility metrics (RND and REF) related to the distance between $D2D_{Tx}$ and the eNB do not achieve the highest spectral efficiencies. However, a selfish metric related only to the distance between the D2D pair (PAIR) achieves the highest spectral efficiency, with gains that reach $24\,\%$.

about $63\,\%$. PAIR considers the distance between the D2D pair to group the UEs, while DIST considers the distance between $D2D_{Tx}$ and the eNB, thus implying that the gain brought by PAIR in the D2D layer (since the distances between $D2D_{Tx}$-$D2D_{Rx}$ is small, the SINR tends to be high) is larger than the gain brought by DIST in the cellular layer (since the interference created by the D2D UEs in the cellular UEs tends to be smaller).

In Figure 2.8(c), the total system spectral efficiency is shown. The RND algorithm shows the worst result, followed by REF and DIST, which has a relative gain of approximately $4\,\%$ compared to the former. The best result is achieved by PAIR, with a substantial relative gain ($\approx 29\,\%$) compared to RND and REF ($\approx 24\,\%$) algorithm.

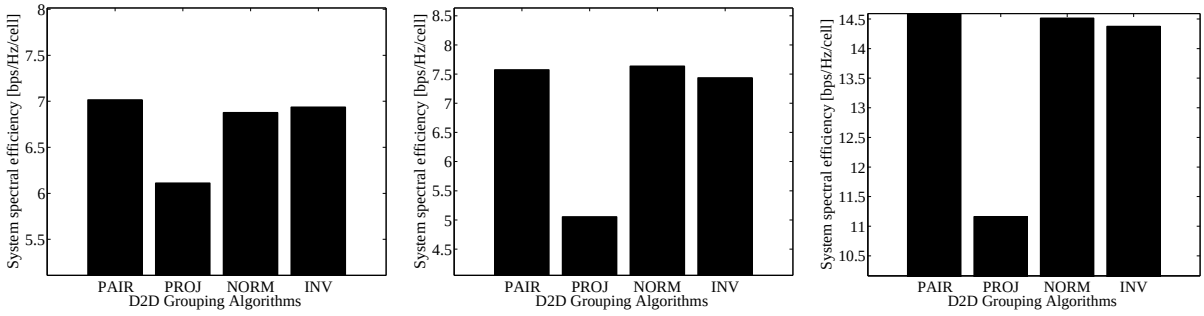

(a) Cellular UEs **(b)** D2D UEs **(c)** Total aggregated

Figure 2.9: System spectral efficiency for 2×1 **MISO with orthogonal projection-based algorithms**, which illustrate that the orthogonality between the cellular and the D2D users shall not be taken into account alone. Nevertheless, considering it with more compatibility indicators, the achieved relative gains compared to the RND and REF algorithms can reach $26\,\%$ and $21\,\%$, respectively.

Since PAIR achieves the best results, it will be used as comparison now for the orthogonal projection-based algorithms, which are presented in Figure 2.9. Regarding the cellular UEs, the PROJ algorithm presents the worst result, followed by the NORM and INV algorithms, which have a gain of approximately $13\,\%$ compared to PROJ. The PAIR algorithm presents a small gain over NORM and INV ($\approx 2\,\%$). Notice that both NORM and INV are close to the performance of PAIR, and therefore show a marginal gain over REF ($\approx 1\,\%$) and a substantial gain over RND ($\approx 17\,\%$). The PROJ algorithm is slightly better than RND, with a relative gain of approximately $4\,\%$, thus showing that the impact of the orthogonality between the grouped UEs alone is small.

These results show that a grouping algorithm that only considers the D2D UEs that are most orthogonal to the cellular UE (the PROJ algorithm) is marginally better than a random

one (the RND algorithm). Although the D2D UEs chosen by PROJ are the most orthogonal to the cellular UE, they may be to far from their $D2D_{Rx}$ or also close to the eNB, thus increasing the interference to other UEs. Therefore, it suggests that another compatibility indicator must be taken into account. Indeed, the two algorithms that consider orthogonal projections and other compatibility indicator, namely NORM and INV algorithms, have a substantial gain compared to the RND and practically the same performance of REF. For the DIST algorithm, which chooses the farthest D2D UE to be grouped with a cellular UE, the interference on the cellular UE will be seriously decreased, thus reducing the impact of D2D communications on the cellular communication.

For the D2D UEs in Figure 2.9(b), the PROJ algorithm presents the worst result, but is still better than REF and DIST, with relative gains of $9\,\%$ and $2\,\%$, respectively. The NORM algorithm has the highest spectral efficiency, with a relative gain of $51\,\%$ to the former. However, the relative gain of NORM over PAIR and INV is low ($\approx 2\,\%$).

Thus, the results suggest that a group formed by the farthest D2D from the chosen cellular UE cannot reach spectral efficiencies as high as a group formed by the most orthogonal to the cellular UE. However, for a group formed by the D2D UEs which have the lowest pair distance, a grouping algorithm can achieve results as good as the ones achieved by algorithms that use orthogonal projection and other compatibility indicators, such as the norm of the cellular UE channel and the D2D large-scale fading gain.

In Figure 2.9(c), the total system spectral efficiency is shown. The PROJ algorithm shows the worst result, being worse than RND, which has a relative gain of approximately $2\,\%$ compared to the former. The best result is achieved by PAIR, followed closely by NORM and INV, with a relative difference between them of approximately $1\,\%$.

These results illustrate again that the orthogonality between the cellular and the D2D users shall not be taken into account alone, because it achieves a spectral efficiency even worse than the RND. Nevertheless, if the orthogonality is considered with the norm of the channel of the cellular UE and/or the D2D channel large-scale fading gain, the achieved relative gains compared to RND can reach $29\,\%$ and compared to the reference scheme proposed by Zulhasnine et al. [12] it can reach $24\,\%$. The PAIR algorithm has the lowest computational complexity and also achieves the highest spectral efficiency in this scenario. However, its overall performance may vary if the hotspot is close to the eNB, because the interference on the cellular layer will increase.

2.6.3 Performance Analysis for Grouping Algorithms - 4×1 MISO System

Now the performance of the seven D2D UE grouping techniques described in Section 2.5 is presented for a 4×1 antenna configuration in Figure 2.10, where now the number of D2D pairs to share a resource can be up to three. As it was shown in Section 2.6.2, the grouping algorithms that do not use orthogonal projections are presented (RND,REF,DIST and PAIR) and then PROJ, NORM and INV are compared with the best algorithm among the ones shown before. In Figures 2.10(a) and 2.10(b), the system spectral efficiency for both cellular and D2D UEs is presented.

Regarding the cellular UEs and the results for $M = 1$ in Figure 2.10(a), a similar behavior to the 2×1 antenna configuration can be observed. The DIST algorithm has the highest spectral efficiency among the analyzed algorithms and RND has the worst. When two pairs are considered, all the algorithms show losses that can be up to $16\,\%$, which is a result of the additional interference introduced by the increased resource reuse.

When $M = 3$, all the algorithms show additional losses. Compared to the case with two

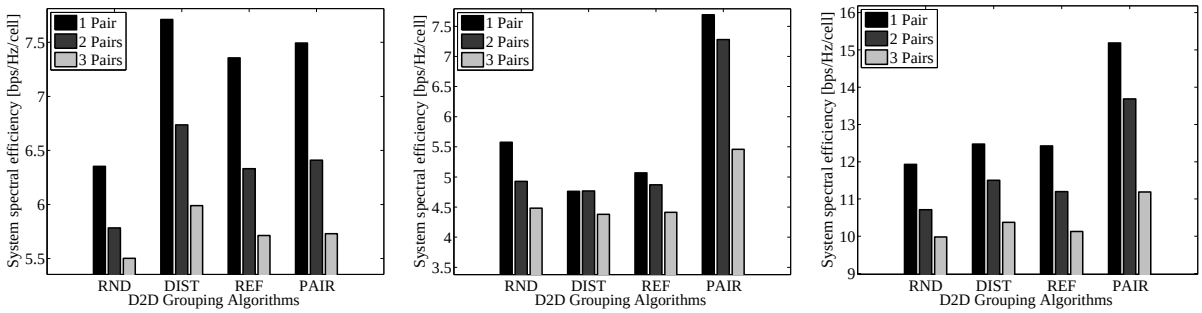

(a) Cellular UEs **(b)** D2D UEs **(c)** Total aggregated

Figure 2.10: System spectral efficiency for 4×1 **MISO**, which illustrate that if non-orthogonality is considered, the losses relative to the case with only one D2D pair are high and can reach $11\,\%$. Moreover, the proposed scheme PAIR achieves better results than REF proposed by Zulhasnine [12].

D2D pairs, RND, REF and DIST algorithms show losses up to $11\,\%$. Compared to the case with one D2D pair, the losses are about $22\,\%$ for REF and DIST and $13\,\%$ for RND. For PAIR, the loss by adding one more D2D pair is about $10\,\%$, but they still have the highest spectral efficiency values.

Regarding the D2D UEs and when $M = 1$ in Figure 2.10(b), the results show again the same behavior of the 2×1 configuration. The DIST algorithm is the worst and PAIR has the highest spectral efficiency. When $M = 2$, all the algorithms show losses, where RND, REF and PAIR algorithms present losses of approximately $13\,\%$, $4\,\%$ and $5\,\%$, respectively. By increasing the number of pairs to three, I have additional losses. The RND and REF algorithms show a loss of approximately $9\,\%$, while PAIR has the highest spectral efficiency and a loss of about $7\,\%$.

Figure 2.10(c) shows the total system spectral efficiency. When $M = 1$, the results show a behavior similar to the 2×1 antenna configuration. When M is increased to two, all the algorithms show losses, with losses up to $10\,\%$ and with PAIR as the best algorithm. When $M = 3$, PAIR shows the highest loss, about $18\,\%$, but it has a gain of approximately $10\,\%$ over REF and RND.

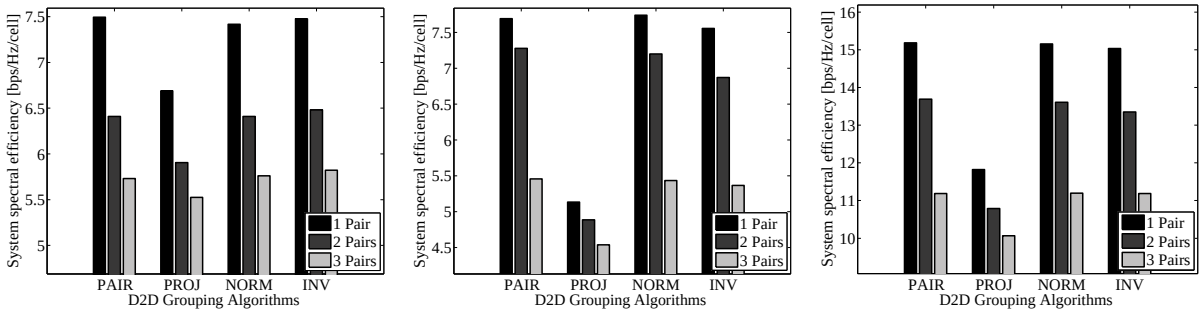

(a) Cellular communications **(b)** D2D communications **(c)** Total aggregated

Figure 2.11: System spectral efficiency for 4×1 **MISO with orthogonal projection-based algorithms**, where once more orthogonality between the cellular and the D2D UEs is desirable with multiple D2D pairs, because it reaches higher values than the REF.

Since PAIR achieves the best results, it will be used once more as comparison for the orthogonal projection-based algorithms, which is present in Figure 2.11. Regarding the cellular UEs, the results for $M = 1$ in Figure 2.11(a), a similar behavior to the 2×1 antenna configuration can be observed. When $M = 2$, the algorithms show losses that are up to $14\,\%$, where now PAIR has a marginal gain over NORM ($\approx 0.006\,\%$).

For $M = 3$, the algorithms show additional losses. For NORM and INV, the losses are

similar (about $10\,\%$), where INV shows the highest spectral efficiency, followed by NORM and PAIR.

Regarding the D2D UEs and when $M = 1$ in Figure 2.11(b), the PROJ algorithm is the worst and the NORM, PAIR and INV have almost the same spectral efficiencies and also the best results. When $M = 2$, all the algorithms show losses, where for PROJ, NORM and INV, they are approximately $5\,\%$, $7\,\%$ and $9\,\%$, respectively. With these losses, PAIR becomes the algorithm with the highest spectral efficiency and a relative gain of $1\,\%$ over NORM, which is still higher than RND and REF.

By increasing the number of pairs to three, there are more losses. PAIR has now the highest spectral efficiency and a loss of about $7\,\%$, while for the PROJ, NORM and INV algorithms, the losses by adding one more D2D pair are about $20\,\%$. Although the losses are higher for these algorithms, NORM and INV are close to PAIR ($\approx 1\,\%$) and still better than REF, with a relative gain of $18\,\%$. Therefore, as well as the cellular UEs, with the proposed grouping algorithms, it is possible to further increase the spectral efficiency of the D2D UEs when compared to the reference schemes.

Figure 2.11(c) shows the total system spectral efficiency. For $M = 1$, the results are similar to what was shown before to the 2×1 antenna configuration. When M is increased to two, PAIR shows loss of approximately $10\,\%$ and presents the highest spectral efficiency. The PROJ, NORM and INV algorithms show losses that are up to $11\,\%$, where the difference between NORM and PAIR is about $0.5\,\%$. When $M = 3$, PAIR and NORM algorithms show the highest losses, about $18\,\%$, followed by INV, about $16\,\%$. Although NORM and PAIR present the highest losses, they achieve the highest spectral efficiencies, with a difference between them of $0.1\,\%$.

These results illustrate that the orthogonality between the cellular and the D2D UEs is desirable with multiple D2D pairs, because it reaches higher values than of spectral efficiency the REF proposed by Zulhasnine et al. [12] and RND. Nevertheless, if non-orthogonality is considered as in the PAIR algorithm, the spectral efficiency achieved is practically the same of NORM, and much better than REF.

2.7 Conclusions and Future Perspectives

In this chapter, algorithms to group UEs as well as algorithms to wisely choose between cellular and D2D communications with the goal of minimizing intra-cell interference and improving the system spectral efficiency have been formulated for both cellular and D2D UEs. The fundamental idea behind mode selection and D2D UE grouping has been presented as well as one algorithm for mode selection — rate-based — and seven algorithms for D2D UE grouping — RND, REF, PAIR, PROJ, NORM and INV — were described, wherein the cellular mode and RND algorithm were used as benchmark, respectively. The metrics used by each grouping algorithm are based on some relevant indicators on the compatibility between the channels of cellular and D2D UEs.

Considering the mode selection, either using forcedly the D2D mode or employing the rate-based mode selection, the spectral efficiency of the system is improved. This spectral efficiency gain comes at the cost of a reduction in the spectral efficiency of cellular communications. For the D2D-capable UEs, the rate-based mode achieved a slightly worse performance than the D2D mode, but provided higher protection to the cellular communications. Although the rate-based mode selection algorithm presented the highest spectral efficiency values among the three considered modes, its gain compared to the D2D mode was marginal, which implies that most of the spectral efficiency improvement with D2D communications can be achieved by employing a suitable grouping algorithm, such as the

proposed DIST grouping.

With this knowledge, the D2D UEs grouping algorithms were then compared. Considering the total spectral efficiency for a 2×1 antenna configuration, the PAIR, NORM and INV algorithms achieved the highest spectral efficiencies, while the PROJ algorithm was the worst. The REF algorithm had a low performance, whereas PAIR, NORM and INV presented a gain of approximately $23\,\%$. The PAIR algorithm is the most simple one, and it achieved the highest spectral efficiency in the simulated scenario. However, its overall performance may vary if the hotspot is close to the eNB, so it can be recommended whenever the D2D UEs are far from the eNB.

For a 4×1 antenna configuration, and when there are multiple D2D pairs, the NORM and PAIR algorithms have losses, but they are able to reach higher spectral efficiency values than the compared schemes (RND and REF), with relative gains of approximately $10\,\%$.

For future works, I intend to address scenarios with D2D pairs within the whole cell and not only confined to the hotspot and, to extend the grouping metrics for Multi-User Multiple Input Multiple Output (MU-MIMO) with different spatial filtering approaches, to investigate the interactions between UE grouping and other RRM schemes and also the impact of channel knowledge on the performance of the grouping metrics.

Chapter 3

Mode Selection and Resource Allocation for Two-Hop Device-to-Device Communications

3.1 Introduction

Although the ideas of integrating ad hoc relaying systems into cellular networks are not new [8, 9], the advantages of D2D communications in cellular spectrum have been identified and analyzed only recently [6, 10]. Specifically, it has been found that D2D communications can increase the spectral and energy efficiency by taking advantage of the proximity, reuse and hop gains when radio resources are properly allocated to the cellular and D2D layers [11].

Another line of research suggests that relay-assisted Multi-Hop (MH) communications, including mobile relays and relay-assisted D2D communications can not only enhance the achievable transmission capacity, but can also improve coverage in cellular networks [34–37].

Recognizing the potential of combining D2D and relay technologies, the standardization and research communities have initiated studies on the achievable gains and enabling technology components to support network-assisted MH D2D communications in operator licensed spectrum. Integrating MH D2D communications can also help to meet the evolving requirements of next generation wireless networks [2, 3]. In all these cases, both spectral and energy efficiency requirements must be met due to the limited spectrum resources and the requirement on providing broadband services.

3.1.1 Related Work

As mentioned before, combining D2D and relay technologies are recognized as potential applications of D2D communications [2, 3]. There are some recent works that consider the usage of fixed and mobile relays to improve the communication [34–36], either on ad hoc or cellular networks, but only a few in the network-assisted D2D communication scenario [37–40].

Conti et al [34] discuss the state of the art for Mobile Ad hoc Networks (MANETs) and why they have failed in their role. Moreover, the article also discusses some research directions as mesh, sensor, opportunistic, vehicular and people-centric networking. Chen et al [35] discuss the role and benefits of mobile relays in LTE-Advanced systems. Zafar et al [36] analyzes MH relaying networks and the impact of the number of hops and antennas on the system's

performance. The main differences between my work and theirs are that I consider a D2D network-assisted system and the fact that a new infrastructure for the relays is not necessary, since the users are the relays, which reduces costs of implementation.

In Wen et al [37] MH D2D relaying is considered, where it derives closed expressions for power and capacity based on the distance between the mobiles and the number of D2Ds and the optimization of spatial density and transmit power of D2D UEs are considered. Finally, they obtain the achievable transmission capacity of MH D2D system with constraints that guarantee the outage probability. The results show that the relay-assisted transmission can effectively enhance the performance of D2D, both in spectral and energy efficiency.

In Romero et al [38], the considered problem is the joint selection of the relay, which will help the UE to connect with the eNB, and the spectrum to be used in the D2D link, which may be licensed or not. The proposed method can achieve better results than a random selection strategy.

In Mastronarde et al [39] the relaying strategies in cellular D2D networks are discussed. They consider that the UE wants to have access to the eNB services and the D2D may help it as a relay. However, for that to happen some incentives are necessary, which is the main topic of the article. They conclude that individual devices have the greatest incentive to cooperate when the network contains highly mobile users.

In Hasan et al [40] Layer-3 (L3) relays are considered to assist the D2D communication, which are fixed and responsible for resource allocation and power control independent of the eNB. The proposed problem aims at maximizing the rate with Quality of Service (QoS), power and interference constraints. It considers also that the UEs shall use only one RB. In other formulation, the problem is rewritten in a convex form, where the powers allocated are given by a multi-level water filling. The results show that compared to Zulhasnine's work [12], the rate gain increases with the D2D distance.

3.1.2 Contributions

Extending the key enabling technology components of single-hop network-assisted D2D communications to MH D2D communication is non-trivial, because (Figure 3.1):

i. Existing single-hop *Mode Selection* (MS) algorithms must be extended to select between the single-hop D2D link, MH D2D paths and cellular communications.

ii. Existing single-hop *Resource Allocation* (RA) algorithms must be further developed to be able not only to manage spectrum resources between cellular and D2D layers, but also to comply with resource constraints along MH paths.

In this chapter, I concentrate on the mode selection and resource allocation problems for two-hop D2D communications within an LTE-like cellular network. Specifically, I formulate and analyze methods to first select whether a D2D UE will transmit to its receiver through an eNB, directly to the receiver or using a relay and then allocate the resource that shall decrease the intra-cell interference, thus improving the overall spectral efficiency of the system.

I adopt a two-step approach: firstly, I apply the mode selection algorithm proposed to determine if the D2D UEs will transmit through the eNB – in cellular mode – or directly to their receivers – in D2D mode – or through D2D relay, in two-hop D2D mode. Secondly, I select one or more D2D UEs to share the resources with conventional cellular UEs. However, resource reuse leads to intra-cell interference and combined with the resource constraints along the MH path, the resource allocation problem is even more interesting. The mode selection and

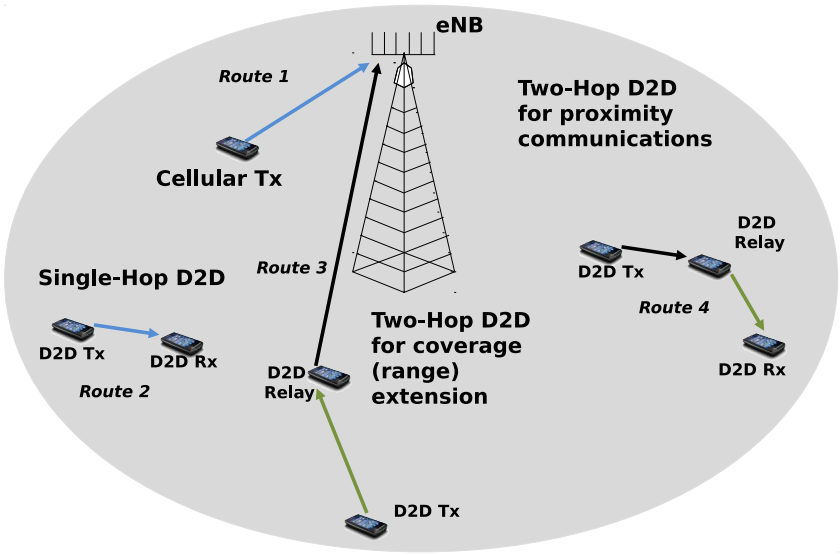

Figure 3.1: An example of a cellular network supporting single- and MH D2D communications in cellular spectrum. I use different colors to indicate different time-frequency resources, while the same color for different links indicate the possibility for intra-cell resource reuse. In this chapter I assume that in the MH case, the incoming and outgoing links of a relay node must use orthogonal resources. Notice that a given source-destination (S-D) pair may have the possibility to communicate in *cellular* mode through the base station or using single- or MH D2D communications.

resource allocation algorithms now must take into account that a relaying device cannot receive and transmit data on the same frequency resource at the same time.

I propose mode selection and resource allocation algorithms that can suitably select the communication mode and assign resources to the D2D UEs that may decrease the intra-cell interference or increase protection to the cellular layer. However, only a few works tackle the resource allocation problem [38, 40], while the mode selection is treated only by [38]. In contrast to previous works which evaluated only single-cell scenarios [37, 39, 40], I consider a seven-cell system with wrap-around in the UL. Moreover, differently from [37–40], I consider two different scenarios for two-hop communications that follow 3GPP Proximity Services (ProSe) use cases [3, §5.9, 5.11]: proximity communication and coverage (range) extension. The proximity communication case comprises scenarios where a D2D UE acts as a relay to the D2D receiver, while in the range extension a D2D UE acts also as a relay, but to the eNB aiming at the extension of cell coverage.

In summary, the main contributions of this chapter are:

i. Proposal of heuristic mode selection and resource allocation strategies that are applicable in cellular networks integrating MH D2D communications;

ii. Performance evaluation of the proposed methods considering a Single Input Single Output (SISO) multi-cellular and two-hop D2D system aligned with 3GPP ProSe use cases for UL.

The remaining sections are organized as follows. In Section 3.2 the system modeling is presented as well as the main simulation parameters; Section 3.3 proposes a mode selection algorithm, while Section 3.4 solves the resource allocation problem considering three different algorithms; Section 3.5 presents numerical results for two different MH D2D communication scenarios and the chapter ends with conclusions and some perspectives, in Section 3.6.

3.2 System Modeling

In this section, I present the models adopted to evaluate the performance of the cellular system with MH D2D underlaying communications considered in this chapter. I have used a modified version and extended to MH D2D the well-known simulator developed by Zander [65], RUdimentary Network Emulator (RUNE), to run the system-level simulations for this chapter. The simulator is different from the one in Chapter 2 because RUNE was used in my internship at Ericsson. Similarly to Section 2.2, I assume that each eNB is placed at the center of a site, which is represented by a regular hexagon and the propagation environment considered is urban-macrocell, cf. [56].

In the considered notation, it is assumed that the multi-cell scenario is composed of 7 cells, each one serving N_{UE} UEs uniformly distributed over its coverage area. Also, it is assumed that frequency resources can be fully reused in all cells. Furthermore, each cell and UE are equipped with one antenna, which are omnidirectional in the urban-macrocell environment [56].

The UL communication link is considered, where each frame is composed of N_{PRB} PRBs, which have frequency dimension only. I assume that the channel coherence bandwidth is larger than the bandwidth of a PRB, thus leading to a *flat fading channel* over each PRB. In addition, no fast fading is considered and I assume that each UE can use at most one RB, which is reused if necessary.

The distance dependent pathloss in the macrocell environment is based on the propagation model from [66]. Slow channel variations due to shadowing are modeled by a zero-mean lognormal distribution with standard deviation σ_{sh}. Particular aspects of the large-scale fading model for the urban-macrocell environment used are described in [66] and its basic parameters are presented in Table 3.1.

Table 3.1: Parameters of the large-scale fading model for cellular links

Parameter	**Urban-macrocell**
Inter-site distance	$1\,\text{km}$
eNB transmit power	$40\,\text{dBm}$
UE transmit power	$15\,\text{dBm}$
Pathloss model	$128.1 + 37.6\log_{10}(d)$ dB
Shadowing standard deviation	$8\,\text{dB}$

For D2D communications, the shadowing is defined in Table 3.1 and the pathloss model employed is given by $PL = 144.7 + 39.7\log_{10}(d)$, where d is the distance in meters [66]. The channel response for the link between the UE u and cell c can be represented by a channel matrix $\mathbf{H}_{u,c} \in \mathbb{R}^{M_U \times M_C}$, while the channel response for the link between the UEs r and t can be represented by $\mathbf{H}_{r,t} \in \mathbb{R}^{M_U \times M_U}$.

Hotspots will not be analyzed herein, because the D2D UEs need to be spread over the cell in order to make MH D2D communications desirable to the UEs. I consider that all neighbors able to establish D2D communication with a reference UE are detected by a peer-discovery procedure (not covered in this thesis).

In order to evaluate the system's performance, a proper UE dropping must be created, since the geometry can affect directly the mode selection, resource allocation and power control. Since I am dealing with two-hop D2D communications, the UEs shall be dropped in *triplets* within the cell, which are composed of a D2D transmitter (D2D_{Tx}), a D2D relay candidate (D2D_{Re}) and the D2D receiver (D2D_{Rx}). For the sake of benchmarking, one dropping is proposed, the ellipse ring, which is a two-hop friendly dropping, where the UEs are dropped

randomly in a manner that two-hop communication might take advantage of the proximity.

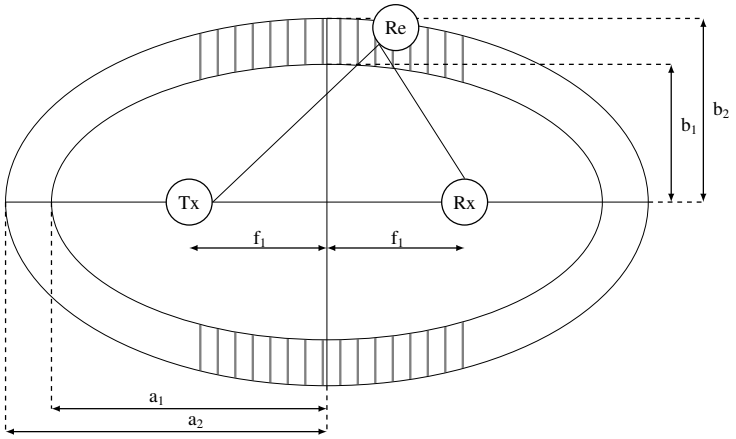

Figure 3.2: The D2D UEs are dropped within the ellipse, where I restrict the $D2D_{Re}$ to be dropped in the ellipse ring created by the intersection of those two ellipses, illustrated as the region with gray lines.

The ellipse ring model presented in Figure 3.2 is based on the fact that the sum of the distances from any point P on the ellipse to those two foci is constant and equal to the major axis $2a$. Thus, $D2D_{Tx}$ and $D2D_{Rx}$ are dropped with a mean distance predetermined between them and defined as the two foci of an ellipse around them, where the major and minor semi-axes are defined based on the focal distance f_1:

$$a_1 = 1.1 f_1$$
$$b_1 = \sqrt{a_1^2 - f_1^2}.$$

Around the first ellipse, another one is created with the same center and foci, with dimensions given by:

$$a_2 = 1.3 f_1$$
$$b_2 = \sqrt{a_2^2 - f_1^2}.$$

Then, I allow the $D2D_{Re}$ to be dropped in the ellipse ring created by the intersection of those two ellipses, illustrated in Figure 3.2 and that can be defined as:

$$2a_1 \leq d_{Tx-Re} + d_{Re-Rx} \leq 2a_2. \tag{3.1}$$

In order to keep the relay close to both transmitter and receiver, I restrict the relay to be dropped in the regions with gray lines shown in Figure 3.2, while the other ones are forbidden. This can be accomplished by restricting the difference between d_{Tx-Re} and d_{Re-Rx}, such as $d_{Tx-Re} \leq 1.1a_2$ and $d_{Re-Rx} \leq 1.1a_2$, which limits the difference between the hops.

3.2.1 Multi-Hop D2D Scenarios: Proximity Communication and Coverage (Range) Extension

Recall from Figure 3.1 that MH D2D communications can be advantageously used in two distinct scenarios. In the *proximity communication* scenario, a $D2D_{Re}$ node helps a D2D pair to communicate [3, Section 5.2.9], while in the *coverage* or *range extension* scenario a $D2D_{Re}$ node assists a coverage limited $D2D_{Tx}$ node to boost its link budget to an eNB [3, Section

5.2.10]. In the proximity communication scenario, the mode selection problem consists of deciding whether the $D2D_{Tx}$ node should communicate with the $D2D_{Rx}$ node:

i. via a direct D2D (single-hop) link,

ii. via a 2-hop path through the $D2D_{Re}$ node,

iii. through the cellular eNB.

In contrast, in the range extension scenario, the mode selection problem consists of deciding whether the $D2D_{Tx}$ node should communicate via a direct transmission with its serving eNB or via the $D2D_{Re}$ node.

3.2.2 Network-assisted RRM Techniques for MH D2D Communications

The main problems to be solved by the network-assisted RRM techniques for MH D2D communications in this chapter are the mode selection considering a two-hop path and the decision of which cellular and D2D UEs will share the PRBs. The assignment decisions are taken independently for each cell and PRB.

In the following, network-assisted RRM techniques such as resource allocation and mode selection are discussed. Figure 3.3 presents the flowchart of the network-assisted RRM techniques developed in this chapter.

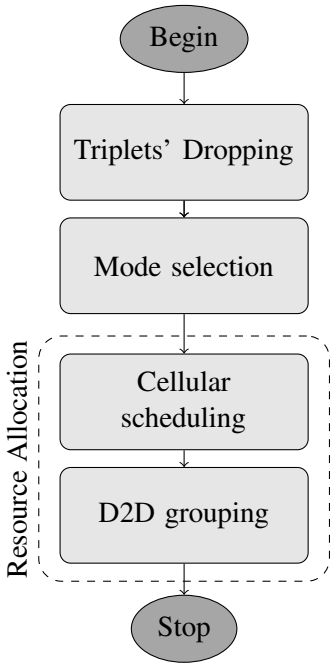

Figure 3.3: Flowchart of the network-assisted RRM techniques for MH D2D communications.

The RRM techniques considered in this chapter for D2D communications and presented in Figure 3.3 are detailed as follows:

1) The initialization step includes the triplets' dropping using the ellipse ring model as mentioned in Section 3.2.

2) Differently from Section 2.2, the mode selection procedure comes before the resource allocation, because now a resource must be allocated to the $D2D_{Re}$ that is going to transmit, which is only decided after the mode selection.

3) In the following, the resource allocation for network-assisted MH D2D communications is composed of two parts: cellular scheduling and D2D grouping. After the mode selection,

cellular scheduling is performed. Actually, the cellular scheduling is not considered a RRM technique in this chapter, because the fast fading is not considered, so that just a random allocation of the PRB is enough. The grouping of D2D pairs takes into account the cellular scheduling decisions in order to establish D2D communications and manage the intra-cell interference in the same resource. Moreover, it is necessary to include the new constraint due to MH path, such that a $D2D_{Tx}$ and $D2D_{Re}$ do not share a resource.

3.3 Mode Selection Algorithms

In mixed cellular and D2D systems, the mode selection is an important procedure that must be done to avoid cases where D2D communications should not be used. Usually, the mode selection must decide whether a D2D candidate should transmit in cellular or D2D modes. However, in my work there is an even more difficult task, because I permit the usage of a relay to help the communication.

For both communication scenarios I define the Harmonic Mode Selection (HMS), which is based on an equivalent channel from $D2D_{Tx}$ to its receiver (either $D2D_{Rx}$ or $D2D_{Re}$). In the proximity communication, I use the notion of the equivalent channel from $D2D_{Tx}$ to $D2D_{Rx}$ through $D2D_{Re}$, which is based on the harmonic mean of the channel coefficients from $D2D_{Tx}$ to $D2D_{Re}$ (G_{Tx-Re}) and from $D2D_{Re}$ to $D2D_{Rx}$ (G_{Re-Rx}):

$$\frac{1}{G_{eq}} = \frac{1}{G_{Tx-Re}} + \frac{1}{G_{Re-Rx}}. \tag{3.2}$$

The intuition on defining the equivalent channel according to (3.2) is that the equivalent channel gain tends to be high only when both involved channels have high gain (initially considered for subcarrier matching [67]) and therefore it is an appropriate single measure for mode selection purposes. A pseudo code of HMS is given in Algorithm 3.1, where the channel gains from the $D2D_{Tx}$ to the eNB (G_{Tx-eNB}) and to the $D2D_{Rx}$ (G_{Tx-Rx}) are also necessary. In addition to the HMS, I consider a single-hop Mode Selection (MS) algorithm termed D2D Mode Selection (D2DM), which will select D2D communications if the direct gain between $D2D_{Tx}$-$D2D_{Rx}$ (G_{Tx-Rx}) is greater than the gain of $D2D_{Tx}$-eNB (G_{Tx-eNB}).

Algorithm 3.1 Harmonic Mode Selection (HMS) for Proximity Communication

1: **if** $G_{eq} \geq \max\{G_{Tx-Rx}, G_{Tx-eNB}\}$ **then**
2: Choose D2D two-hop communications
3: **else if** $G_{Tx-Rx} \geq G_{Tx-eNB}$ **then**
4: Choose D2D single-hop communications
5: **else**
6: Choose cellular mode, that is $D2D_{Tx}$ and $D2D_{Rx}$ communication through the eNB.
7: **end if**

Recall from Section 3.2.1 that in the range extension scenario, there are only two possible communication modes (direct or relay-assisted) between the $D2D_{Tx}$ device and the eNB. Therefore, in this scenario, I modify the definition of the equivalent channel such that it includes the path gain between the relay device and the eNB (G_{Re-eNB}):

$$\frac{1}{G_{eq}} = \frac{1}{G_{Tx-Re}} + \frac{1}{G_{Re-eNB}},$$

and use a modified version of the HMS algorithm (Algorithm 3.2).

Algorithm 3.2 Harmonic Mode Selection (HMS) for Range Extension

1: **if** $G_{eq} \geq G_{Tx-eNB}$ **then**
2: Choose D2D relay assisted communication
3: **else**
4: Choose cellular mode that is $D2D_{Tx}$ transmits directly to the eNB.
5: **end if**

3.4 Two-Hop D2D Grouping Algorithms

Relevant problems in the context of D2D communications in cellular systems are how to allocate the unused resources and how to select which cellular and D2D links should share a resource. They are called *resource allocation*, which is comprised of a scheduling of the cellular UE and *grouping* of the D2D UE, respectively.

In a MH D2D communications, the resource usage may be high, since another resource for each $D2D_{Re}$ must be assigned. In this new scenario, new constraints to guarantee a realistic resource usage and to minimize the intra-cell interference must be assured, such as:

- Cellular or D2D UEs in cellular mode must use orthogonal resources, that is, cellular transmissions maintain intra-cell orthogonality;
- $D2D_{Tx}$ and $D2D_{Re}$ must use orthogonal resources, because the mode selection and resource allocation algorithms must take into account that a relaying device cannot receive and transmit data on the same frequency resource at the same time.

For the unused resources, I use a random strategy, in which they are allocated randomly first for the cellular UEs and then for the D2Ds. This approach is used since I disregard the fast fading, therefore the channel gains are the same in all resources. For the grouping, i.e., the assignment of the already used resources, I consider three different strategies proposed by Pradini [68] and extended to multi-hop cases: Balanced Random Allocation (BRA), Cellular Protection Algorithm (CPA) and MinInterf.

3.4.1 Balanced Random Allocation - BRA

BRA is as an improvement of the random grouping. It introduces a new variable ρ_q, which indicates the number of times resource q has been assigned. Using ρ_q, BRA allocates first the unused resources randomly and once all the resources have been used at least one time, it will allocate randomly the most unused ones.

The main idea of BRA is to balance the resource usage, trying to equally reuse all of the available ones. With this, the interference will be spread among all the resources available, instead of concentrating in a few resources. A pseudo-code of the algorithm is given in Algorithm 3.3.

3.4.2 Cellular Protection Allocation - CPA

CPA is a protection mechanism to cellular communication. It takes into account ρ_q and the large-scale fading of the users (either cellular or D2D) using that to allocate first the unused resources randomly. Once all the resources have been used at least once, it will allocate the most unused ones for which the channel coefficients between the transmitter already using that resource to the eNB are the highest.

The strategy of CPA is to take advantage of strong links (either cellular or D2D) using the resources and reuse them while keeping the weak users with a low resource reuse. Hence the term cellular protection, because most of the protected UEs are using cellular communication. A pseudo-code of the algorithm is given in Algorithm 3.4.

Algorithm 3.3 Balanced Random Allocation (BRA)

for each cellular UE **do**
  Allocate orthogonal resource-q to cellular UEs
  Set $\rho_q = 1$ for the assigned resources
end for
$\rho_{min} \leftarrow \min_{q=1,\cdots,N_{\text{PRB}}} \rho_q$
for each D2D_{Tx} and D2D_{Re} **do**
  if $\rho_{min} == 0$ **then**
    if D2D_{Tx} **or** (D2D_{Re} **and** two-hop) **then**
      Allocate the resource-q for which $\rho_q == \rho_{min}$
    end if
  else
    if D2D_{Tx} **or** (D2D_{Re} **and** two-hop) **then**
      Allocate randomly the resource-q for which $\rho_q == \rho_{min}$
    end if
  end if
  $\rho_q \leftarrow \rho_q + 1$
  Update $\rho_{min} \leftarrow \min_{q=1,\cdots,N_{\text{PRB}}} \rho_q$
end for

Algorithm 3.4 Cellular Protection Algorithm (CPA)

for each cellular UE **do**
  Allocate orthogonal resource-q to cellular UEs
  Set $\rho_q = 1$ for the assigned resource
  Store the channel coefficients to the eNB in g_q
end for
$\rho_{min} \leftarrow \min_{q=1,\cdots,N_{\text{PRB}}} \rho_q$
for each D2D_{Tx} and D2D_{Re} **do**
  if $\rho_{min} == 0$ **then**
    if D2D_{Tx} **or** (D2D_{Re} **and** two-hop) **then**
      Allocate the resource-q for which $\rho_q == \rho_{min}$
    end if
  else
    if D2D_{Tx} **or** (D2D_{Re} **and** two-hop) **then**
      Allocate randomly the resource-q for which $\rho_q == \rho_{min}$ and $q = \arg\max_q g(q)$
      Update the channel coefficients to the eNB of the chosen user i: $g_q \leftarrow g_q + g_i$
    end if
  end if
  $\rho_q \leftarrow \rho_q + 1$
  Update $\rho_{min} \leftarrow \min_{q=1,\cdots,N_{\text{PRB}}} \rho_q$
end for

3.4.3 Minimum Interference Allocation

MinInterf tries to allocate the D2D UEs that might cause and suffer less interference, hence the term MinInterf, which comes from Minimum Interference. With full channel knowledge, i.e., the algorithm assumes that all the channel coefficients for cellular and D2D UEs are known, it assigns the resource $\tilde{q}$ for which the interference generated and received by the possible transmitters and receivers is the lowest. Therefore, MinInterf also avoids the UEs' concentration in the resources.

The interference generated by the transmitter (either cellular UE, D2D_{Tx} or D2D_{Re}) using resource-q is estimated as the sum of the channel coefficients between the transmitter and the R receivers, named G_r, that are sharing it:

$$G_{\text{interf.gen},q} = \sum_{r}^{R} G_r. \tag{3.3}$$

The interference perceived by the receiver related to the previous transmitter using resource-q is also estimated as the sum of the path gains between the receiver and the T transmitters, named G_t, that are sharing it:

$$G_{\text{interf.rec},q} = \sum_{t}^{T} G_t. \tag{3.4}$$

Therefore, MinIntef will assign the resource-$\tilde{q}$ for which the sum of these two interference terms, termed $S(q)$, is the lowest, i.e.,

$$S(q) = G_{\text{interf.gen},q} + G_{\text{interf.rec},q} \tag{3.5}$$

$$\tilde{q} = \arg\min_q S(q) \tag{3.6}$$

A pseudo-code of the algorithm is given in Algorithm 3.5.

Algorithm 3.5 Minimum Interference Allocation

for each cellular UE **do**
  Allocate orthogonal resource-q to cellular UEs
  Set $\rho_q = 1$ for the assigned resource
end for
$\rho_{min} \leftarrow \min_{q=1,\cdots,N_{\text{PRB}}} \rho_q$
for each D2D_{Tx} and D2D_{Re} **do**
  if $\rho_{min} == 0$ **then**
    if D2D_{Tx} **or** (D2D_{Re} **and** two-hop) **then**
      Allocate the resource-q for which $\rho_q == \rho_{min}$
    end if
  else
    if D2D_{Tx} **or** (D2D_{Re} **and** two-hop) **then**
      for each available resource q **do**
        $S(q) \leftarrow G_{\text{interf.gen,q}} + G_{\text{interf.rec,q}}$
      end for
      Allocate the resource-$\tilde{q}$ for which $\tilde{q} = \arg\min_q S(q)$
    end if
  end if
  $\rho_{\tilde{q}} \leftarrow \rho_{\tilde{q}} + 1$
  Update $\rho_{min} \leftarrow \min_{q=1,\cdots,N_{\text{PRB}}} \rho_q$
end for

3.5 Numerical Results and Discussions

To evaluate and compare the performance of the proposed two-hop D2D mode selection and grouping algorithms, I performed *system-level simulations* considering an LTE-like cellular system, whose main parameters are summarized in Table 3.2 and are aligned with the 3GPP LTE architecture [56, 57, 66].

To collect statistics on the measured SINR and transmit power levels, I perform Monte Carlo simulations, such that in each Monte Carlo experiment in the Resource Allocation (RA) analysis I randomly drop two different numbers of users:

i. Normal load: 7 D2D triplets and 11 cellular UEs in the proximity communication and 12 D2D pairs in the range extension, which guarantees intra-cell orthogonality;

ii. Interference load: 25 D2D triplets and 25 cellular UEs in the proximity communication and 25 D2D pairs in the range extension, which guarantees intra-cell reuse.

Recall that in the proximity communication scenario a D2D_{Tx} transmits to a D2D_{Rx} node (possibly via a D2D_{Re}), while in the range extension scenario, a D2D_{Tx} node transmits to its

Table 3.2: Simulation parameters

Parameter	**Value**
Number of eNBs (N_{CELL})	7 (with wrap-around)
Communication link	Uplink (UL)
Minimum distance eNB-UE	50 m (Prox. Comm.)/400 m (Range Ext.)
Minimum distance UE-UE	10 m
Mean distance D2D_{Tx}-D2D_{Rx}	100 m
Central carrier frequency	2 GHz
System bandwidth	5 MHz
Number of PRBs (N_{PRB})	25 PRBs [57]
Noise power	-116.4 dBm
Channel model	Table 3.1 [66]
CSI knowledge	Ideal channel information
Relaying protocol	Decode and Forward (DF)
Power allocation among PRBs	Equal Power Allocation (EPA)
Traffic model	Full buffer [56]
Antenna configuration	1×1
Number of Monte Carlo realizations	100

serving eNB (possibly via a D2D_{Re}). In the range extension scenario, the D2D_{Rx} node does not exist, as well as cellular UEs.

A random assignment policy is applied to assign resources to the cellular UEs. The D2D communication uses uplink RBs in both proximity communication and range extension scenarios. The average spectral efficiency and the power consumption are the metrics chosen to compare the performance between the different modes and grouping algorithms. The relaying protocol considered is DF, on which the relay only decodes the message and forward it to the receiver.

To gain insights into the performance impacts of mode selection algorithms, I evaluate the MS alternatives listed in Table 3.3. For the proximity communication, the HMS will be compared with the forced cellular mode (termed Cmode) and a simple mode selection, the D2DM, which considers only the single-hop and the cellular mode. However, for the range extension, the HMS will be compared with the forced cellular mode (termed Cmode) only, because the D2DM is not present.

Table 3.3: Mode selection algorithms

Name	**Proximity Communications Scenario**	**Range Extension Scenario**
Cellular mode (**Cmode**)	Forced cellular mode (no D2D communications)	Forced cellular mode (no D2D communications)
D2D mode (**D2DM**)	Mode selection between single-hop D2D mode and cellular mode	Not present
Adaptive mode selection with the HMS algorithms (**HMS**)	Mode selection by Algorithm 3.1	Mode selection by Algorithm 3.2

The simulation results are presented in terms of the performance achieved by users employing cellular communications and users employing D2D communication (either single or two-hop), which are measured in terms of the system spectral efficiency[1] [bps/Hz/cell] and power consumption [W].

In addition, all the two-hop D2D grouping algorithms presented in Section 3.4 are compared using the HMS. Spectral efficiency values are presented for the cellular (in the

[1]The system spectral efficiency measures the number of bits received per frequency unit and per cell.

proximity communication scenario) and D2D UEs separately, as to illustrate the impact of each algorithm on the performance of each type of UEs. The results related to power consumption are shown in bar charts, where the y axis is adjusted in each figure as to better shown the differences among the algorithms which have their names shown in the x axis.

3.5.1 Performance Analysis for Mode Selection

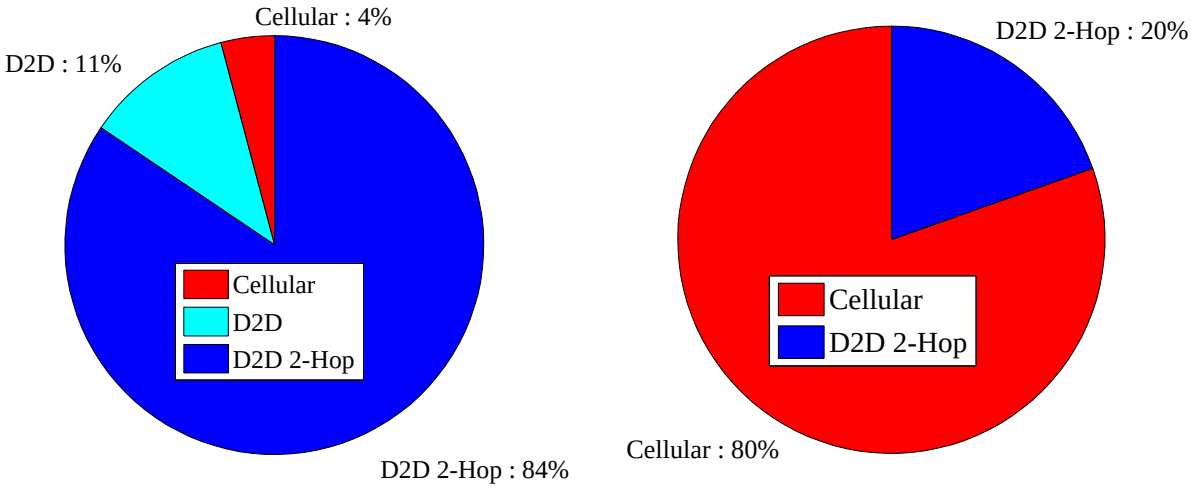

(a) *Harmonic Mode Selection* (HMS) for proximity communication - Algorithm 3.1

(b) *Harmonic Mode Selection* (HMS) for range extension - Algorithm 3.2

Figure 3.4: Percentage of D2D candidates using different communication modes and at different scenarios, which illustrates that the ellipse ring is indeed D2D and two-hop friendly for both scenarios.

Now in Figure 3.4, the percentage of D2D candidates that are using D2D communication is presented for the mode selection algorithms in both scenarios, the HMS presented at Algorithm 3.1 and Algorithm 3.2. Notice in Figure 3.4(a) that the ellipse ring dropping proposed in Section 3.2 is indeed two-hop friendly, because at least $84\,\%$ of the D2D candidates are using two-hop communications. However, in Figure 3.4(b) only $20\,\%$ of the UEs are using the relay in the range extension, which shows that even with a mean distance to the eNB of $400\,\mathrm{m}$, a low percentage of the UEs will use two-hop communication.

In Figure 3.5 the Cumulative Distribution Function (CDF) of the SINR for both cellular UEs (red) and for the D2D candidates (black and dashed line) is presented when employing the mode selection schemes of Table 3.3 in the proximity communication scenario. For the cellular UEs (termed '-Cell'), the HMS presents a loss of approximately $2\,\mathrm{dB}$ over Cmode and D2DM at the 50^{th} percentile, which have the same SINR. The HMS has this loss because the interference for the cellular UEs increases due to the usage of the second hop by the $\mathrm{D2D_{Re}}$. In addition, the D2DM has the same SINR of the Cmode because from the perspective of the cellular UE, regardless of the communication, there will be one interferer with the same transmitting power, which suggests that if a power control were applied, this behavior would not happen.

Regarding the D2D candidates (termed '-D2D'), either single or two-hop, there is a gain of at least $23\,\mathrm{dB}$ over Cmode at the the 50^{th} percentile, where the gap between D2DM and HMS is approximately $3\,\mathrm{dB}$. The intuitive explanation of this is that D2D communication takes advantage of the proximity gain and thus increases the SINR. At the same time, D2D UEs benefit from an improved link budget due to the proximity of the two-hop path, which explains the additional gain of HMS over D2DM ($\approx 3\,\mathrm{dB}$).

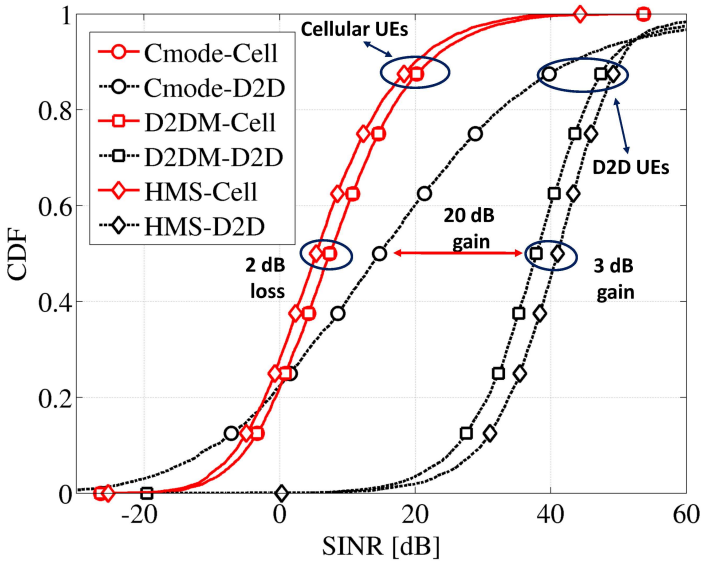

Figure 3.5: Proximity communication scenario: CDF of the SINR for both cellular UEs and for the D2D candidates. HMS is superior for the D2D candidates and considering all the modes. The cellular UEs do not benefit from two-hop D2D communications, which is explained by the power allocation (EPA) used. For the D2D candidates, the mode selection gain is much more pronounced ($\approx 25\,\mathrm{dB}$) with the HMS.

In Figures 3.6 comprises the bar chart of the average spectral efficiency and system power consumption. In Figure 3.6(a), notice that using D2D communications the relative spectral efficiency gain is at least $54\,\%$ compared to Cmode, and the D2DM and HMS present almost the same spectral efficiency. When looking at Figure 3.6(b), the Cmode is the one that uses more power, because I consider the power consumption of the DL transmission from the eNB to the $\mathrm{D2D_{Rx}}$. In addition, the HMS presents the lowest power consumption, with a relative power efficiency of $51\,\%$ over the D2DM. This behavior is due the fact that in HMS there will be less cellular communications, which demand power for both UL and DL (higher power than the UL).

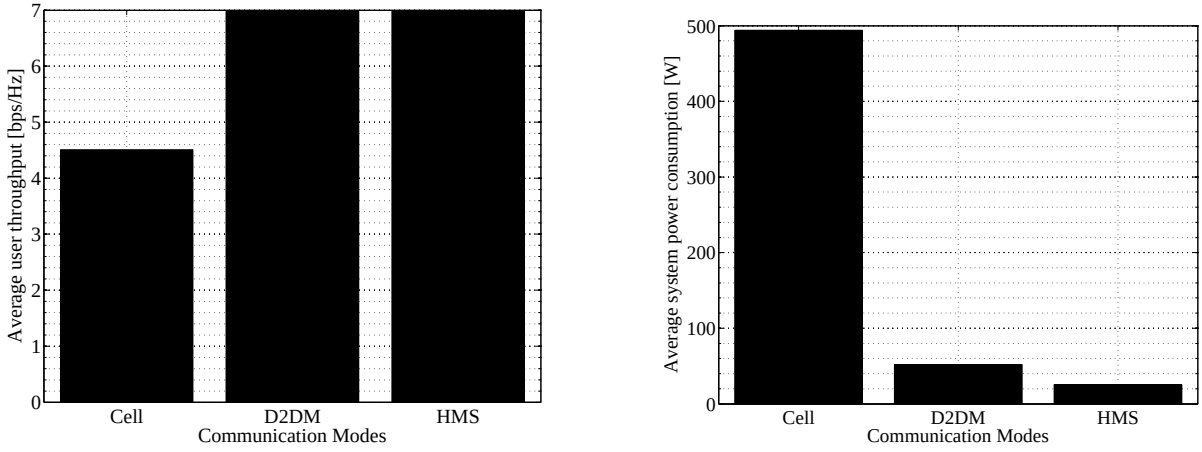

(a) Average spectral efficiency

(b) Average system power consumption

Figure 3.6: Proximity communication scenario: Bar chart of the average spectral efficiency and system power consumption when considering different communication modes. We notice that Cmode results in lower spectral efficiency values with a higher power consumption than all the other modes. In addition, HMS reaches almost the same value of spectral efficiency as single hop D2D mode with a lower power consumption, which suggests that in addition to the SINR gains, two-hop communications outperform the single-hop D2D mode in terms of energy efficiency.

Therefore, in the proximity communication scenario, Cmode results in lower SINR values

with a higher power consumption than all the other modes. Moreover, HMS reaches higher SINR values than single-hop D2D mode with a lower power consumption, which suggests that in addition to the SINR gains, two-hop communications outperform single-hop D2D mode in terms of energy efficiency.

Regarding the range extension scenario, Figure 3.7 shows the CDF of the SINR for those UEs that had SINR below $0\,\mathrm{dB}$ in the Cmode, which are usually at the cell-edge. As it can be seen, all the UEs have substantial gains when using HMS instead of Cmode, where at the 50^{th} percentile the gain is of approximately $7.5\,\mathrm{dB}$ and can reach $20\,\mathrm{dB}$.

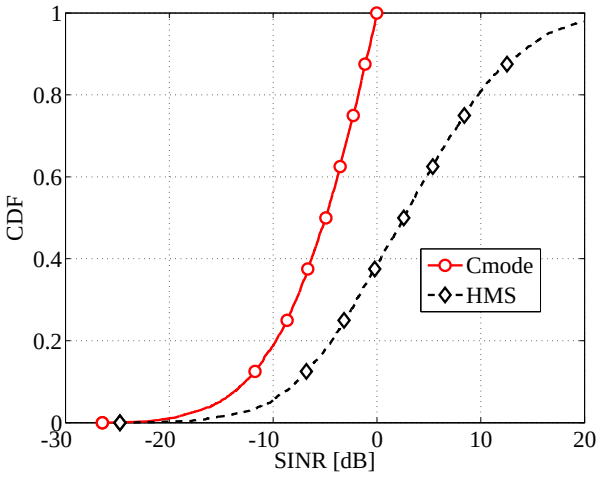

Figure 3.7: Range extension scenario: CDF of the SINR for those UEs that had SINR below than 0 in the Cmode, which are commonly the *cell-edge* users. Notice that the gain between the two communication modes is substantial and can reach $20\,\mathrm{dB}$.

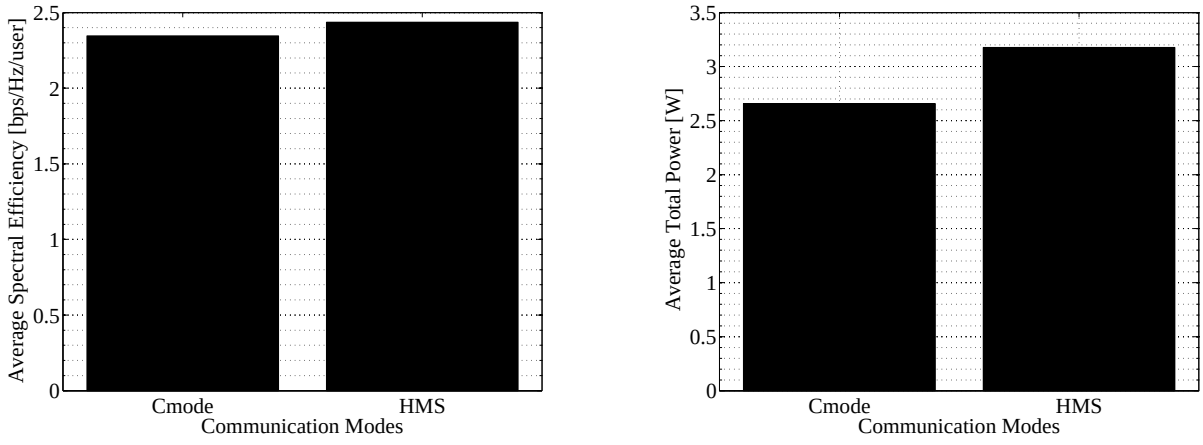

(a) Average spectral efficiency

(b) Average system power consumption

Figure 3.8: Range extension scenario: Bar chart of the average spectral efficiency and system power consumption when considering different communication modes. HMS presents a slightly higher average spectral efficiency (approximately $4\,\%$), but at the expense of a higher power consumption (approximately $19\,\%$).

Figure 3.8 presents the bar chart for the average spectral efficiency and system power consumption for the range extension scenario. Notice that in Figure 3.8(a), the relative gain of HMS over Cmode in spectral efficiency is marginal, approximately $4\,\%$. However, this small gain comes at the expense of a higher power consumption, presented in Figure 3.8(b), which is approximately $19\,\%$. Although this overuse of the power was not expected, this is explained by the EPA used, which forces even nearby links to use the same power, instead of a lower one. If a proper power control were used, this behavior might not happen.[2]

[2]Power control techniques for two-hop D2D communications are addressed on the next chapter.

3.5.2 Performance Analysis for Resource Allocation

At this section, the total average rate of the grouping algorithms for two-hop D2D communications is analyzed for both communication scenarios (proximity communication and range extension) as well as for two different loads (normal and interference).

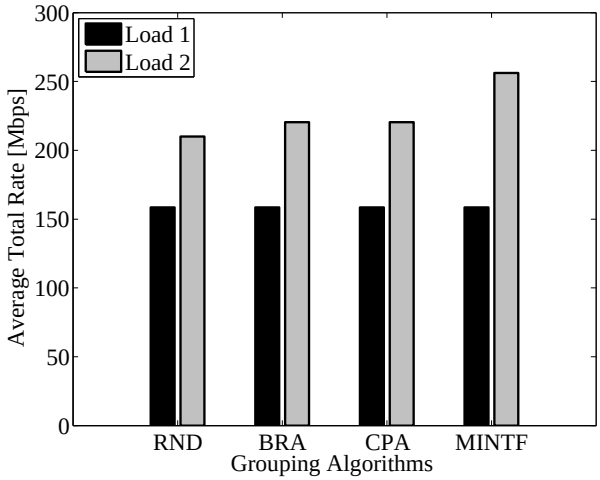

Figure 3.9: Proximity communication scenario: The algorithms have the same rate for the normal load, which is expected. As for the interference load, MinInterf is the best grouping algorithm, providing a gain of $46\,\mathrm{Mbps}$ over RND, which is the worst one.

In Figure 3.9 the total average rate for the grouping algorithms at Section 3.4 is presented for the proximity communication scenario. For the normal load all the algorithms have the same rate, which is expected since there is no intra-cell interference, thus all the groups are equal. In the interference load the RND is the worst one, whereas BRA and CPA have almost the same rate. MinInterf is the best grouping algorithm, with a gain of $46\,\mathrm{Mbps}$ (approximately $22\,\%$) over RND.

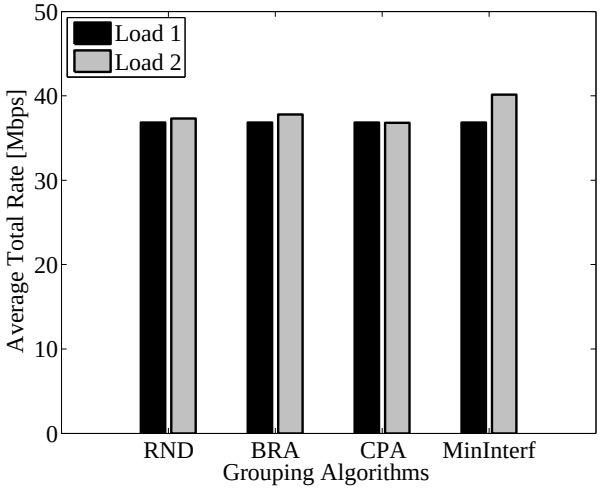

Figure 3.10: Range extension scenario: As expected, the algorithms present the same rate for the normal load. For the interference load, MinInterf has the best performance, with a gain of $3\,\mathrm{Mbps}$ over CPA, which is the worst one.

For the range extension, Figure 3.10 presents the average total rate for the two loads and four grouping algorithms shown previously. As expected, for normal load the algorithms have the same rate. However, CPA has the worst performance for the interference load, which shows that by protecting the cellular communication the overall rate decreases. MinInterf shows again the best performance among the algorithms, with a gain of $3\,\mathrm{Mbps}$ (approximately $9\,\%$) over CPA.

3.6 Conclusions

In this chapter, I concentrated on the mode selection and resource allocation problems for two-hop D2D communications within an LTE-like cellular network and two ProSe scenarios proposed by 3GPP. More specifically, I formulated and analyzed methods to first select whether a D2D UE would transmit to its receiver through an eNB, directly to the receiver or using a relay and then allocate the resource that might decrease the intra-cell interference, thus improving the overall spectral efficiency of the system. Moreover, from the simulation perspective I proposed the ellipse ring dropping to act as a two-hop friendly scenario for $D2D_{Tx}$, $D2D_{Re}$ and $D2D_{Rx}$.

The proposed adaptive *Harmonic Mode Selection* (HMS) scheme can improve the throughput and the energy efficiency of a system that does not support D2D communications or employs traditional mode selection schemes. HMS can also decrease the outage probability and improve the average throughput using fixed transmit power levels for all the users in the relay extension scenario.

Moreover, the proposed grouping algorithms for two-hop communications have also shown gains over an RND algorithm. MinInterf has the highest gains for both communication scenarios, but it needs full channel knowledge, which might not always be available. Thus, BRA might be a good choice when some channel coefficients are unknown.

Therefore, two-hop D2D communications have gains over single-hop D2D when using a proper mode selection strategy and can be even increased if a grouping algorithm is used.

Chapter 4

Power Control for Two-Hop Device-to-Device Communications

4.1 Introduction

Power Control (PC) is a well-known Radio Resource Management (RRM) strategy for interference management in multi-user communication systems, where the performance of a User Equipment (UE) depends on its own transmit power as well as on the transmit powers of interfering UEs. Power control usually improves system performance by adjusting transmit powers of the co-channel UEs so that each of them attains its target Quality of Service (QoS), often expressed as a Signal to Interference-plus-Noise Ratio (SINR) value. In this way, links with in-excess QoS will have their transmit powers lowered, thus reducing (battery) power consumption as well as interference levels in the system [20, 21, 69].

In particular, power control algorithms originally designed for multi-cell systems can be adapted to scenarios with Device-to-Device (D2D) communications by looking at D2D transmitters as the transmitters of interfering cells. Because D2D communications in a Long Term Evolution (LTE)-like system can be seen as an underlay, some works focused on limiting the impact of these communications on the cellular ones.

As it was explained in Chapter 3, integrating Multi-Hop (MH) D2D communications can also help to meet the evolving requirements of next generation wireless networks [2]. Apart from mode selection and resource allocation techniques analyzed in the previous chapter, power control is another key technique to deal with inter- and intra-cell interference. With more D2D UEs in the cell due to MH transmissions, a proper power control is necessary to keep the interference low and further increase the gains brought by the integration between D2D communications and MH relaying.

4.1.1 Related Work

In Yu et al [28], the SINR distribution of D2D and cellular users is determined and a simple power control algorithm that limits the impact of D2D communications on the cellular users is investigated, while in Yu et al [29] two power control algorithms are analyzed: a power optimization with greedy sum-rate maximization and a power optimization with rate constraints. Similarly, different power control schemes for D2D UEs communicating in the uplink of an LTE system have been studied by Xing et al [30]. In these works the authors reached the same conclusions: power control can improve the whole system performance in comparison with a pure cellular system and, with proper resource allocation and mode

selection algorithms, also minimize the generated interference.

Belleschi et al. [70] extended the power control algorithm proposed by Papandriopoulos et al. [69], making it distributed and separating the operation in the PHY/MAC and transport layer while maintaining optimality. This power control scheme was then considered in an environment with cellular and D2D UEs by Fodor et al. [71], which have shown that the optimal scheme provides gains in terms of the SINR distribution and total power consumption.

Joint optimization has also been studied by some authors, which mainly include joint power control, resource allocation and mode selection problems. In Belleschi et al. [31] the authors studied a joint mode selection, resource allocation and power control problem, which aimed to minimize the total transmitting power. The scenario was composed of two circular cells, one D2D-capable pair and two cellular UEs. The authors developed a suboptimal algorithm considering mode selection and resource allocation, because the joint problem was Non-Polynomial Time (NP)-hard and, therefore, the optimum solution might not be useful in practice. Results showed that when the D2D communications could reuse the cellular spectrum resources, the overall capacity was increased, mainly when the joint mode selection and power control were used.

In Jung et al. [32] the authors also studied the joint mode selection and power allocation problem, but aiming at a sum power minimization and capacity maximization. The scenario was composed of one circular cell, one D2D-capable pair and one cellular UE. In order to jointly consider those goals, it was proposed an utility function as power efficiency measure, which was defined as the overall system capacity divided by the total consumed power. The authors also derived an upper and lower bounds to the utility function. Based on the utility function and the bounds, an algorithm was proposed which performs an exhaustive search in the set of all possible mode sequences and chooses the best one. From the results, the proposed algorithm performed close to the delivered upper bound, but had the disadvantage of demanding a huge computational effort.

In the MH ad-hoc relaying networks, power control has also been studied. Choi et al. [72] consider multi-hop in ad-hoc networks, where the algorithm performs power control using iterations [20] and updates the rate using the average rate of nearby (and known or sharing) nodes.

4.1.2 Contributions

Extending the power control algorithms proposed for single-hop network-assisted D2D communications to MH D2D communication is non-trivial, because the available D2D PC algorithms must be made capable of taking into account the rate constraints of MH paths, called the *solidarity property* [72], which specifies that the end-to-end throughput of the MH path is limited by the weakest link of the route. Specifically, it must be taken into account that along the multiple links of a given path, only a single rate can be sustained without requiring large buffers or facing buffer underflow situations at intermediate nodes.

In this chapter I analyze heuristic mode selection strategies from Chapter 3 that are applicable in cellular networks integrating MH D2D communications and extend an utility optimal distributed PC scheme that takes into account both the achievable rates along MH paths and the overall energy consumption.

The PC scheme can now operate in concert with both the PC schemes and the mode selection and resource allocation algorithms available in cellular networks. Therefore, it is necessary to take into account that a relaying device cannot receive and transmit data on the same frequency resource at the same time, which means that I also extended the algorithm

to a multi-resource environment.

I adopt a three-step approach: firstly, I apply the proposed Harmonic Mode Selection (HMS) algorithm to determine if the D2D UEs will transmit through the Evolved Node B (eNB)– in cellular mode – or directly to their receivers – in D2D mode – or through D2D relay, in two-hop D2D mode. Secondly, I select one or more D2D nodes to share the resources with conventional cellular UEs. Lastly, I apply the power control over all the users in the system, which needs to take into account the resource constraints along the MH path.

Therefore, the main contribution here is the MH power control scheme that is analyzed by means of a realistic system simulator when performing practically feasible mode selection and resource allocation.

The remaining sections are organized as follows. In Section 4.2 the system modeling is presented, where the main simulation parameters are quite similar to the ones used in Chapter 3; in Section 4.3 I show the utility optimal distributed PC scheme with its optimality; in Section 4.4 I present the LTE PC schemes that will be used to compare the proposed PC scheme; Section 4.5 presents numerical results for two different MH D2D communication scenarios comparing first the impact on the mode selection of the proposed scheme and then the comparison between all the PC algorithms; and the chapter ends with conclusions and some perspectives, in Section 4.6.

4.2 System Modeling

The system model for the system level simulations is equal to the one presented in Section 3.2, but here I will present two additional parts with important concepts to help the reader throughout the chapter. First, the *routing matrix* describes the network topology and associates links with resources. Secondly, the *utility function* associated with a Source-Destination (S-D) pair characterizes the utility of supporting some communication rate between the end nodes of the pair.

4.2.1 Network Topology

I model the integrated cellular-D2D network as a set of L transmitter-receiver (Tx-Rx) pairs. A Tx-Rx pair can be a cellular UE transmitting to its serving eNB, a D2D_{Tx} node transmitting to a D2D_{Rx} node in single-hop D2D mode, a D2D_{Tx} node transmitting to a D2D_{Re} node or a D2D_{Re} node transmitting to a D2D_{Rx} node. A *link* refers to a single-hop transmission between a Tx-Rx pair, while a *route* is a concatenation of one or more links between an S-D pair. For example, a two-hop route consists of two Tx-Rx pairs, in which case the middle node must be a D2D-capable relay node (Figure 4.1). The links and routes are labeled as $l = 1, \ldots, L$ and $i = 1, \ldots, I$ respectively.

Next, I define the 3-dimensional *routing matrix* that associates links with routes and resources and thereby describes both the network topology in terms of links and routes and the resources assigned to links. The routing matrix is defined as $\mathbf{R} = [r_{liq}] \in \{0,1\}^{L \times I \times N_{\text{PRB}}}$, where the entry r_{liq} is 1 if data between the S-D pair i is routed across link l and resource q, and zero otherwise. With this definition, the routing matrix can be seen as a set of N_{PRB} single-resource matrices, $\mathbf{R}_q \in \{0,1\}^{L \times I}$, such that the r_{li} element of $\mathbf{R}_q$ indicates whether link l is part of route i on resource q. For the example of Figure 4.1, the $N_{\text{PRB}} = 3$ routing matrices

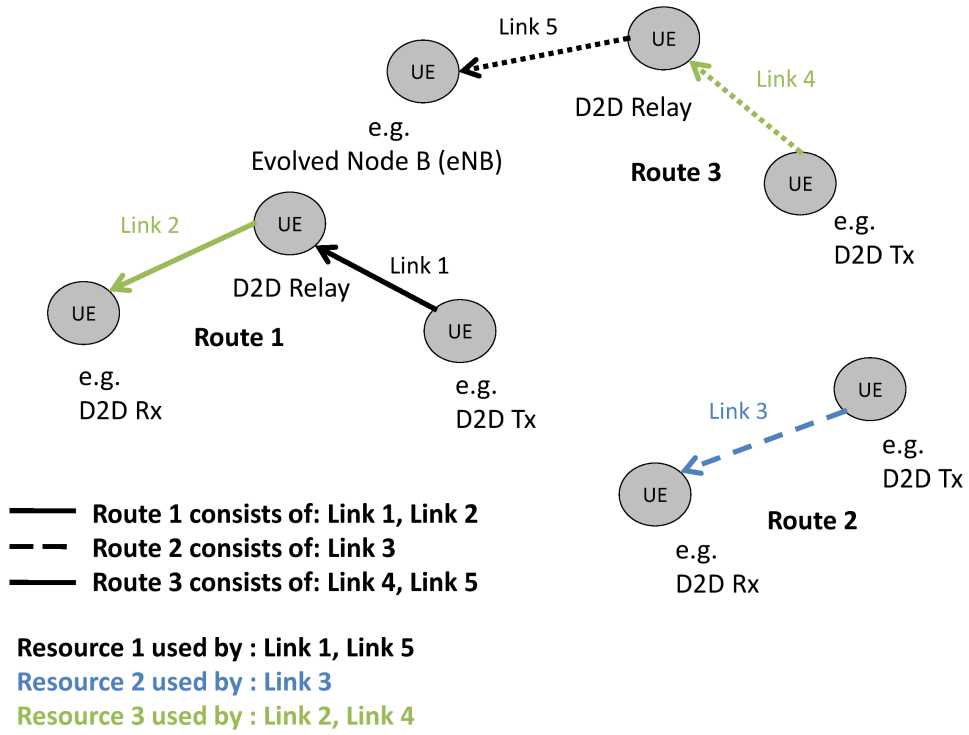

Figure 4.1: An example of a network with 3 routes, where Route 1 and Route 3 are two-hop routes, and Route 2 consists of a single-hop route. In the specific case of Figure 3.1, Route 1, 2 and 3 can model the two-hop D2D route for proximity communication, the two-hop D2D route for coverage extension and the single-hop D2D link. Note that the resources allocated to the incoming and outgoing links of a relay node must be orthogonal, as indicated in this Figure. A node can represent a User Equipment (UE) or an Evolved Node B (eNB).

are the following:

$$\mathbf{R}_1 = \begin{pmatrix} 1 & 0 & 0 \\ 0 & 0 & 0 \\ 0 & 0 & 0 \\ 0 & 0 & 0 \\ 0 & 0 & 1 \end{pmatrix}, \mathbf{R}_2 = \begin{pmatrix} 0 & 0 & 0 \\ 0 & 0 & 0 \\ 0 & 1 & 0 \\ 0 & 0 & 0 \\ 0 & 0 & 0 \end{pmatrix}, \mathbf{R}_3 = \begin{pmatrix} 0 & 0 & 0 \\ 1 & 0 & 0 \\ 0 & 0 & 0 \\ 0 & 0 & 1 \\ 0 & 0 & 0 \end{pmatrix}$$

For example, $\mathbf{R}_1$ corresponds to resource $q = 1$ and describes that it is (re-)used by link $l = 1$ (first hop of route $i = 1$) and link $l = 5$ (second hop of route $i = 3$).

It is useful to define the 2-dimensional equivalent routing matrix, given by $\tilde{\mathbf{R}} = \sum_{q=1}^{N_{\text{PRB}}} \mathbf{R}_q$ and entries $\tilde{r}_{li}$. I assume the data to be routed along a single fixed link, i.e., I do not allow the data flow between a Tx-Rx pair to be spread between 2 or more resources.

To associate links with resources, I define the following two functions. Let $f : I \to \{1, 2\}$ denote the number of hops in the route i; $\mathbf{t} : I \times \{1, \ldots, f(i)\} \to L \times N_{\text{PRB}}$ denote the link and resource used in route i and hop h respectively. In addition, I denote by $t_1(i, h)$ and $t_2(i, h)$ the first and second outputs of $\mathbf{t}$, which represent the link and resource respectively. Table 4.1 gives an example of how these functions help to describe the relationship between routes, links and resource usage.

4.2.2 Assigning a Utility to an S-D Pair

I let s_i denote the end-to-end *rate* for communication between the S-D pair i, which is in correspondence with the SINR *targets* for hop h of route i denoted by $\gamma^{tgt}_{t_1(i,h)}$. In a multi-hop communication, the SINR targets of each link in a specific route must be the same, in line with the so-called *solidarity property* [72]. Thus, $\gamma^{tgt}_{t_1(i,h)}$ needs to be indexed with the single

Table 4.1: An example of how the network in Figure 4.1 can be described using the three functions defined above.

Function	Description	Example in the Network of Figure 4.1
$f(i)$	Number of hops in route i	$f(1) = f(3) = 2$
$\mathbf{t}(i,h)$	Link and resource indexes in route i and hop h	$\mathbf{t}(3,2) = (5,1)$
$t_1(i,h)$	Link index l in route i and hop h	$t_1(3,2) = 5$
$t_2(i,h)$	Resource index q in route i and hop h	$t_2(3,2) = 1$

index $t_1(i,h)$.

Associated with each S-D pair i is a function $u_i(.)$, which describes the utility of the S-D pair communicating at rate s_i. I assume that u_i is *increasing* and *strictly concave*, with $u_i \to -\infty$ as $s_i \to 0^+$. In this chapter I use $u_i(x) \triangleq \ln(x), \forall i$ [69].

The matrix of link capacities is denoted by $\mathbf{C} = [\mathbf{c}_1 \cdots \mathbf{c}_q] \in \mathbb{R}^{L \times N_{\text{PRB}}}$, which depends on the communication bandwidth W of one resource and the *achieved* actual SINR along route i and hop h, $\gamma_{\mathbf{t}(i,h)}$. Notice that the achieved SINR $\gamma_{\mathbf{t}(i,h)}$ is indexed by $\mathbf{t}(i,h)$, because the SINRs are generally different at different resources.

The vector of total traffic across the links of a route is given by $\tilde{\mathbf{R}}\mathbf{s}$ and the network flow imposes the following set of constraints on the source-destination rate vector $\mathbf{s}$:

$$\tilde{\mathbf{R}}\mathbf{s} \preceq \sum_{q=1}^{N_{\text{PRB}}} \mathbf{c}_q \qquad\qquad \mathbf{s} \succeq 0,$$

where $\succeq$ is a component-wise inequality. In this formulation, it is convenient to think of the $\mathbf{s}$ vector as the vector of rates while the $\mathbf{c}_q$ vectors represent the Shannon capacity that can be achieved by the particular power vector $\mathbf{p}_q = [P_{1q}, \ldots, P_{Lq}] \in \mathbb{R}^L$ on resource q. Therefore, the vector of rates along the links is constrained by the Shannon capacity that can be achieved by the link.

Let $G_{\mathbf{t}(i,h)}$ denote the desired link gain on route i and hop h, which includes both large- and small-scale fading gains. The thermal noise power is denoted by σ^2, and the transmission power on route i and hop h is $P_{\mathbf{t}(i,h)}$. The SINR on route i and hop h is given by

$$\gamma_{\mathbf{t}(i,h)}(\mathbf{P}) = \frac{G_{\mathbf{t}(i,h)} P_{\mathbf{t}(i,h)}}{\sigma^2 + (P^{tot}_{\mathbf{t}(i,h)} - G_{\mathbf{t}(i,h)} P_{\mathbf{t}(i,h)})}, \tag{4.1}$$

where $P^{tot}_{\mathbf{t}(i,h)}$ represents the total received power measured by the receiver on route i and hop h and $\mathbf{P} = [\mathbf{p}_1, \ldots, \mathbf{p}_{N_{\text{PRB}}}] \in \mathbb{R}^{L \times N_{\text{PRB}}}$ is the power allocation matrix.

Finally, it will be useful to view each link on route i and hop h as a single Gaussian channel with Shannon capacity

$$c_{\mathbf{t}(i,h)}(\mathbf{P}) = W_{t_2(i,h)} \log_2 \left(1 + \gamma_{\mathbf{t}(i,h)}(\mathbf{P})\right), \tag{4.2}$$

which represents the maximum rate that can be achieved on route i and hop h. Since I will consider that all the Resource Blocks (RBs) have the same bandwidth, $W_{t_2(i,h)}$ can be replaced by W.

4.3 Distributed Power Control Optimization

Assuming that the communication-mode has already been selected for the D2D candidates, and all (cellular and D2D) links have been assigned a frequency channel or a Physical Resource Block (PRB), I formulate the problem of target rate setting and power control as:

$$\begin{aligned} \underset{\mathbf{P},\mathbf{s}}{\text{maximize}} \;& \textstyle\sum_{i=1}^{I} u_i(s_i) - \omega \sum_{i=1}^{I} \sum_{h=1}^{f(i)} P_{\mathbf{t}(i,h)} \\ \text{subject to} \;& \tilde{\mathbf{R}}\mathbf{s} \preceq \textstyle\sum_{q=1}^{N_{\text{PRB}}} \mathbf{c}_q(\mathbf{P}), \quad \forall i,h, \\ & \mathbf{P},\mathbf{s} \succeq 0 \end{aligned} \tag{4.3}$$

which aims at maximizing the utility while taking into account the transmit powers (through a predefined weight $\omega \in (0,+\infty)$ [69]), so as to increase spectrum efficiency while reducing the sum power consumption.

Unfortunately, Problem (4.3) is not convex and to the best of my knowledge, it has not been addressed previously. However, exploiting the results presented in [69], I can transform it into the following equivalent form:

$$\begin{aligned} \underset{\tilde{\mathbf{s}},\tilde{\mathbf{P}}}{\text{maximize}} \;& \textstyle\sum_{i} u_i(e^{\tilde{s}_i}) - \omega \sum_{i=1}^{I} \sum_{h=1}^{f(i)} e^{\tilde{P}_{\mathbf{t}(i,h)}} \\ \text{subject to} \;& \log(\tilde{\mathbf{R}}\mathbf{e}^{\tilde{\mathbf{s}}}) \leq \log\left(\textstyle\sum_{q=1}^{N_{\text{PRB}}} \mathbf{c}_q(e^{\tilde{\mathbf{P}}})\right) \quad \forall i,h, \end{aligned} \tag{4.4}$$

where $s_i \leftarrow e^{\tilde{s}_i}$ and $P_{\mathbf{t}(i,h)} \leftarrow e^{\tilde{P}_{\mathbf{t}(i,h)}}$. The transformed Problem (4.4) can be proved to be convex (now in the $\tilde{s}_i$-s and $\tilde{P}_{\mathbf{t}(i,h)}$-s), since the utility functions $u_i(\cdot)$ are selected to be $(\log, x)$-concave over their domains [69].

Under the utility's condition, I can solve it to optimality by means of an iterative algorithm where the $\tilde{s}_i$ (equivalent to the SINR targets) are set by an **outer loop**. The transmit powers $\tilde{P}_{t(i,h)}$ that meet the particular SINR targets (set in each outer loop cycle) are in turn set by a Zander type iterative SINR target loop [20] following thus an **inner loop**. This separation of SINR targets setting and corresponding power levels are detailed in the following.

4.3.1 SINR Target Setting and Power Control Problem - Utility Maximization

I now reformulate Problem (4.4) as a problem in the user rate $\tilde{s}$ (*Problem I*), which due to convexification, can be solved for a given (assumed known) power allocation ($\tilde{\mathbf{P}}$). I define *Problem I* as:

$$\begin{aligned} \underset{\tilde{\mathbf{s}}}{\text{maximize}} \;& \nu(\tilde{\mathbf{s}}) \\ \text{subject to} \;& \tilde{\mathbf{s}} \in \tilde{\mathbf{S}}, \end{aligned} \tag{4.5}$$

where $\tilde{\mathbf{S}}$ represents the set of feasible rate vectors that, for a given power vector $\tilde{\mathbf{P}}$, fulfill the constraints of Problem (4.4):

$$\tilde{\mathbf{S}} = \left\{ \tilde{\mathbf{s}} | \log\left(\sum_{j=1}^{I} \tilde{r}_{t_1(i,h)j} e^{\tilde{s}_j}\right) \leq \log\left(\sum_{q=1}^{N_{\text{PRB}}} c_{\mathbf{t}(i,h)}(e^{\tilde{\mathbf{P}}})\right) \quad \forall i,h \right\},$$

Notice that $\sum_{q=1}^{N_{\text{PRB}}} \mathbf{c}_q(\mathbf{P})$ was modified by $\sum_{q=1}^{N_{\text{PRB}}} c_{\mathbf{t}(i,h)}(e^{\tilde{\mathbf{P}}})$, for it will be easier to show the proofs ahead.

Comparing (4.4) and (4.5), it follows that the objective function in (4.5) is defined as $\nu(\tilde{\mathbf{s}}) \triangleq \sum_{i=1}^{I} u_i(e^{s_i}) - \varphi(\tilde{\mathbf{P}})$, where $\varphi(\tilde{\mathbf{P}}) \triangleq \omega \sum_i \sum_h e^{\tilde{P}_{\mathbf{t}(i,h)}}$ represents the cost in terms of the total transmit power for achieving a given rate $\tilde{s}$. Accordingly, I denote with $\varphi^\star(\tilde{\mathbf{P}}) \triangleq \omega \sum_i \sum_h e^{\tilde{P}_{\mathbf{t}(i,h)}}$ the cost of achieving the optimum rates $\tilde{\mathbf{s}}^\star$ that solves the utility maximization Problem (4.5).

Therefore, *Problem II*, for a given $\tilde{\mathbf{s}}$ vector, can be formulated as

$$\begin{aligned} \underset{\tilde{\mathbf{P}}}{\text{minimize}} \quad & \omega \sum_{i=1}^{I} \sum_{h=1}^{f(i)} e^{\tilde{P}_{\mathbf{t}(i,h)}} \\ \text{subject to} \quad & \log\left(\sum_{j=1}^{I} \tilde{r}_{t_1(i,h)j} e^{\tilde{s}_j}\right) \leq \log\left(\sum_{q=1}^{N_{\text{PRB}}} W \log_2\left(1+\gamma_{\mathbf{t}(i,h)}(e^{\tilde{\mathbf{P}}})\right)\right) \forall i,h. \end{aligned} \tag{4.6}$$

4.3.2 Solving the Rate (SINR target) Setting Problem

I am now concerned with setting the SINR targets by solving Problem I (4.5). Provided that the objective function $\nu(\tilde{\mathbf{s}})$ in (4.5) is concave and differentiable, I can determine the optimal $\tilde{\mathbf{s}}^\star$ by means of *projected gradient iterations* [73], with a fixed predefined step ϵ:

$$\tilde{s}_i^{(k+1)} = \tilde{s}_i^{(k+1)} + \epsilon \nabla_i \nu(\tilde{\mathbf{s}}^{(\mathbf{k})}) \quad \forall i, \tag{4.7}$$

where

$$\begin{aligned} \nabla_i \nu(\tilde{\mathbf{s}}) &= \tfrac{\partial}{\partial \tilde{s}_i}\left[\textstyle\sum_{i=1}^{I} u_i(e^{\tilde{s}_i}) - \varphi^\star(\tilde{\mathbf{P}})\right] \\ &= u_i{}'(e^{\tilde{s}_i}) e^{\tilde{s}_i} - \frac{\partial}{\partial \tilde{s}_i}\left[\varphi^\star(\tilde{\mathbf{P}})\right]. \end{aligned} \tag{4.8}$$

In order to compute (4.8), I first need to find $\varphi^\star(\tilde{\mathbf{P}})$ by solving the primal problem, i.e., Problem II in (4.6). Since it is convex in $\tilde{\mathbf{P}}$, it can be conveniently solved by the so called *Lagrange Duality* as follows. Let $\boldsymbol{\lambda}$ be the Lagrange multipliers (the dual variables) for the constraint in (4.6) and form the Lagrangian function:

$$\mathcal{L}(\boldsymbol{\lambda}, \tilde{\mathbf{P}}) = \omega \sum_{i=1}^{I} \sum_{h=1}^{f(i)} e^{\tilde{P}_{\mathbf{t}(i,h)}} + \sum_{i=1}^{I} \sum_{h=1}^{f(i)} \lambda_{\mathbf{t}(i,h)} \left[\log\left(\sum_{j=1}^{I} \tilde{r}_{t_1(i,h)j} e^{\tilde{s}_j}\right) - \log\left(\sum_{q=1}^{N_{\text{PRB}}} c_{\mathbf{t}(i,h)}(e^{\tilde{\mathbf{P}}})\right)\right] \tag{4.9}$$

The Lagrangian dual of Problem II is given by:

$$\begin{aligned} \underset{\boldsymbol{\lambda}}{\text{maximize}} \quad & \left[\mathcal{L}(\boldsymbol{\lambda}) = \min_{\tilde{\mathbf{P}}} \quad \mathcal{L}(\boldsymbol{\lambda}, \tilde{\mathbf{P}})\right] \\ \text{subject to} \quad & \boldsymbol{\lambda} \succeq 0. \end{aligned} \tag{4.10}$$

Thus, I can now calculate the rate for both communication modes. For the routes with one-hop D2D communications, the rate s_i is updated according to:

$$s_i{}^{(k+1)} = s_i{}^{(k)} \exp\left(\epsilon\, s_i{}^{(k)} \left[u_i{}'(s_i{}^{(k)}) - \frac{\lambda^\star_{\mathbf{t}(i,1)}}{(s_i{}^{(k)})}\right]\right). \tag{4.11a}$$

As well as for the routes with two-hop D2D communications:

$$s_i{}^{(k+1)} = s_i{}^{(k)} \exp\left(\epsilon\, s_i{}^{(k)} \left[u_i{}'(s_i{}^{(k)}) - \frac{\lambda^\star_{\mathbf{t}(i,1)} + \lambda^\star_{\mathbf{t}(i,2)}}{(s_i{}^{(k)})}\right]\right), \tag{4.11b}$$

where $\lambda^\star_{\mathbf{t}(i,1)}$ holds for the one-hop link in route i and for the k-th iteration rate $s_i{}^{(k)}$, $\lambda^\star_{\mathbf{t}(i,2)}$ holds for the two-hop link and also for the k-th rate $s_i{}^{(k)}$.

Proof: Since the original problem is convex, if strong duality conditions hold[1] then the solution of Problem (4.10) corresponds to the solution of Problem II (4.6), i.e. $\mathcal{L}(\boldsymbol{\lambda}^\star) = \varphi^\star(\tilde{\mathbf{P}})$. Assuming that $(\boldsymbol{\lambda}^\star, \tilde{\mathbf{P}}^\star)$ represents the optimum solution of it, I can calculate now $\varphi^\star(\tilde{\mathbf{p}})$ from

[1] For more information about strong duality, see Boyd et al. [74, Section 5.2.3].

(4.9):

$$\varphi^{\star}(\tilde{\mathbf{P}}) = \sum_{i=1}^{I}\sum_{h=1}^{f(i)}\left[\omega e^{\tilde{P}_{\mathbf{t}(i,h)}} - \lambda^{\star}_{\mathbf{t}(i,h)} log\left(\sum_{q=1}^{Q} c_{\mathbf{t}(i,h)}(e^{\tilde{\mathbf{P}}})\right)\right] + \sum_{i=1}^{I}\sum_{h=1}^{f(i)}\lambda^{\star}_{\mathbf{t}(i,h)} log\left(\sum_{j=1}^{I}\tilde{r}_{t_1(j,h)i}e^{\tilde{s}_i}\right) \quad (4.12)$$

and

$$\frac{\partial}{\partial\tilde{s}_i}\left[\varphi^{\star}(\tilde{\mathbf{P}})\right] = \sum_{m=1}^{I}\sum_{h=1}^{f(m)}\tilde{r}_{t_1(m,h)i}\frac{\lambda^{\star}_{\mathbf{t}(m,h)}e^{\tilde{s}_i}}{\sum_{j=1}^{I}\tilde{r}_{t_1(m,h)j}e^{\tilde{s}_j}}. \quad (4.13)$$

Recalling (4.8), I have now:

$$\begin{aligned}\nabla_i\nu(\tilde{\mathbf{s}}) &= {u_i}'(e^{\tilde{s}_i})e^{\tilde{s}_i} - \frac{\partial}{\partial\tilde{s}_i}\left[\varphi^{\star}(\tilde{\mathbf{p}})\right] \\ &= e^{\tilde{s}_i}\left[{u_i}'(e^{\tilde{s}_i}) - \sum_{m=1}^{I}\sum_{h=1}^{f(m)}\tilde{r}_{t_1(m,h)i}\frac{\lambda^{\star}_{\mathbf{t}(m,h)}}{\sum_{j=1}^{I}\tilde{r}_{t_1(m,h)j}e^{\tilde{s}_j}}\right], \end{aligned} \quad (4.14)$$

and so the final rate update, for all i is:

$$s_i{}^{(k+1)} = e^{\tilde{s}_i^{(k+1)}} = s_i{}^{(k)}\exp(\epsilon\nabla_i\nu(\tilde{\mathbf{s}}^{(k)})). \qquad \blacksquare \quad (4.15)$$

The updating rules of the outer loop given by (4.11) are useful to determine the $(k+1)$-th iteration rate and the SINR that should be targeted by the inner power control. Note that as a natural consequence of the decomposition approach, the rate' updates equations require the knowledge of the Lagrange multipliers $\lambda^{\star}_{\mathbf{t}(i,h)}$ associated with Problem II, which can be found by solving the power control problem associated with the k-th outer loop iteration.

4.3.3 Solving the Power Allocation for a given SINR Target

I now consider the power control problem (Problem II) (4.6) for a given SINR target as follows. Given $\tilde{\mathbf{s}}^{(k)} \in \tilde{\mathbf{S}}$, the constraints in (4.6) require that the SINRs of the links exceed a target value, i.e.

$$\log\left(\sum_{j=1}^{I}\tilde{r}_{t_1(i,h)j}e^{\tilde{s}_j}\right) \leq \log\left(\sum_{q=1}^{N_{\text{PRB}}} c_{\mathbf{t}(i,h)}(e^{\tilde{\mathbf{P}}})\right) \quad \Leftrightarrow \quad \gamma_{\mathbf{t}(i,h)}(\mathbf{P}) \geq \gamma^{tgt}_{\mathbf{t}(i,h)}(\tilde{\mathbf{s}}^{(k)})\forall i,h,$$

where $\gamma_{\mathbf{t}(i,h)}(\mathbf{P})$ is defined in (4.1), and

$$\gamma^{tgt}_{\mathbf{t}(i,h)}\left(\tilde{s}_i^{(k)}\right) \triangleq 2^{\frac{\sum_{j=1}^{I}\tilde{r}_{t_1(i,h)j}e^{\tilde{s}_j}}{W}} - 1. \quad (4.16)$$

For the one-hop communications, the previous expression reduces to:

$$\gamma^{tgt}_{\mathbf{t}(i,1)}\left(\tilde{s}_i^{(k)}\right) = 2^{\left(\frac{e^{\tilde{s}_i}}{W}\right)} - 1, \quad (4.17a)$$

while for two-hop communications:

$$\gamma^{tgt}_{\mathbf{t}(i,1)}\left(\tilde{s}_i^{(k)}\right) = \gamma^{tgt}_{\mathbf{t}(i,2)}\left(\tilde{s}_i^{(k)}\right) = 2^{\left(\frac{e^{\tilde{s}_i}}{W}\right)} - 1. \quad (4.17b)$$

Therefore, for the two-hop communications and considering that a link is not included in other route than i, the links shall fulfill the SINR target, implying that the power shall not be

wasted in any of the links.

Therefore, Problem (4.6) can be rewritten as:

$$\begin{aligned} \underset{\tilde{\mathbf{P}}}{\text{minimize}} \quad & \omega \sum_{i=1}^{I} \sum_{h=1}^{f(i)} e^{\tilde{P}_{\mathbf{t}(i,h)}} \\ \text{subject to} \quad & \gamma_{\mathbf{t}(i,h)}(\mathbf{P}) \geq \gamma_{\mathbf{t}(i,h)}^{tgt}(\tilde{\mathbf{s}}^{(k)}) \quad \forall i,h, \\ & \tilde{\mathbf{P}} \succeq 0 \end{aligned} \tag{4.18}$$

and solved with an iterative SINR target following a Closed Loop Power Control (CLPC) scheme proposed by Zander et al. [20] for each given route i and hop h:

$$P_{\mathbf{t}(i,h)}{}^{(t+1)} = \frac{\gamma_{\mathbf{t}(i,h)}^{tgt}(\tilde{s}_i)}{\gamma_{\mathbf{t}(i,h)}\left(\mathbf{P}^{(t)}\right)} P_{\mathbf{t}(i,h)}{}^{(t)}. \tag{4.19}$$

Thus, for a given $\gamma_{\mathbf{t}(i,h)}^{tgt}(\tilde{s}_i)$, the (4.19) power control inner loop provides an efficient means to set the transmit powers at each transmitter in loop $(t+1)$, provided that the transmitter knows the SINR measured at the receiver in the preceding loop $\left(\gamma_{\mathbf{t}(i,h)}\left(\mathbf{P}^{(t)}\right)\right)$.

4.3.4 Determining the $\lambda_l^\star$-s

Therefore, it is now possible to determine the $\boldsymbol{\lambda}^\star$-s for the outer loop update (4.11) by exploiting the intimate relationship between the optimal $\mathbf{p}^\star$ and the associated Lagrange multipliers $\boldsymbol{\lambda}^\star$.

For this purpose, I will rewrite the interfering term in equation (4.1) as:

$$P_{\mathbf{t}(i,h)}^{tot} - G_{\mathbf{t}(i,h)} P_{\mathbf{t}(i,h)} = \sum_{j \neq i} \sum_{n} G_{\mathbf{t}(j,n)-\mathbf{t}(i,h)} P_{\mathbf{t}(j,n)}, \tag{4.20}$$

where $G_{\mathbf{t}(j,n)-\mathbf{t}(i,h)}$ denotes the undesired link gain between the transmitting user on route j and hop n and the receiving user on route i and link h, which is only possible if they are in the same PRB ($t_2(i,h) = t_2(j,n)$). Thus, it is now possible to rewrite the constraints in (4.18):

$$\begin{aligned} \frac{G_{\mathbf{t}(i,h)} P_{\mathbf{t}(i,h)}}{\sigma^2 + \sum_{j \neq i} \sum_n G_{\mathbf{t}(j,n)-\mathbf{t}(i,h)} P_{\mathbf{t}(j,n)}} - \gamma_{\mathbf{t}(i,h)}^{tgt} \geq 0 \quad \forall i,h \\ P_{\mathbf{t}(i,h)} - \gamma_{\mathbf{t}(i,h)}^{tgt} \sum_{j \neq i} \sum_n \frac{G_{\mathbf{t}(j,n)-\mathbf{t}(i,h)}}{G_{\mathbf{t}(i,h)}} P_{\mathbf{t}(j,n)} - \frac{\gamma_{\mathbf{t}(i,h)}^{tgt} \sigma^2}{G_{\mathbf{t}(i,h)}} \geq 0 \quad \forall i,h. \end{aligned} \tag{4.21}$$

Therefore, after rewriting some equations, it is possible to note that problem (4.18) can be written as a Linear Programming (LP) problem. Let $\mathbf{V} \in \mathbb{R}^{L \times L}$ and $\boldsymbol{\eta} \in \mathbb{R}^L$ be defined as follows:

$$\mathbf{V} = [v_{\mathbf{t}(j,m)-\mathbf{t}(i,h)}] \triangleq \begin{cases} -1 & \text{if } \mathbf{t}(i,h) = \mathbf{t}(j,m) \\ \gamma_l^{tgt} \dfrac{G_{\mathbf{t}(j,n)-\mathbf{t}(i,h)}}{G_{\mathbf{t}(i,h)}} & \text{if } \mathbf{t}(i,h) \neq \mathbf{t}(j,n) \end{cases} \tag{4.22a}$$

$$\boldsymbol{\eta} = [\eta_{\mathbf{t}(i,h)}] \triangleq \left[\frac{\gamma_{\mathbf{t}(i,h)}^{tgt} \sigma^2}{G_{\mathbf{t}(i,h)}}\right]. \tag{4.22b}$$

Using this notation, it is possible to reformulate Problem (4.18) as the following LP problem:

$$\begin{aligned} \underset{\mathbf{p}}{\text{minimize}} \quad & \omega \mathbf{1}^T \mathbf{p} \\ \text{subject to} \quad & \mathbf{V}\mathbf{p} \preceq -\boldsymbol{\eta}, \\ & \mathbf{p} \succeq 0, \end{aligned} \tag{4.23}$$

with the corresponding dual problem

$$\begin{aligned} \underset{\boldsymbol{\lambda}^{(\mathrm{LP})}}{\text{maximize}} \quad & \boldsymbol{\eta}^T \boldsymbol{\lambda}^{(\mathrm{LP})} \\ \text{subject to} \quad & \mathbf{V}^T \boldsymbol{\lambda}^{(\mathrm{LP})} \succeq -\omega \mathbf{1}, \\ & \boldsymbol{\lambda}^{(\mathrm{LP})} \succeq 0, \end{aligned} \tag{4.24}$$

which is necessary to compute the Lagrange multipliers in equation (4.11) for the rate update.

The inequality constraints in (4.24) can be rewritten explicitly as:

$$\frac{\lambda^{(\mathrm{LP})}_{\mathbf{t}(i,h)}}{\omega} - \sum_{j \neq i} \sum_{n} \frac{G_{\mathbf{t}(j,n)-\mathbf{t}(i,h)}}{G_{\mathbf{t}(j,n)}} \gamma^{tgt}_{\mathbf{t}(j,n)} \frac{\lambda^{(\mathrm{LP})}_{\mathbf{t}(j,n)}}{\omega} \leq 1, \quad \forall i, h. \tag{4.25}$$

Proof:

$$\begin{aligned} \mathbf{V}^T \boldsymbol{\lambda}^{(\mathrm{LP})} &\succeq -\omega \mathbf{1} \\ \sum_{j=1}^{I} \sum_{n=1}^{f(j)} v_{\mathbf{t}(j,n)-\mathbf{t}(i,h)} \lambda^{(\mathrm{LP})}_{\mathbf{t}(j,n)} &\geq -\omega, \quad \forall i, h; \\ -v_{\mathbf{t}(i,h)} \lambda^{(\mathrm{LP})}_{\mathbf{t}(i,h)} + \sum_{j \neq i}^{I} \sum_{n=1}^{f(j)} v_{\mathbf{t}(j,n)-\mathbf{t}(i,h)} \lambda^{(\mathrm{LP})}_{\mathbf{t}(j,n)} &\geq -\omega, \\ \frac{\lambda^{(\mathrm{LP})}_{\mathbf{t}(i,h)}}{\omega} - \sum_{j \neq i}^{I} \sum_{n=1}^{f(j)} \frac{G_{\mathbf{t}(j,n)-\mathbf{t}(i,h)}}{G_{\mathbf{t}(j,n)}} \gamma^{tgt}_{\mathbf{t}(j,n)} \frac{\lambda^{(\mathrm{LP})}_{\mathbf{t}(j,n)}}{\omega} &\leq 1, \quad \forall i, h. \end{aligned}$$ ■

By defining

$$\mu_{\mathbf{t}(i,h)} \triangleq \frac{\lambda^{(\mathrm{LP})}_{\mathbf{t}(i,h)}}{\omega} \frac{\gamma^{tgt}_{\mathbf{t}(i,h)} \sigma^2}{G_{\mathbf{t}(i,h)}} = \frac{\lambda^{(\mathrm{LP})}_{\mathbf{t}(i,h)}}{\omega} \eta_{\mathbf{t}(i,h)}, \tag{4.26}$$

inequality (4.25) can be interpreted as an SINR requirement:

$$\begin{aligned} \gamma^{FC}_{\mathbf{t}(i,h)}(\boldsymbol{\mu}) \triangleq & \frac{\mu_{\mathbf{t}(i,h)} G_{\mathbf{t}(i,h)}}{\sigma^2 + \sum_{j \neq i}^{I} \sum_{n=1}^{f(j)} G_{\mathbf{t}(j,n)-\mathbf{t}(i,h)} \frac{\sigma^2}{\sigma^2_{\mathbf{t}(j,n)}} \mu_{\mathbf{t}(j,n)}} \\ & \leq \gamma^{tgt}_{\mathbf{t}(i,h)}, \quad \forall i, h, \mathbf{t}(j,n) \neq \mathbf{t}(i,h). \end{aligned} \tag{4.27}$$

Proof:

$$\frac{\lambda^{(\text{LP})}_{\mathbf{t}(i,h)}}{\omega} - \sum_{j\neq i}^{I}\sum_{n=1}^{f(j)} \frac{G_{\mathbf{t}(j,n)-\mathbf{t}(i,h)}}{G_{\mathbf{t}(j,n)}} \gamma^{tgt}_{\mathbf{t}(j,n)} \frac{\lambda^{(\text{LP})}_{\mathbf{t}(j,n)}}{\omega} \leq 1$$

$$\frac{\lambda^{(\text{LP})}_{\mathbf{t}(i,h)}}{\omega} \frac{\gamma^{tgt}_{\mathbf{t}(i,h)}\sigma^2}{G_{\mathbf{t}(i,h)}} \frac{G_{\mathbf{t}(i,h)}}{\gamma^{tgt}_{\mathbf{t}(i,h)}\sigma^2} - \sum_{j\neq i}^{I}\sum_{n=1}^{f(j)} \frac{G_{\mathbf{t}(j,n)-\mathbf{t}(i,h)}}{G_{\mathbf{t}(j,n)}} \gamma^{tgt}_{\mathbf{t}(j,n)} \frac{\lambda^{(\text{LP})}_{\mathbf{t}(j,n)}}{\omega} \frac{\sigma^2_{\mathbf{t}(j,n)}}{\sigma^2_{\mathbf{t}(j,n)}} \leq 1$$

$$\frac{\mu_{\mathbf{t}(i,h)} G_{\mathbf{t}(i,h)}}{\gamma^{tgt}_{\mathbf{t}(i,h)}\sigma^2} \leq \sum_{j\neq i}^{I}\sum_{n=1}^{f(j)} \frac{G_{\mathbf{t}(j,n)-\mathbf{t}(i,h)}}{\sigma^2_{\mathbf{t}(j,n)}} \mu_{\mathbf{t}(j,n)} + 1$$

$$\gamma^{FC}_{\mathbf{t}(i,h)}(\boldsymbol{\mu}) \triangleq \frac{\mu_{\mathbf{t}(i,h)} G_{\mathbf{t}(i,h)}}{\sigma^2 + \sum_{j\neq i}^{I}\sum_{n=1}^{f(j)} G_{\mathbf{t}(j,n)-\mathbf{t}(i,h)} \frac{\sigma^2}{\sigma^2_{\mathbf{t}(j,n)}} \mu_{\mathbf{t}(j,n)}} \leq \gamma^{tgt}_{\mathbf{t}(i,h)}, \quad \forall i,h. \qquad \blacksquare$$

Therefore, the dual Problem (4.24) can be reformulated as:

$$\begin{aligned} \underset{\boldsymbol{\mu}}{\text{maximize}} \quad & \omega \mathbf{1}^T \boldsymbol{\mu} \\ \text{subject to} \quad & {\lambda_{\mathbf{t}(i,h)}}^{FC} \leq \gamma^{tgt}_{\mathbf{t}(i,h)}, \quad \forall i,h, \\ & \boldsymbol{\mu} \succeq 0, \end{aligned} \tag{4.28}$$

where the solution $\boldsymbol{\mu}$ can be found through the following distributed iterations

$$\mu^{(t+1)}_{\mathbf{t}(i,h)} = \frac{\gamma^{tgt}_{\mathbf{t}(i,h)}}{\gamma^{FC}_{\mathbf{t}(i,h)}(\boldsymbol{\mu}^{(t)})} \mu^{(t)}_{\mathbf{t}(i,h)} \quad \forall i,h. \tag{4.29}$$

Note that (4.29) can be interpreted as a reverse link power control problem, in which the receiver in route i and hop h becomes a transmitter (transmitting with power $\mu_{\mathbf{t}(i,h)}$) and the transmitter measures the experienced SINR at its position. In this sense, equation (4.26) represents the SINR requirement of the "forward channel" (FC), that is the SINR requirement related to the transmission from the receiver to the transmitter of the link in route i and hop h. Once the iterative procedure (4.29) converges to the optimum $\boldsymbol{\mu}^\star$, the optimal dual variables $\boldsymbol{\lambda}^{\star(\text{LP})}$ can be retrieved from equation equation (4.26) as

$$\lambda^{\star(\text{LP})}_{\mathbf{t}(i,h)} = \omega \mu^\star_{\mathbf{t}(i,h)} \eta^{-1}_{\mathbf{t}(i,h)}, \quad \forall i,h. \tag{4.30}$$

The original nonlinear power control problem (4.6) and its LP formulation (4.23) are equivalent in the sense that there is a specific relation between their optimal solutions $(\tilde{\mathbf{p}}^\star, \boldsymbol{\lambda}^\star)$ and $(\mathbf{p}^\star, \boldsymbol{\lambda}^{\star(\text{LP})})$:

$$\begin{aligned} P^\star_{\mathbf{t}(i,h)} &= e^{\tilde{P}^\star_{\mathbf{t}(i,h)}} \qquad \forall i,h \\ \lambda^\star_{\mathbf{t}(i,h)} &= \log(1+\gamma^{tgt}_{\mathbf{t}(i,h)}) \frac{1+\gamma^{tgt}_{\mathbf{t}(i,h)}}{\gamma^{tgt}_{\mathbf{t}(i,h)}} P^\star_{\mathbf{t}(i,h)} \log(2) \lambda^{\star(\text{LP})} \, \forall i,h. \end{aligned} \tag{4.31}$$

Hence, when I achieve both $P^\star_{\mathbf{t}(i,h)}$ and $\mu^\star_{\mathbf{t}(i,h)}$ by means of Equations (4.30) and (4.31), I am able to compute $\boldsymbol{\lambda}^\star$ as

$$\lambda^\star_{\mathbf{t}(i,h)} = \log(1+\gamma^{tgt}_{\mathbf{t}(i,h)}) \frac{1+\gamma^{tgt}_{\mathbf{t}(i,h)}}{\gamma^{tgt}_{\mathbf{t}(i,h)}} P^\star_{\mathbf{t}(i,h)} \log(2) \omega \mu^\star_{\mathbf{t}(i,h)} \frac{G_{\mathbf{t}(i,h)}}{\sigma^2 \gamma^{tgt}_{\mathbf{t}(i,h)}} \qquad \forall i,h, \tag{4.32}$$

and use it to update the user rates of equation (4.11).

Therefore, a pseudo-code of the the distributed power control algorithm is given in Algorithm 4.1:

Algorithm 4.1 Distributed utility maximizing PC

Initialize power for the inner-loop
Initialize SINR target for the outer-loop
for each **outer-loop** iteration **do**
  for each **inner-loop** iteration **do**
    Calculate $\gamma_{\mathbf{t}(i,h)}(\mathbf{P}^{(t)})$ (direct link)
    Update $P_{\mathbf{t}(i,h)}{}^{(t+1)}$
    Calculate $\gamma^{FC}_{\mathbf{t}(i,h)}(\boldsymbol{\mu}^{(t)})$ (reverse link)
    Update $\mu^{(t+1)}_{\mathbf{t}(i,h)}$
  end for
  Calculate $\lambda_{\mathbf{t}(i,h)}$
  Update $s_i{}^{(k+1)}$ and then $\gamma^{tgt}_{\mathbf{t}(i,h)}$
end for

4.4 Power Control Options Based on LTE Mechanisms

Due to intra-cell and new inter-cell interference scenarios, the question naturally arises whether the available LTE power control is suitable for D2D communications integrated in a MH LTE network. Also, the ad-hoc networking community has proposed efficient distributed schemes for MH communications in unlicensed spectrum, such as [72]. Such schemes can also serve as a basis for D2D multi-hop power control design in cellular spectrum.

The LTE PC scheme can be seen as a 'toolkit' from which different PC strategies can be selected depending on the deployment scenario and operator preference [75]. It employs a combination of Open Loop (OL) and Closed Loop (CL) control to set the UE transmit power (up to a maximum level of $P_{MAX} = 24$ dBm) as follows:

$$P_{\text{UE}} = \min\left\{ P_{max},\ \underbrace{P_0 - \alpha \cdot G}_{\text{OL operating point}} + \underbrace{f\big(\Delta_{\text{TPC}}\big)}_{\text{dynamic offset}} + \underbrace{10 \cdot \log_{10} m_{\text{PRB}}}_{\text{BW factor}} \right\}, \tag{4.33}$$

where the OL operating point allows for *Pathloss (PL) compensation* and the dynamic offset can further adjust the transmit power taking into account the current Modulation and Coding Scheme (MCS) and explicit Transmit Power Control (TPC) commands from the network. The bandwidth factor takes into account the minimum number of scheduled RBs per user (m_{PRB}). For the OL operating point, P_0 is a base power level used to control the Signal to Noise Ratio (SNR) target, α is the PL compensation factor, G is the path gain between the UE and the eNB. For the dynamic offset, Δ_{TF} is the transport format MCS dependent component, $f\big(\Delta_{\text{TPC}}\big)$ represents the explicit TPC commands.

For the integrated D2D communications scenario, I consider the following options:

- Equal Power Allocation (EPA): The transmit power of D2D UEs are set to some fixed value $P_{fix} \leq P_{max}$;
- Open Loop Power Control (OL) : The OL scheme allows users to transmit with variable power levels, depending on their path loss. Therefore, the OL compensates for the fraction of the path loss by setting α to some suitable value in the range $[0, 1]$ and $P_0 = \gamma^{tgt} + P_{IN}$, where γ^{tgt} is a predefined SNR target and P_{IN} is the interference plus noise power (in practice and for simplicity, P_{IN} can be assumed a fixed value, e.g. $P_{IN} \approx -106$ dBm) [30];
- Closed Loop Power Control (CL) : CL extends the OL scheme by adding the dynamic offset $f(\Delta_{TF})$ in (4.33) and by correcting the closed loop proposed by Hakola et al. [30],

which could neither reach nor compensate the SINR target. The tuning step can now be computed as follows:

$$f(\Delta_{TPC})^k = \left(\frac{\gamma^{tgt} - \widehat{\gamma}}{2}\right) + f(\Delta_{TPC})^{k-1}. \tag{4.34}$$

For cellular UEs communicating with their respective eNB, OL provides a well proven alternative, typically used in practice, for it avoids the complexity and overhead associated with the dynamic offset of the CL scheme.

4.5 Numerical Results and Discussion

4.5.1 Simulation Setup and Parameters

The simulation environment performed for this chapter is the same presented in Chapter 3, where I consider a seven cell system with a cell radius of 500 m supporting 25 uplink PRBs in each cell. The D2D communication uses uplink RBs in both the proximity communication and the range extension scenarios. For simplicity and to gain insights, I assume that each UE and D2D pair uses a single uplink RB. The most important system parameters are summarized in Table 4.2.

Table 4.2: Simulation parameters

Parameter	**Value**
Number of eNBs (N_{CELL})	7 (with wrap-around)
Communication link	Uplink (UL)
Minimum distance eNB-UE	$50\,\text{m}$ (Prox. Comm.)/$400\,\text{m}$ (Range Ext.)
Minimum distance UE-UE	$10\,\text{m}$
Mean distance D2D_{Tx}-D2D_{Rx}	$100\,\text{m}$
Central carrier frequency	$2\,\text{GHz}$
System bandwidth	$5\,\text{MHz}$
Number of PRBs (N_{PRB})	25 PRBs [57]
Noise power	$-116.4\,\text{dBm}$
Channel model	3GPP [66]
CSI knowledge	Ideal channel information
Traffic model	Full buffer [56]
Antenna configuration	1×1
Monte Carlo realizations	100
eNB transmit power	$40\,\text{dBm}$
UE min/max transmit power	$-23\,\text{dBm}/23\,\text{dBm}$
Fixed Power for EPA	$23\,\text{dBm}$
Path loss compensation factor (α)	0.8
SNR/SINR target for LTE PC	$15\,\text{dB}$
Number of outer-loop iterations	70
Number of inner-loop iterations	10
ϵ for the outer-loop	0.05
Initial power for the inner-loop	$10\,\text{dBm}$
Initial γ^{tgt} for the outer-loop	$0\,\text{dB}$
ω of Eq. (4.3)	[0.01 0.1 1 10 100]

To collect statistics on the measured SINR and transmit power levels, I consider the Normal load proposed in Section 3.5, with 7 D2D triplets and 11 cellular UEs in the proximity communication and 12 D2D pairs in the range extension, which guarantees intra-cell orthogonality.

Recall that in the proximity communication scenario a D2D transmitter transmits to a D2D receiver node (possibly via a D2D_{Re}), while in the range extension scenario, a D2D transmitter node transmits to its serving eNB (possibly via a D2D_{Re}). In the range extension scenario, the

D2D receiver node is not used. To gain insight into the performance impacts of MS algorithms, I evaluate the alternatives listed in Table 3.3.

To evaluate and benchmark the performance of the utility maximizing power control scheme, I compare its SINR and power consumption statistics with those based on the well known LTE power control schemes, as listed in Table 4.3. For the utility maximizing power control, the values of ω were chosen arbitrarily, because the optimal value of ω is an optimization problem.

Table 4.3: Power control algorithms

Name	Cellular UE power control	D2D power control
EPA	LTE Open Loop	Fixed Power
Open Loop **(OL)**	LTE Open Loop	LTE Open Loop
Closed Loop **(CL)**	LTE Open Loop	LTE Closed Loop
Utility Maxim. **(UM-ω)**	Utility maximizing PC with parameter ω	Utility maximizing PC with parameter ω

4.5.2 Impact of Mode Selection Algorithms

Since the mode selection does not depend on the power control algorithm used, the statistics when using the utility maximizing PC are the same shown in Section 3.5.1. Figures 4.2-4.3 compare the performance of the forced cellular mode, D2D mode (mode selection between single hop and cellular communications, D2DM) and HMS (see Table 3.3) for proximity communication when using the utility maximizing PC with $\omega = 1$.

Figure 4.2 shows the SINR distributions of cellular UEs and D2D pairs when employing the mode selection schemes of Table 3.3 in the proximity communication scenario. This figure shows that cellular UEs (transmitting to their serving eNB) benefit somewhat ($\approx 3\,\mathrm{dB}$) from D2D communications, especially when adaptive mode selection (the HMS algorithm) is used for mode selection.

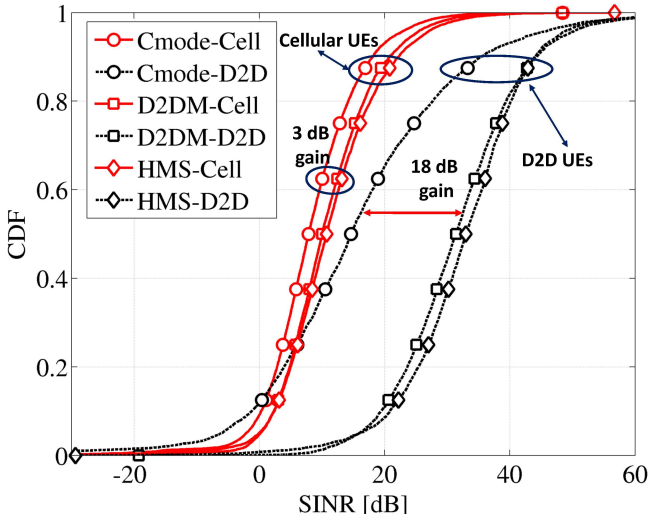

Figure 4.2: Proximity communication scenario: CDF of the SINR for both cellular UEs and D2D candidates with Cmode, D2DM and HMS (see Table 3.3). HMS is superior for both the cellular UEs (denoted '-Cell') and the D2D candidates and considering all the modes. The cellular UEs benefit somewhat ($\approx 2\,\mathrm{dB}$) from D2D communications. For the D2D candidates, the mode selection gain is much more pronounced ($\approx 18\,\mathrm{dB}$) with the HMS.

For the D2D users the mode selection gain is much more pronounced ($\approx 18\,\mathrm{dB}$). The intuitive explanation of this is that D2D communication with adaptive power control takes advantage of the proximity gain and reduces inter-cell interference. At the same time, D2D UEs benefit from an improved link budget due to the proximity, which allows for lower transmit power and higher SINR at the D2D receivers. HMS can adaptively take advantage of

the two-hop path, which explains the additional gain of HMS over D2D Mode Selection (D2DM) ($\approx 2\,\mathrm{dB}$).

Figure 4.3 is the CDF of the transmit power levels of all UEs in the proximity communication scenario, which shows that cellular UEs have a higher power consumption than the D2D users, where below the 50-th percentile HMS shows a higher power consumption for the cellular UEs than D2DM. For the D2D UEs, HMS can reduce the power consumption, reaching a $7\,\mathrm{dB}$ gain at the 50th percentile. Therefore, the results suggest that in addition to the SINR gains, two-hop communications outperform single-hop D2D mode in terms of power efficiency.

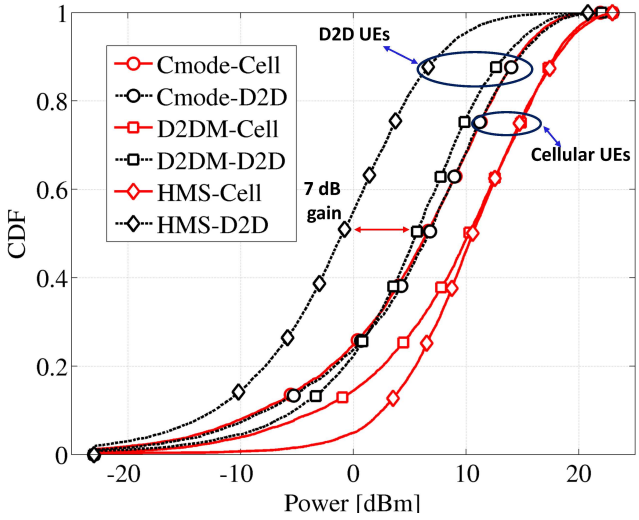

Figure 4.3: Proximity communication scenario: CDF of the transmit power levels for both cellular UEs and D2D candidates when considering different communication modes. I notice that the cellular UEs have higher higher power consumption than D2D UEs. In addition, HMS has a lower power consumption for the D2D UEs than D2DM, which suggests that in addition to the SINR gains, two-hop communications outperform the single-hop D2D mode in the power consumption.

Figure 4.4 shows the SINR distribution for the D2D nodes using the Cmode and the HMS algorithms in the range extension scenario. Figure 4.4 shows that HMS outperforms Cmode with a margin of $2\,\mathrm{dB}$ in the low SINR regime. Moreover, notice that $15\,\%$ of the UEs have SINR below $0\,\mathrm{dB}$, which is due to the severity of our simulation environment for both communication modes (all the transmitters are at least $400\,\mathrm{m}$ away from the eNB).

Figure 4.5 shows the CDF specifically for users that are in outage (SINR < 0) when using Cmode. Notice that HMS dramatically improves the SINR for these UEs and thereby reduces the probability of outage by exploiting the MH route.

Figure 4.6 shows the power distribution for the D2D nodes (aggregated between $\mathrm{D2D_{Tx}}$ and relay) using the Cmode and the HMS algorithms in the range extension scenario. Notice that HMS leads to a somewhat higher power consumption than Cmode for low SINR regime ($\approx 9\,\mathrm{dB}$), but this difference disappears as the power increases, where HMS shows a power gain of $1\,\mathrm{dB}$. Considering the average power consumption of both modes (average sum of all the power consumption along the Monte Carlo iterations), there is an efficiency gain of about $16\,\%$ of HMS over Cmode. That is, HMS can harvest the improvement on the SINR using less power than Cmode.

4.5.3 Impact of Power Control Algorithms

To gain insight into the impact of power control, I consider the power control algorithms of Table 4.3 using HMS for both the proximity communication and range extension scenarios.

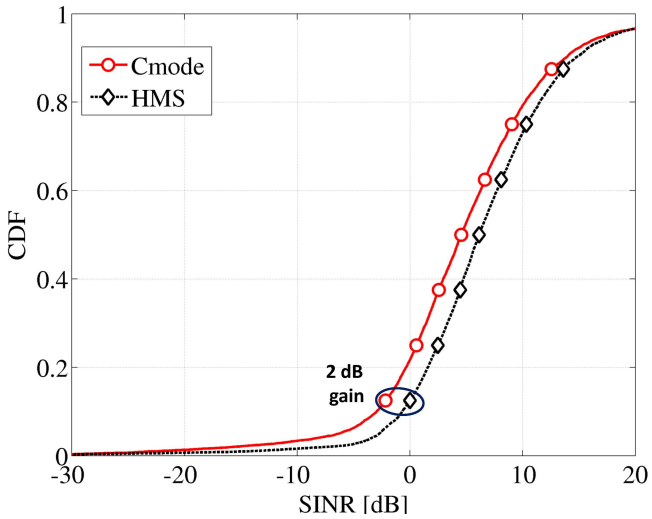

Figure 4.4: Range extension scenario: CDF of the SINR for D2D candidates when considering different communication modes. Notice that the HMS outperforms the Cmode in the low SINR regime. Moreover, HMS decreases the occurrence of SINR values below $0\,\mathrm{dB}$.

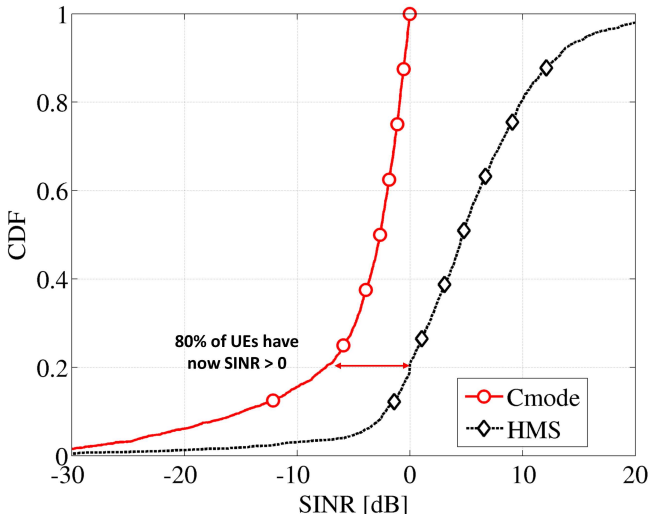

Figure 4.5: Range extension scenario: CDF specifically for the UEs that are in outage when using Cmode. HMS ensures coverage for $80\,\%$ of these originally 'out-of-coverage' users.

For the utility maximizing PC scheme, I employ five different values of ω, $(\omega = 0.01; 0.1; 1; 10; 100)$ which controls the spectral and energy efficiency trade-off.

Figure 4.7 is the CDF of the SINR for cellular and D2D candidates in the proximity communication scenario. Notice that utility maximizing PC with different values of ω has better SINRs than LTE PC schemes, with a gain of approximately $5\,\mathrm{dB}$ at the 50th percentile compared with LTE OL. However, for the high SINR regime EPA achieves higher SINR values than utility maximizing PC with $\omega = 0.01$ ($\approx 3\,\mathrm{dB}$). This behavior is explained due to the usage of maximum power by the best users, which causes more interference to users with low SINR, thus reducing it to values lower than utility maximizing PC. Moreover, it can be seen how ω improves the SINR, translating to an enhancement on the throughput as ω goes from 100 to 0.01.

Figure 4.8 is the scatter plot for the proximity communication scenario. With $\omega = 0.01$ the average throughput gain is low ($\approx 1\,\%$) over EPA, but using approximately $30\,\%$ less power. With $\omega = 100$ the average throughput gain is approximately $34\,\%$ using similar transmit power levels as LTE OL and CL.

Figure 4.9 is the CDF of the SINR for cellular and D2D candidates in the range extension

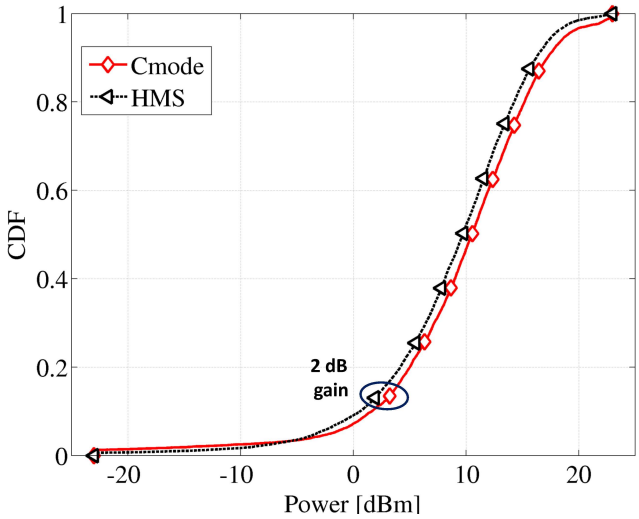

Figure 4.6: Range extension scenario: CDF of the power for D2D candidates when considering different communication modes. Notice that the power consumption of HMS is higher than Cmode (9 dB) in the low SINR regime but lower in the high SINR regime (1 dB). However, the average power consumption is lower in HMS.

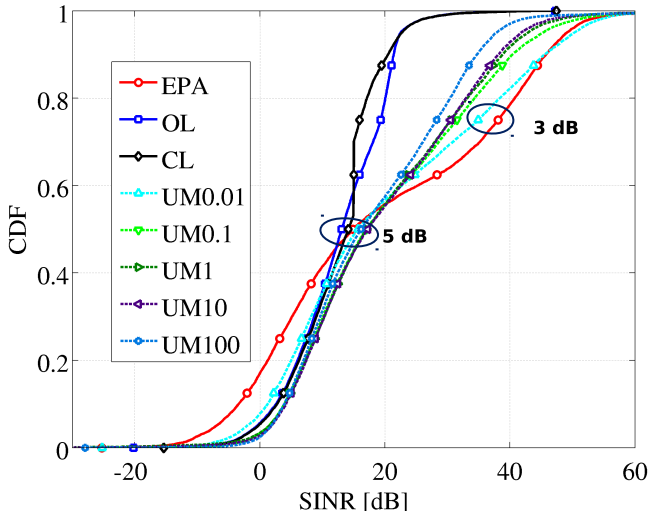

Figure 4.7: Proximity communication scenario: CDF of the SINR for cellular and D2D candidates users when considering different PC algorithms. Notice that utility maximizing PC shows a better performance with all values of ω than LTE PC, with a gain of approximately 5 dB at the 50th percentile to both LTE PC schemes and EPA. For the high SINR regime, EPA achieves a gain of approximately 3 dB over utility maximizing PC.

scenario. The utility maximizing PC schemes do not show the best SINRs for some cases, because the algorithm tries to reduce the SINR of some users while increasing the SINR for others. However, in most cases the utility maximizing PC with different values of ω has better SINRs than LTE PC, with a gain of approximately 3 dB at the 50th percentile to CL and OL, while only 1 dB to EPA. Moreover, it can be seen that increasing ω now decreases the SINR, which is also explained by the fact that some users have low SINR because the system tries to improve the SINR of users with better chance to achieve a high throughput.

Figure 4.10 is the scatter plot for the range extension scenario. Similarly to Figure 4.8, for $\omega = 0.01$ the utility maximization reaches the highest average throughput, although it does not show the best SINR for some users, with a throughput gain of approximately 8 % over EPA and 37 % over LTE CL. Moreover, it uses less power than EPA ($\approx$ 38 %). This behavior explains how utility maximizing PC achieves the highest throughput. With $\omega \geq 10$ the utility maximizing PC minimizes power consumption and it still reaches higher throughput values than LTE PC

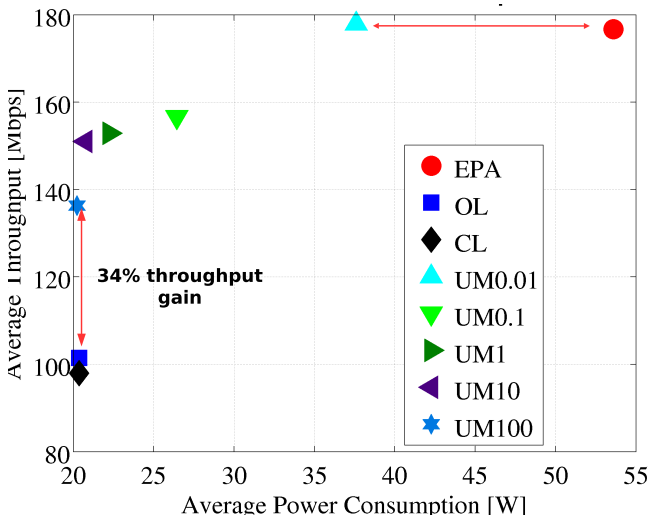

Figure 4.8: Proximity communication scenario: Scatter plot of the total power consumption and average throughput achieved by the examined power control algorithms. The utility maximizing PC can reach the highest throughput (with lower values of ω) and the LTE OL provides a reasonable engineering trade-off. Note that UM0.01 can maintain the same average throughput of EPA, but using $30\,\%$ less power.

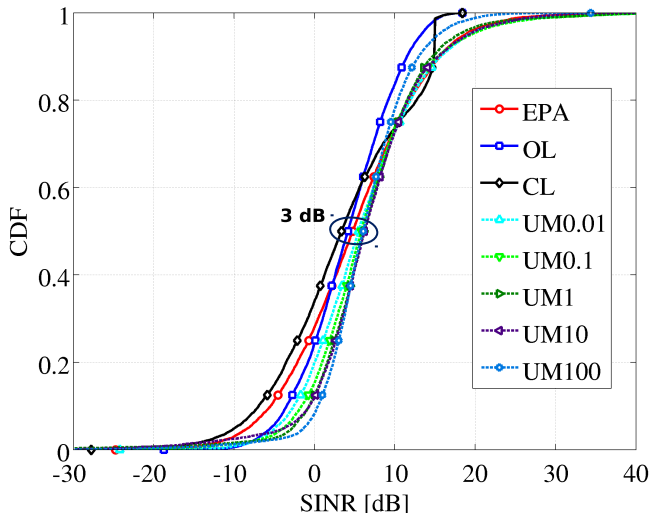

Figure 4.9: Range extension scenario: CDF of the SINR for cellular and D2D candidates users when considering different PC algorithms. In most cases the utility maximizing PC with different values of ω has better SINRs than LTE PC, with a gain of approximately $3\,\mathrm{dB}$ at the 50th percentile to LTE schemes. Moreover, it can be seen that ω now decreases the SINR.

schemes ($\approx 14\,\%$). Clearly, utility maximizing PC can reach high throughput when using low values of ω. However, if the power consumption has to be kept at low values with reasonable throughput values, utility maximization with higher ω values or using the LTE PC can be satisfactory.

4.6 Conclusions

In this chapter I extended a power control algorithm to multi-resource network-assisted MH D2D scenarios, including the proximity communication and the range extension ones. The proposed adaptive Harmonic Mode Selection (HMS) scheme together with a utility maximizing distributed PC scheme can improve the throughput and the energy efficiency of a system that does not support D2D communications or employs traditional mode selection and power control schemes. HMS can also decrease the outage probability and improve the average throughput using similar transmit power levels as users employing traditional PC

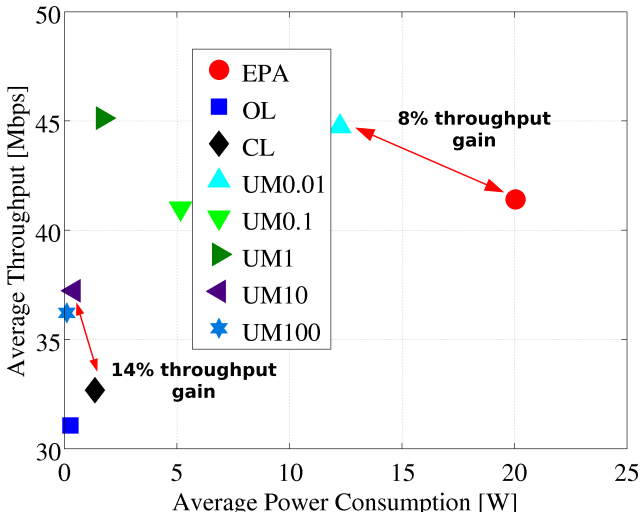

Figure 4.10: Range extension scenario: Scatter plot of the total power consumption and average throughput achieved by the examined power control algorithms. The utility maximizing PC can reach the highest throughput (with lower values of ω) or the lowest power consumption (with higher ω values). LTE OL provides a reasonable engineering trade-off.

techniques. LTE OL power control can also provide a reasonable trade-off between throughput and energy efficiency, especially in the range extension MH scenario. The numerical results clearly show that MH D2D communications have the potential of improving the performance not only of traditional cellular networks, but also that of cellular networks supporting only single hop D2D communications.

Chapter 5

Conclusions and Future Work

"It's the questions we can't answer that teach us the most. They teach us how to think. If you give a man an answer, all he gains is a little fact. But give him a question and he'll look for his own answers."

Patrick Rothfuss

This master's thesis has dealt with Radio Resource Management (RRM) in network-assisted Device-to-Device (D2D) communications. Mode selection, grouping and power control have been considered, at first for single-hop communications and then for multi-hop communications.

In Chapter 2, algorithms to group User Equipments (UEs) as well as algorithms to wisely choose between cellular and D2D communications with the goal of minimizing intra-cell interference and improving the system spectral efficiency have been formulated for both cellular and D2D UEs. Considering the mode selection, either using forcedly the D2D mode or employing the rate-based mode selection, the spectral efficiency of the system is improved. With this knowledge, the D2D UEs grouping algorithms were then compared. When there are multiple D2D pairs, the Normalized Projection-based Grouping (NORM) and D2D Pair Gain-based Grouping (PAIR) algorithms have losses, but they are able to reach higher spectral efficiency values than the compared schemes (Random Grouping (RND) and Reference Grouping (REF)), with relative gains of approximately $10\,\%$. The PAIR algorithm is the most simple one and it achieves the highest spectral efficiencies in the simulated scenario. However, its overall performance may vary if the hotspot is close to the Evolved Node B (eNB), so it can be recommended whenever the D2D UEs are far from the eNB.

In Chapter 3, I concentrated on the mode selection and resource allocation problems for two-hop D2D communications within a Long Term Evolution (LTE)-like cellular network and two Proximity Services (ProSe) scenarios proposed by the 3rd Generation Partnership Project (3GPP). The results show that the proposed adaptive *Harmonic Mode Selection* (HMS) scheme can improve the throughput and the energy efficiency of a system that does not support D2D communications or employs traditional mode selection schemes. Harmonic Mode Selection (HMS) can also decrease the outage probability and improve the average throughput using fixed transmit power levels for all the users in the relay extension scenario. Moreover, the proposed grouping algorithms for two-hop communications have also shown gains over an RND algorithm.

In Chapter 4, I extended a power control algorithm to a multi-resource applicability in network-assisted Multi-Hop (MH) D2D scenarios, including the proximity communication and the range extension scenarios. The proposed adaptive HMS scheme together with a utility maximizing Power Control (PC) scheme can improve the throughput and the energy efficiency

of a system that does not support D2D communications or employs traditional mode selection and power control schemes. LTE Open Loop (OL) power control can also provide a reasonable trade-off between throughput and energy efficiency, especially in the range extension MH scenario. The numerical results clearly show that MH D2D communications have the potential of improving the performance not only of traditional cellular networks, but also that of cellular networks supporting only single hop D2D communications.

In summary, this master's thesis has provided important results for RRM on D2D communications. The grouping algorithms have been proposed with the goal of minimizing intra-cell interference and improving the system spectral efficiency, as well as providing a mode selection algorithm that can wisely select between single- and multi-hop communications, and also extending a multi-hop power control algorithm to multi-resource D2D communications. Nevertheless, there are still several open issues and problems to be investigated by further works in the area, such as: the impact of imperfect channel knowledge on the performance of the algorithms, the extension to Multiple Input Multiple Output (MIMO) scenarios, the proposal of a joint resource allocation and power control algorithm for multi-hop D2D communications, among others.

Bibliography

[1] Ericsson, "RWS-120003 LTE release 12 and beyond," 3GPP Radio Access Network Workshop on Release 12 and Onwards, Ljubljana, Slovenia, Jun. 2012.

[2] METIS Project, Work Package 1, "Scenarios, Requirements and Key Performance Indicators for 5G Mobile and Wireless Systems," *European Project METIS*, April 2013.

[3] 3GPP, "Feasibility study for Proximity Services (ProSe)," 3rd Generation Partnership Project (3GPP), TR 22.803, Dec. 2012. [Online]. Available: http://www.3gpp.org/ftp/Specs/html-info/22803.htm

[4] E. C. Committee, "User Requirements and Spectrum Needs for Future European Broadband PPDR Systems," *European Conference on Postal and Telecommunications Administration*, February 2013.

[5] K. Doppler, M. Rinne, P. Janis, C. Ribeiro, and K. Hugl, "Device-to-Device Communications; Functional Prospects for LTE-Advanced Networks," in *IEEE International Conference on Communications Workshops, 2009*, Jun. 2009, pp. 1–6.

[6] G. Fodor, E. Dahlman, G. Mildh, S. Parkvall, N. Reider, G. Mikló, and Z. Turányi, "Design aspects of network assisted device-to-device communications," *IEEE Communications Magazine*, vol. 50, no. 3, pp. 170–177, Mar. 2012.

[7] C. F. Silva, J. M. B. da Silva Jr., and T. F. Maciel, "Radio Resource Management for Device-to-Device Communications in Long Term Evolution Networks," in *Resource Allocation and MIMO for 4G and Beyond*, F. R. P. Cavalcanti, Ed. Springer New York, 2014, vol. 105-156.

[8] H. Wu, C. Qiao, S. De, and O. Tonguz, "Integrated Cellular and Ad Hoc Relaying Systems:iCAR," *IEEE Journal on Selected Areas in Communications*, vol. 19, no. 10, pp. 2105–2115, 2001.

[9] F. H. Fitzek, M. Katz, and Q. Zhang, "Cellular controlled short range communication for cooperative p2p networking," in *Wireless World Research Forum (WWRF) 17*, November 2006.

[10] K. Doppler, M. Rinne, C. Wijting, C. B. Ribeiro, and K. Hugl, "Device-to-device communication as an underlay to LTE-advanced networks," *IEEE Communications Magazine*, vol. 47, no. 12, pp. 42–49, Dec. 2009.

[11] A. Asadi, Q. Wang, and V. Mancuso, "A survey on device-to-device communication in cellular networks," http://arxiv.org/abs/1310.0720v1, oct 2013.

[12] M. Zulhasnine, C. Huang, and A. Srinivasan, "Efficient resource allocation for device-to-device communication underlaying LTE network," in *Proceedings of the IEEE Wireless and Mobile Computing, Networking and Communications (WiMob)*, Oct 2010, pp. 368–375.

[13] P. Jänis, V. Koivunen, C. B. Ribeiro, K. Doppler, and K. Hugl, "Interference-avoiding MIMO schemes for device-to-device radio underlaying cellular networks," in *IEEE International Symposium on Personal, Indoor and Mobile Radio Communications (PIMRC'09)*, Sep. 2009, pp. 2385 – 2389.

[14] B. Wang, L. Chen, X. Chen, X. Zhang, and D. Yan, "Resource Allocation Optimization for Device-to-Device Communication Underlaying Cellular Networks," in *Proceedings of the IEEE Vehicular Technology Conference (VTC)*, May 2011, pp. 1–6.

[15] P. Tejera, W. Utschick, G. Bauch, and J. A. Nossek, "Subchannel allocation in multiuser multiple-input multiple-output systems," *IEEE Transactions on Information Theory*, vol. 52, no. 10, pp. 4721 –4733, Oct. 2006.

[16] G. Caire and S. Shamai, "On the Achievable Throughput of a Multiantenna Gaussian Broadcast Channel," *IEEE Transactions on Information Theory*, vol. 49, no. 7, pp. 1691 – 1706, Jul. 2003.

[17] P. Jänis, C.-H. Yu, K. Doppler, C. Ribeiro, C. Wijting, K. Hugl, O. Tirkkonen, and V. Koivunen, "Device-to-device communication underlaying cellular communications systems," in *International Journal of Communications, Network and System Sciences,2009*, vol. 2, no. 3, Jun. 2009, pp. 169–178.

[18] S. Hakola, T. Chen, J. Lehtomaki, and T. Koskela, "Device-to-device (D2D) communication in cellular network - performance analysis of optimum and practical communication mode selection," in *Proceedings of the IEEE Wireless Communications and Networking Conference (WCNC)*, Apr. 2010, pp. 1 –6.

[19] K. Doppler, C.-H. Yu, C. B. Ribeiro, and P. Janis, "Mode selection for device-to-device communication underlaying an LTE-advanced network," in *Proceedings of the IEEE Wireless Communications and Networking Conference (WCNC)*, Apr. 2010, pp. 1 –6.

[20] J. Zander, "Distributed cochannel interference control in cellular radio systems," *IEEE Transactions on Vehicular Technology*, vol. 41, no. 3, pp. 305–311, Aug. 1992.

[21] G. J. Foschini and Z. Miljanic, "A Simple Distributed Autonomous Power Control Algorithm and its Convergence," *IEEE Transactions on Vehicular Technology*, vol. 42, no. 4, pp. 641–645, Nov. 1993.

[22] R. D. Yates, "A Framework for Uplink Power Control in Cellular Radio Systems," *IEEE Journal on Selected Areas in Communications*, vol. 13, no. 7, pp. 1341–1347, Sep. 1995.

[23] S. Gupta, R. Yates, and C. Rose, "Soft dropping power control - a power control backoff strategy," in *IEEE International Conference on Personal Wireless Communications, 1997*, Dec. 1997, pp. 210 –214.

[24] M. Schubert and H. Boche, "Solution of the multiuser downlink beamforming problem with individual SINR constraints," *IEEE Transactions on Vehicular Technology*, vol. 53, no. 1, pp. 18–28, Jan. 2004.

[25] J. Papandriopoulos, J. Evans, and S. Dey, "Distributed power control for cellular MIMO systems with temporal and spatial filtering," in *Australian Communications Theory Workshop*, Feb. 2004, pp. 164–175.

[26] R. Chen, J. Andrews, R. Heath, and A. Ghosh, "Uplink power control in multi-cell spatial multiplexing wireless systems," in *IEEE Transactions on Wireless Communications*, vol. 6, no. 7, July 2007, pp. 2700 – 2711.

[27] F. R. P. Cavalcanti and S. Andersson, Eds., *Optimizing Wireless Communication Systems*. Springer, Apr. 2009.

[28] C. Yu, O. Tirkkonen, K. Doppler, and C. Ribeiro, "On the Performance of Device-to-Device Underlay Communication with Simple Power Control," in *Proceedings of the IEEE Vehicular Technology Conference (VTC)*, Apr. 2009, pp. 1–5.

[29] C.-H. Yu, O. Tirkkonen, K. Doppler, and C. Ribeiro, "Power optimization of device-to-device communication underlaying cellular communication," in *Proceedings of the IEEE International Conference on Communications (ICC)*, 2009, pp. 1–5.

[30] H. Xing and S. Hakola, "The investigation of power control schemes for a device-to-device communication integrated into OFDMA cellular system," in *Proceedings of the IEEE Personal, Indoor and Mobile Radio Communications (PIMRC)*, Sep. 2010, pp. 1775–1780.

[31] M. Belleschi, G. Fodor, and A. Abrardo, "Performance Analysis of a Distributed Resource Allocation Scheme for D2D Communications," in *Proceedings of the IEEE Global Telecommunications Conference*, Houston, EUA, December 2011.

[32] M. Jung, K. Hwang, and S. Choi, "Joint Mode Selection and Power Allocation Scheme for Power-Efficient Device-to-Device (D2D) Communication," in *Proceedings of the IEEE Vehicular Technology Conference (VTC)*, may 2012.

[33] P. Phunchongharn, E. Hossain, and D. Kim, "Resource allocation for device-to-device communications underlying lte-advanced networks," *IEEE Wireless Communications Magazine*, vol. 20, no. 4, pp. 91–100, Aug. 2013.

[34] M. Conti and S. Giordano, "Mobile ad hoc networking: Milestones, challenges, and new research directions," *IEEE Communications Magazine*, vol. 52, no. 1, pp. 85–96, Jan. 2014.

[35] L. Chen, Y. Huang, F. Xie, Y. Gao, L. Chu, H. He, Y. Li, F. Liang, and Y. Yuan, "Mobile relay in lte-advanced systems," *IEEE Communications Magazine*, vol. 51, no. 11, pp. 144–151, Nov. 2013.

[36] B. Zafar, S. Gherekhloo, and M. Haardt, "Analysis of multihop relaying networks: Communication between range-limited and cooperative nodes," *IEEE Vehicular Technology Magazine*, vol. 7, no. 3, pp. 40–47, Sep. 2012.

[37] S. Wen, X. Zhu, Y. Lin, Z. Lin, X. Zhang, and D. Yang, "Achievable Transmission Capacity of Relay-Assisted Device-to-Device (D2D) Communication Underlay Cellular Networks," in *Proceedings of the IEEE Vehicular Technology Conference (VTC)*, Sep. 2013.

[38] J. Pérez-Romero and R. A. O. Sallent, "Enhancing cellular coverage through opportunistic networks with learning mechanisms," in *Proceedings of the IEEE Global Telecommunications Conference*, Dec. 2013.

[39] N. Mastronarde, V. Patel, J. Xu, and M. van der Schaar, "Learning Relaying Strategies in Cellular D2D Networks with Token-Based Incentives," in *Proceedings of the IEEE Global Telecommunications Conference*, Dec. 2013.

[40] M. Hasan and E. Hossain, "Resource allocation for network-integrated device-to-device communications using smart relays," in *Proceedings of the IEEE Global Telecommunications Conference*, vol. Workshop - International Workshop on Device-to-Device (D2D) Communication With and Without Infrastructure, 2013.

[41] J. M. B. da Silva Jr., T. F. Maciel, R. L. Batista, C. F. M. e Silva, and F. R. P. Cavalcanti, "UE grouping and mode selection for D2D communications underlaying a multicellular wireless system," in *Proceedings of the IEEE International Workshop on D2D and Public Safety Communications (WPDC)*, Istambul, Turkey, Apr. 2014, pp. 230–235.

[42] R. L. Batista, C. F. M. e Silva, J. M. B. da Silva Jr., T. F. Maciel, and F. R. P. Cavalcanti, "Impact of device-to-device communications on cellular communications in a multi-cell scenario," in *XXXI Telecommunications Brazilian Symposium (SBrT)*, Fortaleza, Brazil, Sep. 2013.

[43] ——, "What happens with a proportional fair cellular scheduling when D2D communications underlay a cellular network?" in *Proceedings of the IEEE International Workshop on D2D and Public Safety Communications (WPDC)*, Istambul, Turkey, Apr. 2014, pp. 260–265.

[44] ——, "Power prediction prior to scheduling combined with equal power allocation for the OFDMA UL," in *Procedings of the European Wireless Conference*, Barcelona, Spain, May 2014.

[45] Y. V. L. Melo, R. L. Batista, T. F. Maciel, C. F. M. e Silva, J. M. B. da Silva Jr., and F. R. P. Cavalcanti, "Power control with variable target SINR for D2D communications underlying cellular networks," in *Procedings of the European Wireless Conference*, Barcelona, Spain, May 2014.

[46] J. M. B. da Silva Jr., R. L. Batista, C. F. M. e Silva, Y. V. L. Melo, T. F. Maciel, and F. R. P. Cavalcanti, "Network-Assisted Device-to-Device Communications," GTEL-UFC-Ericsson UFC.33, Tech. Rep., Aug. 2014, Fourth Technical Report.

[47] R. L. Batista, C. F. M. e Silva, J. M. B. da Silva Jr., Y. V. L. Melo, T. F. Maciel, and F. R. P. Cavalcanti, "Network-Assisted Device-to-Device Communications," GTEL-UFC-Ericsson UFC.33, Tech. Rep., Jan. 2014, Third Technical Report.

[48] J. M. B. da Silva Jr., R. L. Batista, C. F. M. e Silva, Y. V. L. Melo, T. F. Maciel, and F. R. P. Cavalcanti, "Network-Assisted Device-to-Device Communications," GTEL-UFC-Ericsson UFC.33, Tech. Rep., Aug. 2013, Second Technical Report.

[49] R. L. Batista, C. F. M. e Silva, J. M. B. da Silva Jr., T. F. Maciel, and F. R. P. Cavalcanti, "Network-Assisted Device-to-Device Communications," GTEL-UFC-Ericsson UFC.33, Tech. Rep., Feb. 2013, First Technical Report.

[50] C. Xu, L. Song, Z. Han, Q. Zhao, X. Wang, X. Cheng, and B. Jiao, "Efficiency resource allocation for device-to-device underlay communication systems: A reverse iterative combinatorial auction based approach," *IEEE Journal on Selected Areas in Communications*, vol. 31, no. 9, pp. 348–358, 2013.

[51] M. Hajiaghayi, C. Wijting, C. Ribeiro, and M. T. Hajiaghayi, "Efficient and practical resource block allocation for LTE-based D2D network via graph coloring," *Wireless Networks*, vol. 20, no. 4, pp. 1–14, 2013.

[52] C.-P. Chien, Y.-C. Chen, and H.-Y. Hsieh, "Exploiting spatial reuse gain through joint mode selection and resource allocation for underlay device-to-device communications," in *Proceedings of the IEEE Wireless Personal Multimedia Communications (WPMC)*, 2012, pp. 80–84.

[53] D. Bertsimas and J. Tsitsiklis, *Introduction to Linear Optimization*. Athena Scientific, 1997.

[54] T. F. Maciel and A. Klein, "On the performance, complexity, and fairness of suboptimal resource allocation for multiuser MIMO-OFDMA systems," *IEEE Transactions on Vehicular Technology*, vol. 59, no. 1, pp. 406–419, Jan. 2010. [Online]. Available: http://ieeexplore.ieee.org/stamp/stamp.jsp?tp=&arnumber=5196814

[55] X. Chu, D. Lopez-Perez, Y. Yang, and F. Gunnarsson, *Heterogeneous Cellular Networks: Theory, Simulation and Deployment*. Cambridge University Press, 2013.

[56] 3GPP, "Spatial channel model for multiple input multiple output (MIMO) simulations," 3rd Generation Partnership Project, TR 25.996 V7.0.0, Jun. 2007.

[57] ——, "Physical layer aspects for evolved universal terrestrial radio access (UTRA)," 3rd Generation Partnership Project, TR 25.814 V7.1.0, Sep. 2006.

[58] ——, "Further advancements for E-UTRA physical layer aspects," 3rd Generation Partnership Project, TR 36.814 V9.0.0, Mar. 2009.

[59] A. Goldsmith, *Wireless Communications*, 1st ed. Cambridge University Press, 2005.

[60] J. Hong, S. Park, H. Kim, S. Choi, and K. B. Lee, "Analysis of device-to-device discovery and link setup in LTE networks," in *2013 IEEE 24th Annual International Symposium on Personal, Indoor, and Mobile Radio Communications (PIMRC)*, Sep. 2013, pp. 2856–2860.

[61] C. Mehlführer, M. Wrulich, J. C. Ikuno, D. Bosanska, and M. Rupp, "Simulating the long term evolution physical layer," in *Procedings of the European Signal Processing Conference*, Glasgow, Scotland, Aug. 2009. [Online]. Available: http://publik.tuwien.ac.at/files/PubDat_175708.pdf

[62] 3GPP, "Evolved Universal Terrestrial Radio Access (E-UTRA); Physical layer procedures," 3rd Generation Partnership Project (3GPP), TS 36.213, Oct. 2010. [Online]. Available: http://www.3gpp.org/ftp/Specs/html-info/36213.htm

[63] ——, "Evolved Universal Terrestrial Radio Access (E-UTRA); physical layer procedures," 3rd Generation Partnership Project, TS 36.213 V8.6.0, Mar. 2009.

[64] J. C. Ikuno, M. Wrulich, and M. Rupp, "System level simulation of LTE networks," in *Proceedings of the IEEE Vehicular Technology Conference (VTC)*, May 2010, pp. 1–5.

[65] J. Zander and S.-L. Kim, *Radio Resouce Management for Wireless Networks*. Artech House, 2001.

[66] 3GPP, "Radio Frequency (RF) system scenarios," 3rd Generation Partnership Project (3GPP), TR 25.942, Dec. 2009. [Online]. Available: http://www.3gpp.org/ftp/Specs/html-info/25942.htm

[67] W. Wang, S. Yan, and S. Yang, "Optimally Joint Subcarrier Matching and Power Allocation in OFDM Multihop System," *EURASIP J. Adv. Signal Process*, vol. 2008, pp. 146:1–146:8, Jan. 2008.

[68] A. Pradini, "Power control and resource allocation for device-to-device communications in cellular networks," Master's thesis, KTH Information and Communication Technology, 2013.

[69] J. Papandriopoulos, S. Dey, and J. Evans, "Optimal and Distributed Protocols for Cross-Layer Design of Physical and Transport Layers in MANETs," *IEEE/ACM Transactions on Networking*, vol. 16, pp. 1392–1405, 2008.

[70] M. Belleschi, L. Balucanti, P. Soldati, M. Johansson, and A. Abrardo, "Fast Power Control for Cross-Layer Optimal Resource Allocation in DS-CDMA Wireless Networks," in *Proceedings of the IEEE International Conference on Communications (ICC)*, 2009, pp. 1–6.

[71] G. Fodor, D. D. Penda, M. Belleschi, and M. Johansson, "A comparative study of power control approaches for device-to-device communications," in *Proceedings of the IEEE International Conference on Communications (ICC)*, Budapest, Hungary, Jun. 2013.

[72] H.-H. Choi and J.-R. Lee, "Distributed transmit power control for maximizing end-to-end throughput in wireless multi-hop networks," *Wireless Personal Communications*, vol. 74, no. 3, pp. 1033–1044, 2013.

[73] S. Bazaraa, H. Sherali, and C. Shetty, *Nonlinear Programming: Theory and Algorithms*, ser. Wiley-Interscience series in discrete mathematics and optimization. Wiley, 1993.

[74] S. Boyd and L. Vandenberghe, *Convex optimization*, 1st ed. Cambridge University Press, 2004.

[75] A. Simonsson and A. Furuskar, "Uplink power control in LTE - overview and performance," in *Proceedings of the IEEE Vehicular Technology Conference (VTC)*, 2008.